Complex Organic Interstellar Molecules

Eric Herbst[1] and Ewine F. van Dishoeck[2]

[1]Departments of Physics, Astronomy, and Chemistry, The Ohio State University, Columbus, Ohio 43210; email: herbst@mps.ohio-state.edu

[2]Leiden Observatory, Leiden University, 2300 RA Leiden, The Netherlands; email: ewine@strw.leidenuniv.nl,
and Max-Planck Institut für Extraterrrestrische Physik (MPE), 85748 Garching, Germany

Annu. Rev. Astron. Astrophys. 2009. 47:427–80

The *Annual Review of Astronomy and Astrophysics* is online at astro.annualreviews.org

This article's doi:
10.1146/annurev-astro-082708-101654

0066-4146/09/0922-0427$20.00

Key Words

astrochemistry, complex molecules, interstellar medium, interstellar molecules, star formation

Abstract

Of the over 150 different molecular species detected in the interstellar and circumstellar media, approximately 50 contain 6 or more atoms. These molecules, labeled complex by astronomers if not by chemists, all contain the element carbon and so can be called organic. In the interstellar medium, complex molecules are detected in the denser sources only. Although, with one exception, complex molecules have only been detected in the gas phase, there is strong evidence that they can be formed in ice mantles on interstellar grains. The nature of the gaseous complex species depends dramatically on the source where they are found: in cold, dense regions they tend to be unsaturated (hydrogen-poor) and exotic, whereas in young stellar objects, they tend to be quite saturated (hydrogen-rich) and terrestrial in nature. Based on both their spectra and chemistry, complex molecules are excellent probes of the physical conditions and history of the sources where they reside. Because they are detected in young stellar objects, complex molecules are expected to be common ingredients for new planetary systems. In this review, we discuss both the observation and chemistry of complex molecules in assorted interstellar regions in the Milky Way.

1. INTRODUCTION

Astronomical molecules are found in diverse environments, ranging from nearby objects in our solar system to distant sources in the early universe. Although detected in stellar atmospheres, molecules are particularly associated with dense and cool neutral interstellar and circumstellar matter in our galaxy and others; this matter comprises both a gaseous phase and a solid phase of tiny dust particles. The dense interstellar matter can be found in small individual objects known as globules or as part of much larger irregular assemblies ranging up to so-called giant molecular clouds, with size $\approx$100 pc and mass $\approx 10^5\ M_\odot$. Wherever molecules are found, they are useful probes of the physical conditions of their environments and of the lifetimes of these sources. Moreover, nonterrestrial molecules are of interest for what they tell us about the build-up of molecular complexity throughout the universe.

The utility of molecules as probes derives from both their spectra and their chemistry. The richness of molecular spectra yields detailed physical information on the gas and dust in addition to characterization of the species: High-resolution rotational and vibrational spectra tell us about the density and temperature of the gas as well as large-scale motions such as collapse and rotation, whereas vibrational spectra of molecules in dust grains yield information on the polar or nonpolar nature of the mantles surrounding the particles. Simulations, or models, of the chemistry, in which molecular abundances are calculated based on the rates of their formation and destruction by assorted chemical reactions, provide another probe of current physical conditions, since the rates of chemical processes depend on them. Because calculated molecular abundances are functions of time as well as physical conditions, the results of models can yield information about the histories of the sources by comparison with observations. Of course, models are an imperfect tool because our knowledge of the chemical processes is far from complete and because the physical conditions of sources can themselves be time-dependent, which can modify predictions of current-day abundances. With a proper treatment of radiative transfer, models can be used to predict the intensity and shape of spectral transitions as well as abundances.

The study of interstellar molecules has helped to clarify the evolutionary stages of star formation in the Milky Way, especially for low-mass stars with luminosities $\lesssim 10^2\ L_\odot$ (van Dishoeck & Blake 1998). We now understand that such stars are formed from cold, dense prestellar globules or cores ($n_H = n(H) + 2n(H_2) \approx 2 \times 10^4$ cm^{-3}, $T \approx 10$ K) of size 0.1–0.3 pc and rich in both gas-phase molecules and icy mantles of molecules atop dust particles. The dust particles themselves are thought to be composed of silicates and carbonaceous matter, with sizes ranging from 10 nm to 0.5 μm. Both the dust particles and their icy mantles are major reservoirs for heavy elements. The cold cores begin to collapse in an isothermal manner because the atoms and molecules release energy in the form of radiation as the collapse proceeds (Bergin & Tafalla 2007). Once a central condensation of sufficient density ($n_H \approx 10^{5-7}$ cm^{-3}) and radius ($r \approx 0.02$–0.05 pc) is formed, it becomes opaque, starts to heat up as further collapse occurs, and emits a continuum of infrared radiation. The resulting phases of these young stellar objects (YSOs), which include the protostar and its environs, can encompass a variety of phenomena including the following: (*a*) outflows, consisting of jets and shocks, (*b*) warm inner envelopes passively heated by the protostar, with typical temperatures of $\approx$100 K and densities in the range 10^{7-8} cm^{-3}, and (*c*) incipient protoplanetary disks. When associated with complex organic molecule emission, the inner envelopes are known as hot corinos, the low-mass versions of hot cores (Ceccarelli 2005). The size of the hot corinos, of undetermined geometry, is about 100 AU or less (Ceccarelli 2005), which is smaller than a typical protoplanetary disk. There is also some evidence for protostellar sources in which the bulk of the envelope is only partially heated to temperatures well below 100 K; we use the term lukewarm for these sources (Hassel, Herbst & Garrod 2008), the best

known of which is L1527 (Sakai et al. 2008). Eventually, much of the matter is blown away, and the young stellar object (or objects) settles into life as a T Tauri star encircled by a dense protoplanetary disk.

For the formation of higher-mass stars, our understanding is not as well-developed. It is likely that so-called "infrared dark" clouds with local temperature minima and density maxima represent the initial collapsing phase, but the subsequent stages are not yet fully understood. High-mass young stellar objects can be seen within giant clouds, where they are associated with ultra- or hypercompact H II regions, masers, outflows, and/or warm ambient gas at average temperatures of 300 K, known as hot cores. These hot cores are typically warmer and much larger (up to 0.05 pc = 10^4 AU) than their low-mass analogs, the hot corinos, and they often, but not always, show a rich organic chemistry. To what extent disks are associated with high-mass star formation remains uncertain. Most recently, the formation of intermediate mass stars has been subject to extensive study. If newly formed stars are in the proximity of cool interstellar matter, their radiation strongly alters the temperature and molecular composition of the matter, producing heterogeneous Photon-Dominated Regions (PDRs).

1.1. Complex Molecules

In interstellar clouds and related circumstellar envelopes of AGB stars, the gas-phase molecules detected by high-resolution spectroscopy are not large by the standards of terrestrial organic chemistry, ranging in size from 2 to 13 atoms. Although a significant number of molecules have been detected in external galaxies, we focus here on our own galaxy because our knowledge of the more complex species detected at high spectral resolution is strongly confined to the Milky Way. At present, circa 150 different molecules have been detected, mainly via rotational emission spectra, obtained by the use of millimeter-wave telescopes on the ground or in space (Markwick-Kemper 2003, Woon 2008). Some molecules, notably H_3^+, have been detected via vibrational transitions in the infrared in absorption using background stars or internal young stellar objects as lamps, whereas others have been detected by visible and UV electronic spectroscopy against background stars through diffuse interstellar matter. The dominant molecule in all dense sources, H_2, is actually difficult to detect. It can be seen with difficulty in infrared vibrational absorption in cool, dense sources, in UV absorption through diffuse matter, and via rotational and vibrational emission in warm or shocked matter. Other than molecular hydrogen, the gas-phase molecules detected are minor constituents of the gas; carbon monoxide (CO), the second most abundant gaseous molecule, has a typical fractional abundance of 10^{-4} that of molecular hydrogen in dense objects. The larger species range in fractional abundance down to 10^{-11} with respect to H_2. Note that there is very little atomic hydrogen in dense sources so that $n_H \approx 2n(H_2)$. Fractional abundances of molecules are expressed both relative to molecular hydrogen and to n_H, often resulting in possible confusion of a factor of two. In this review, we use molecular hydrogen.

Although many of the molecules detected are also quite common on Earth, others are quite exotic by terrestrial standards. The exotic molecules comprise molecular ions, both positively charged (e.g., HCO^+) and negatively charged (e.g., C_4H^-); radicals, which are species with unpaired electrons (e.g., C_6H); and isomers, which are species with the same atomic constituents but different structures (e.g., HCN and HNC). So-called isotopologues, or molecules containing unusual isotopes such as deuterium, ^{13}C, ^{15}N, ^{17}O, ^{18}O, and ^{34}S, have also been detected. In the absence of chemical fractionation, a process by which chemical reactions produce abundance ratios among isotopologues different from the actual elemental abundance ratios, the isotopologues can be used to determine elemental abundance ratios such as D/H and $^{13}C/^{12}C$ at different places in the universe.

Most interstellar and circumstellar molecules are organic in nature; that is, they are dominated by the heavy element carbon. The preponderance of organic molecules is especially great for the larger molecules detected; 100% of the detected species with six or more atoms are organic. We arbitrarily refer to species with six atoms or more as complex. The detected organic molecules consist of those designated unsaturated and saturated; the term unsaturated refers to molecules that have few hydrogen atoms, such as the bare carbon clusters (C_n; n = 2, 3, 5), the radicals of the form C_nH, (n = 2–8), and the cyanopolyynes (HC_nN; n = 3, 5, 7, 9, 11), whereas the term saturated refers to organic species richer in hydrogen, such as dimethyl ether (CH_3OCH_3). In strict chemical terms, fully saturated molecules are limited to single chemical bonds involving valence electrons. Most common terrestrial organic molecules tend to be saturated or near-saturated.

Absorption spectra arising from molecules in the solid phase are broad and cannot be assigned with as much certainty as narrow gas-phase features (Whittet 2003). Nevertheless, there is strong evidence that assignments of major species are correct. Compared with their gas-phase analogs, molecules detected on grain mantles tend to be smaller in size because the absorption features from complex species are too weak and lack specificity (Gibb et al. 2000b). The most abundant such molecule in cold sources is water ice, which has a fractional abundance with respect to H_2 of typically 10^{-4}, comparable to gas-phase CO. Somewhat smaller abundances are obtained for solid-phase carbon dioxide (CO_2) and CO, the amount of which depends on environment. The fractional abundance of solid methanol (CH_3OH), the only complex species detected unambiguously, appears to be highly variable from source to source, but can be as large as ≈30% of the water ice abundance, or about 3×10^{-5} with respect to H_2. A lesser fractional abundance of 5×10^{-6} for methane (CH_4), an important ingredient for forming complex organic species, has recently been derived (Öberg et al. 2008) (see Section 4.8 for further discussion on ices). As will become clear throughout this review, grain surface chemistry and ice evaporation play a central role in the formation and observation of saturated complex organic molecules.

A number of broad emission features in the infrared, arising from re-emission in regions with strong UV or visible radiation such as PDRs, have been convincingly assigned to vibrational bands from a class of species known as polycyclic aromatic hydrocarbons (PAHs), although the specific molecules have not been assigned (Allamandola, Tielens & Barker 1989; Léger, D'Hendecourt & Defourneau 1989). The PAHs are thought to be much larger than the gas-phase species detected by high-resolution spectroscopy; their estimated size ranges upward from 30 carbon atoms to more than 100 carbon atoms. There is some evidence that these species can coagulate to produce even larger clusters, which can also be thought of as one class of small particles of amorphous carbon (Kimura et al. 2007). There is also some weak evidence that the well-known but unassigned series of diffuse (broad) interstellar bands (DIBs) seen in the visible as starlight passes through diffuse interstellar matter may be caused by PAHs (Cox & Spaans 2006). Because PAHs and DIBs have been discussed recently (Snow & McCall 2006, Tielens 2008), we limit discussion here to the complex interstellar gas-phase species detected under high-resolution spectroscopic conditions and put them into context with other organics only briefly in Section 7.

1.2. Sources of Complex Molecules

The ≈50 complex organic molecules in the gas phase are listed in **Table 1**, divided into five categories depending upon the elements they contain. Also listed are the types of sources where, to the best of our knowledge, these complex molecules have been detected in our galaxy. The sources include circumstellar envelopes around evolved stars, cold interstellar cores, hot cores and corinos, lukewarm corinos, outflows, as well as other regions. These different types of sources can be associated with different types of complex organic molecules. No complex

Table 1 Complex organic interstellar molecules (≥ 6 atoms)

Species	Name	Source	Species	Name	Source
Hydrocarbons			**N-Containing**		
C_2H_4	Ethene	circ	CH_3CN	Acetonitrile	cc, hc, of
HC_4H	Butadiyne	circ	CH_3NC	Methylisocyanide	hc
H_2C_4	Butatrienylidene	circ, cc, lc	CH_2CNH	Keteneimine	hc
C_5H	Pentadiynyl	circ, cc	HC_3NH^+	Prot. cyanoacetylene	cc
CH_3C_2H	Propyne	cc, lc	C_5N	Cyanobutadiynyl	circ, cc
C_6H	Hexatriynyl	circ, cc, lc	HC_4N	Cyanopropynylidene	circ
C_6H^-	Hexatriynyl ion	circ, cc, lc	CH_3NH_2	Methylamine	hc, gc
H_2C_6	Hexapentaenylidene	circ, cc, lc	C_2H_3CN	Vinylcyanide	cc, hc
HC_6H	Triacetylene	circ	HC_5N	Cyanodiacetylene	circ, cc
C_7H	Heptatriynyl	circ, cc	CH_3C_3N	Methylcyanoacetylene	cc
CH_3C_4H	Methyldiacetylene	cc	CH_2CCHCN	Cyanoallene	cc
CH_3CHCH_2	Propylene	cc	NH_2CH_2CN	Aminoacetonitrile	hc
C_8H	Octatetraynyl	circ, cc	HC_7N	Cyanotriacetylene	circ, cc
C_8H^-	Octatetraynyl ion	circ, cc	C_2H_5CN	Propionitrile	hc
CH_3C_6H	Methyltriacetylene	cc	CH_3C_5N	Methylcyanodiacetylene	cc
C_6H_6	Benzene	circ	HC_9N	Cyanotetraacetylene	circ, cc
O-Containing			C_3H_7CN	N-propyl cyanide	hc
CH_3OH	Methanol	cc, hc, gc, of	$HC_{11}N$	Cyanopentaacetylene	circ, cc
HC_2CHO	Propynal	hc, gc	**S-Containing**		
c-C_3H_2O	Cyclopropenone	gc	CH_3SH	Methyl mercaptan	hc
CH_3CHO	Acetaldehyde	cc, hc, gc	**N,O-Containing**		
C_2H_3OH	Vinyl alcohol	hc	NH_2CHO	Formamide	hc
c-CH_2OCH_2	Ethylene oxide	hc, gc	CH_3CONH_2	Acetamide	hc, gc
$HCOOCH_3$	Methyl formate	hc, gc, of			
CH_3COOH	Acetic acid	hc, gc			
$HOCH_2CHO$	Glycolaldehyde	hc, gc			
C_2H_3CHO	Propenal	hc, gc			
C_2H_5OH	Ethanol	hc, of			
CH_3OCH_3	Methyl ether	hc, gc			
CH_3COCH_3	Acetone	hc			
$HOCH_2CH_2OH$	Ethylene glycol	hc, gc			
C_2H_5CHO	Propanal	hc, gc			
$HCOOC_2H_5$	Ethyl formate	hc			

Abbreviations: circ, circumstellar envelope around evolved star/protoplanetary nebula; cc, cold cloud core; hc, hot core/corino; lc, lukewarm corino; gc, galactic center cloud; of, outflow. Not all of these molecules fulfill the strict criteria for identification listed in Section 3.3.

molecules have yet been detected in protoplanetary disks, either in the gas or in the ice. The only complex molecules detected in external galaxies are methyl acetylene (CH_3CCH), methanol (CH_3OH), and acetonitrile (CH_3CN). Detection of the naphthalene molecular ion $C_{10}H_8^+$ has been recently claimed based on three broad UV features in the direction of the Perseus complex (Iglesias-Groth et al. 2008) in either a relatively diffuse interstellar or circumstellar environment. Throughout the remainder of the paper, we refer to the individual

complex molecules by name and chemical structure unless either has been used repeatedly; the confused reader can consult **Table 1** for the names and structures of all complex species.

In cold cores such as TMC-1, the chemistry tends to produce many exotic molecular species, including ions, radicals, and unsaturated organics such as the cyanopolyynes and the C_nH radicals (Ohishi & Kaifu 1998; Smith, Herbst & Chang 2004). The negative ions C_6H^- and C_8H^- have also been detected in TMC-1 (Brünken et al. 2007, McCarthy et al. 2006), as have some more saturated species, such as methanol (CH_3OH), acetaldehyde (CH_3CHO), and propylene (CH_3CHCH_2), all at fractional abundances of a few $\times 10^{-9}$ and below (Marcelino et al. 2007). The growth of molecular complexity appears to be less in many other cold cores, whether collapsing (prestellar), as in L1544, or not. The chemistry of the outer envelope of the carbon-rich AGB star IRC+10216 possesses a molecular inventory very similar to that of TMC-1 (Olofsson 2005), as does the protoplanetary nebula CRL 618 (Pardo et al. 2007). Like TMC-1, the envelopes of these evolved stars are poor in saturated organic molecules (Remijan et al. 2005b). Here we focus on cold cores and star-forming regions.

The complex molecular inventory of hot cores and corinos is dominated by saturated molecules such as methanol, methyl formate ($HCOOCH_3$), dimethyl ether (CH_3OCH_3), and propionitrile (CH_3CH_2CN), which can reach fractional abundances of 10^{-7}. Different hot-core sources can differ strongly in their molecular abundances (see **Figure 1**); perhaps the strongest differentiation occurs between two nearby sources in the Orion Molecular Cloud, a giant cloud located about 400 pc from the Earth and home to much high-mass star formation. The so-called compact ridge source is dominated by O-containing complex molecules, whereas the nearby Hot Core, only ~3000 AU offset, is dominated by N-containing organic molecules (Blake et al. 1987b). The richest molecular source in the galaxy is the hot core Sgr B2 (N), located in the Galactic Center giant cloud Sgr B2 and also called the Large Molecule Heimat (LMH) (Snyder 2006), which contains the organic species acetone (CH_3COCH_3), ethylene glycol [$(CH_2OH)_2$], glycolaldehyde ($HOCH_2CHO$), and others, including N-containing species. Chemical differentiation within hot cores/corinos and between hot corinos and hot cores has been suggested (see Section 4.6), although corinos are smaller and harder to detect, so that only a few examples are currently known, the best known of which is IRAS 16293–2422, a particularly rich but complex source (Ceccarelli 2005).

Other classes of sources also contain significant abundances of complex molecules. The so-called lukewarm corino L1527 ($T \approx 30$ K) contains a number of unsaturated complex species including negative molecular ions, but only about one third to one half of the number of molecules seen in TMC-1 (Sakai et al. 2007, 2008). There is strong evidence that the Central Molecular Zone of the Galactic Center contains a number of dense clouds rich in methanol (CH_3OH), methyl formate ($HCOOCH_3$), and some other oxygen-containing organics seen in hot cores (Requena-Torres et al. 2008), although these clouds are much lower in density than hot cores and tend to have lower rotational excitation temperatures and exceedingly low grain-surface temperatures. Some more exotic molecules such as acetamide (CH_3CONH_2) (Hollis et al. 2006) and keteneimine (CH_2CNH) (Lovas et al. 2006) have been seen at least partially in absorption in the direction of Sgr B2 (N). Although much of the Galactic Center may contain complex molecules, the same cannot be said of all giant molecular clouds. In particular, the Orion Molecular Cloud contains a large and well-studied cool ($T \approx 50$ K) source known as the quiescent ridge, which appears to contain only smaller molecules (Blake et al. 1987b). Previously known only as sources of methanol, outflows can possess more complex species, such as $HCOOCH_3$, CH_3CN, and ethanol (C_2H_5OH) (Arce et al. 2008). The well-studied PDR known as the Horsehead Nebula shows small hydrocarbons including C_4H in regions where the radiation field is high, but not yet longer chains (Pety et al. 2005). CH_3OH has been detected in the Orion Bar PDR (Hogerheijde, Jansen & van Dishoeck 1995).

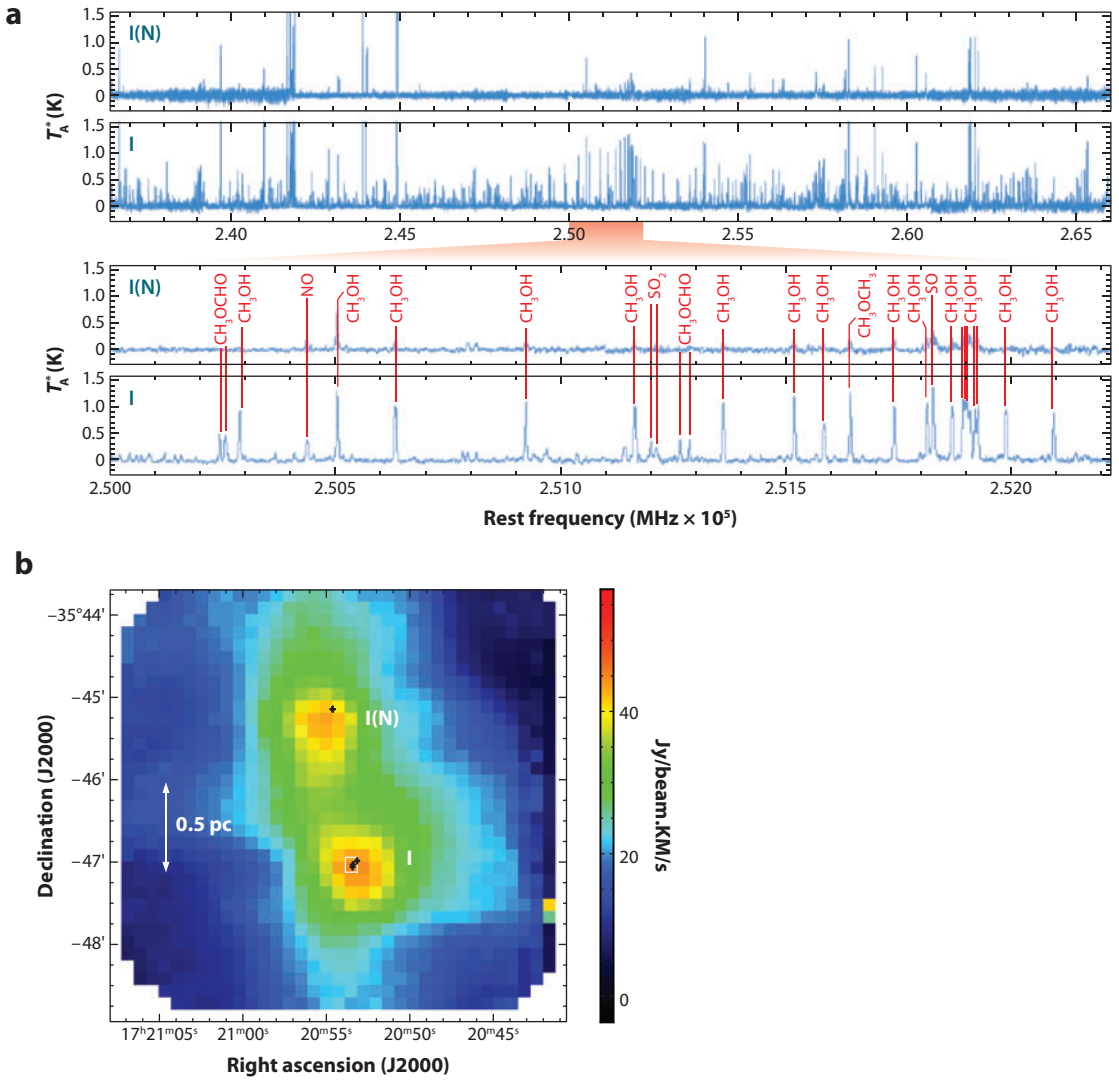

Figure 1

(*a*) Line surveys in the 1 mm atmospheric window toward two massive young stellar objects, I(N) (*top*) and I (*bottom*), in the NGC 6334 star-forming region ($d = 1.7$ kpc; $L \approx 1.1 \times 10^5\ L_\odot$), obtained with the Swedish-ESO Submillimeter Telescope. Note that complex organic molecules are only prominent toward the I source. (*b*) Map of NGC 6334 in the HCN 1–0 line (a tracer of gas with density $n_H \geq 10^6\ cm^{-3}$) obtained with the Mopra telescope (A.J. Walsh, S. Thorwirth, H. Beuther, M.G. Burton, in preparation) illustrating the two sources, which are separated by less than 1 pc. The black plusses mark the positions of CH_3OH masers. Figure based on Thorwirth et al. (2003), with permission.

2. RELEVANT LABORATORY SPECTROSCOPIC STUDIES AND DATABASES

2.1. Rotational Spectroscopy

Most of the detected gaseous interstellar and circumstellar molecules, and virtually all of the complex species listed in **Table 1**, have been observed via their rotational spectral lines. The

rotational spectra of large numbers of molecules have been studied by microwave spectroscopists in the laboratory starting from the late 1930s (Townes & Schawlow 1955). For many years, the preferred frequency range for study was from ≈1–40 GHz, with only selected groups working at higher frequencies, dubbed the millimeter-wave ($\nu \approx 30$–300 GHz; $\lambda \approx 0.10$–1.0 cm) and the submillimeter-wave ($\nu \approx 300$–1000 GHz; $\lambda \approx 0.03$–0.1 cm) (De Lucia et al. 1972). Although a number of groups now work up to 1000 GHz = 1 THz, studies at even higher frequencies, as pioneered by the Cologne group (Xu et al. 2008), which will be important for the *Herschel Space Observatory* and the *Stratospheric Observatory for Infrared Astronomy* (SOFIA), remain rare. Although ab initio quantum chemical calculations have been improving, they are still not capable of experimental accuracy, which is ≈1–10 kHz or even better with selected methods.

Rotational spectroscopists typically interpret their spectra with effective Hamiltonian operators that describe a quasi-rigid-body rotational motion in the presence of vibrational motions of higher frequency. For nonlinear molecules, known as tops, the operators are developed along the principal axes (a, b, c) of the molecule (Gordy & Cook 1984, Townes & Schawlow 1955). Nonlinear rotors can be subdivided into spherical tops, which possess three equal moments of inertia along the principal axes, symmetric tops, which possess two equal moments, and asymmetric tops, in which all three moments of inertia are different. The effective Hamiltonian is normally written as an expansion in terms of products of angular momentum operators raised to even powers that multiply so-called spectroscopic constants, or parameters. Although purely rigid molecules have only second-order terms in angular momenta (a total exponent of 2), nonrigidity is handled through the so-called centrifugal distortion terms, which start from fourth-order terms (a total exponent of 4). For asymmetric tops, the most common type of molecule and the most difficult to treat, diagonalization of the effective Hamiltonian matrix must be utilized to determine the energy levels and eigenkets. For all molecules, the energy levels can be written as a function of the spectroscopic constants, which consist of one or more of the so-called rotational constants, $A \geq B \geq C$, which are the inverses of the moments of inertia ($I_A < I_B < I_C$) in appropriate (frequency or wavenumber) units, and the centrifugal distortion constants. When present, interactions involving unpaired electronic spin and orbital angular momentum (fine structure) and nuclear spin angular momentum (hyperfine structure) split rotational energy levels into multiplets and can help in the identification of molecules.

Once the energy levels and eigenkets are obtained, the energy differences between pairs of levels connected by nonzero dipolar transition moments yield spectral line frequencies, whereas the dipolar matrix elements yield intensities. The selection rules depend on the direction of the dipole moment components; a-, b-, and c-type transitions pertain to dipole components along the a, b, c principal axes. The larger the molecules, the larger the moments of inertia, the smaller the rotational constants, and the more dense the spectrum. **Figure 2** illustrates simulated spectra of different types of molecules for typical excitation temperatures in hot cores. Variation of the rotational and centrifugal distortion constants to achieve the closest agreement with a subset of measured frequencies with assigned quantum numbers in a nonlinear least-squares approach yields the best initial values. The constants can then be used to predict the frequencies of other lines measured in the laboratory and, by inclusion of these new lines in the fit, obtain improved constants. Eventually, the constants can be used to predict lines not studied in the laboratory, although predictions that involve higher rotational quantum numbers than those measured are often inaccurate because more distortion constants are needed. Transitions involving larger rotational quantum numbers generally occur at higher frequencies than those involving smaller rotational quantum numbers; hence it is often difficult to predict higher frequency lines accurately. Thus, if the known spectrum of a molecule is measured only through 600 GHz, it is wise not to take predictions of most line frequencies around 1.5 THz too seriously.

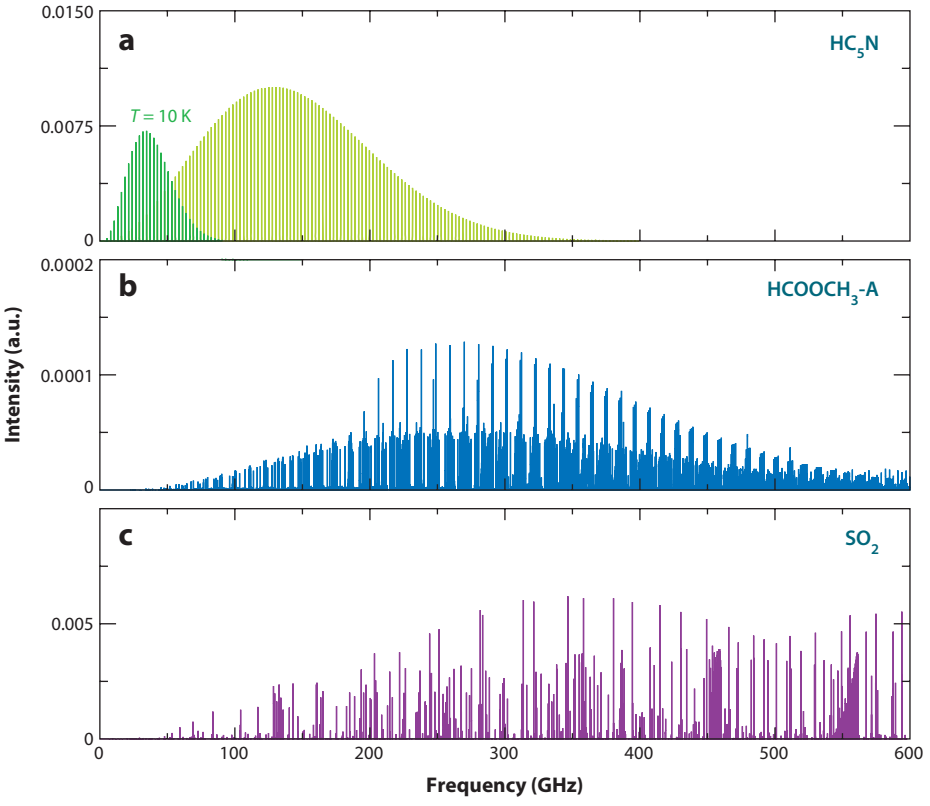

Figure 2

Simulated spectra (in arbitrary units) of (*a*) a linear rotor (HC_5N), (*b*) an asymmetric top with internal rotation ($HCOOCH_3$-A), and (*c*) a more rigid but heavy asymmetric top (SO_2). All spectra assume LTE excitation at a temperature of 150 K, typical of hot cores. For HC_5N, the spectrum for an excitation temperature of only 10 K is shown as well in darker green. Note the highly irregular spectrum of an asymmetric top like SO_2 compared with that of the linear molecule HC_5N, and the shift of peak intensity toward lower frequencies at lower excitation temperatures. Spectra provided by A. Walters using the CASSIS database and package.

Some of the more saturated complex molecules detected in the interstellar gas, such as methanol, have an additional large-amplitude motion known as torsion, or internal rotation (Gordy & Cook 1984). This motion complicates the rotational spectrum in several ways, including the existence of rotational spectra arising from thermally populated excited torsional levels, the splitting of torsional levels into sublevels, and the interaction of the torsion and quasi-rigid rotation. There are a variety of methods to analyze internal rotation spectra (Groner 1997, Kleiner & Hougen 2003, Pickett 1991). If the potential minima corresponding to torsional motion lie at different energies, the structures corresponding to the minima are known as conformers, with names such as *trans* and *gauche*.

The existence of populated torsional levels, the interaction of torsional and rotational motions, and the spectra of different conformers have the effect of increasing the density of spectral lines, which can be quite dense at 100–300 K for complex molecules in the millimeter-wave and submillimeter-wave regions even in the absence of torsional motion (**Figure 2**). In addition to CH_3OH, other internal rotors with many spectral lines in hot-core sources are methyl formate

($HCOOCH_3$) and dimethyl ether (CH_3OCH_3). Internal rotors and heavy species without internal rotation (e.g., propionitrile–C_2H_5CN) that have high fractional abundances in hot cores and corinos are often referred to as weeds. Although weeds are useful probes of physical conditions, their high abundances in hot cores lead to composite spectra that are sufficiently dense that identification of lines of potentially new molecules can be difficult, if not impossible. The problem of weeds is exacerbated by detectable abundances of isotopologues containing isotopes such as ^{13}C, and molecules in low-lying excited vibrational states unrelated to torsion.

The controversy involving the possible detection of the amino acid glycine (NH_2CH_2COOH), a species clearly associated with biology, illustrates the problem caused by weeds. Kuan et al. (2003) claimed to have detected 27 spectral lines of a conformer of glycine in the hot cores Sgr B2(N), Orion KL, and W51 e1/e2. The claim was disputed by Snyder et al. (2005), who concluded that the lines identified as due to glycine are more likely due to weeds such as C_2H_5CN, C_2H_3CN, and *gauche*-ethanol. The analysis of these researchers was based partially on the fact that the observation of some lines of a candidate species implies the existence of other lines, and that some intense lines of glycine were missing. The controversy raised the question of how many lines are needed for secure identification of a complex species via its rotational spectrum, an issue further discussed in Section 3.3.

The problem of weeds can be ameliorated if their spectral lines can in some manner be partially or totally removed from composite interstellar spectra so that the "flowers" can stand out. There are two approaches leading to this removal. The first involves the classical boot-strap approach of spectroscopists, in which lines are measured and assigned quantum numbers, then used to determine spectroscopic constants, which in turn can be used to predict the frequencies of many unmeasured or previously unassigned lines. Despite the many laboratory unidentified lines (U-lines), progress can be made, especially with databases (see Section 2.2). The second method is based on the idea that one can remove all lines of a given weed even if their spectral assignments (that is, quantum numbers) are unknown (Medvedev & De Lucia 2007). The method is currently being developed in the laboratory.

2.2. Databases

The assignment of interstellar molecular lines is made easier by the existence of spectral databases for rotational transitions. These compendia contain the quantal assignments, frequencies, and intensities of both measured and predicted rotational lines for many species. They have useful computer interfaces, so that astronomers can download single-molecule or composite spectra in assorted frequency ranges. The best known of the databases are the JPL Catalog (**http://spec.jpl.nasa.gov/home.html**), the Cologne Database for Molecular Spectroscopy (CDMS, **http://www.astro.uni-koeln.de/site/vorhersagen/**), and the Lovas/NIST database of recommended rest frequencies for known astronomical transitions (**http://physics.nist.gov/PhysRefData/Micro/Html/contents.html**). The relatively new CDMS database is a continuation of older databases, one of which, the Lovas/NIST catalog, has not been updated since 2002. A new database from Japan, known as the Toyama Microwave Atlas, has recently appeared (**http://www.sci.u-toyama.ac.jp/phys/4ken/atlas/**).

In addition to these, there are several new databases associated with telescopic projects or synthetic spectra. The *Splatalogue* Database for Astronomical Spectroscopy (Remijan, Markwick-Kemper, & ALMA Working Group on Spectral Line Frequencies 2007) (**http://www.splatalogue.net/**) contains data from the catalogs already mentioned as well as from the SLAIM source (Spectral Line Atlas of Interstellar Molecules), a publicly unavailable compilation of Lovas' spectroscopic analyses of molecules already detected in space. *Splatalogue* is VO

(virtual observatory)-compliant and can be queried under the IVOA SLAP standard. Another very interesting database is known as CASSIS (**http://www.cesr.fr/∼walters/web_cassis/index.html**); it allows users to "choose the most appropriate data and model to create a synthetic spectrum for the region to be studied" (see **Figure 2** for examples). As with *Splatalogue*, the spectral data come mainly from the standard databases. According to the current manual, both local thermodynamic equilibrium (LTE) and large velocity gradient (LVG) models can be chosen (see also Section 3). A version of the popular Grenoble CLASS line data analysis system called XCLASS has been developed by P. Schilke (following initial work by T. Groesbeck) to include the JPL and other databases to interactively identify features in spectra and create synthetic spectra for overlay. Such analyses give investigators a sense of which features of the composite spectra are carried by weeds and whether they can be removed (see above).

The spectral databases tend to be incomplete for a variety of reasons. There is little external funding for such projects and therefore new additions to the catalogs are likely to come slowly. In addition, the databases are somewhat biased toward existing interstellar species, so that astronomers searching for exotic or unusual molecules may not find their spectra. Finally, the database contributors tend not to list data without some reanalysis, in part so that incorrect assignments can be eliminated before listing. This cautious approach has on occasion hindered the inclusion of data from internal rotors, since specific expertise in complex methods of analysis is often needed. Even if absent or partially absent from databases, internal rotor data can be found in original references, such as the most recent study of methanol (Xu et al. 2008) through terahertz (THz) frequencies, and studies of methyl formate, a ^{13}C isotopologue, and the $v_t = 1$ excited torsional state through 600 GHz (Carvajal et al. 2007, Kobayashi et al. 2007, Maeda et al. 2008, Willaert et al. 2006). As our knowledge of the spectra of important interstellar molecules spreads into the THz region, a similar degree of knowledge for rotational spectra of their major isotopologues and excited torsional and even vibrational states is still needed.

As an example of the incompleteness of catalogs even at lower frequencies, a recent 80–280 GHz IRAM-30m line survey of Orion-KL by B. Tercero & J. Cernicharo (in preparation) reveals ∼16,000 lines of which ∼8000 were unidentified in 2005. Two years later, thanks to new laboratory data on just two molecules—CH_3CH_2CN and CH_2CHCN—together with their isotopes and vibrationally excited states, the number of U-lines has been reduced to ∼6000. Significantly more laboratory work is needed to speed up this process.

3. TECHNIQUES OF OBSERVATIONAL ANALYSIS

3.1. Rotation Diagrams

Owing to improvements in detector technology and the availability of telescopes on high and dry sites, observations of individual spectral lines of complex molecules at (sub)millimeter wavelengths have become quite routine. A single-frequency setting covering up to a GHz of bandwidth can take as little as a few minutes of telescope time before the confusion limit is reached on strong sources. Although getting a complete, well-calibrated spectral survey across an atmospheric window is still a significant observational effort, especially at the higher frequencies (**Figure 3**), the main challenge actually lies in the analysis of the thousands of lines that are readily obtained. This procedure starts with line identification using the catalogs described in Section 2.2. In the case of spectra taken in double-sideband mode (DSB), a deconvolution first has to be performed to obtain single-sideband spectra. In case of severe line blending, care has to be taken not to produce any ghosts in the deconvoluted spectra (see **Figure 3**, insert). Another observational issue is that spectral survey data are usually taken over different observing nights, sometimes months or even

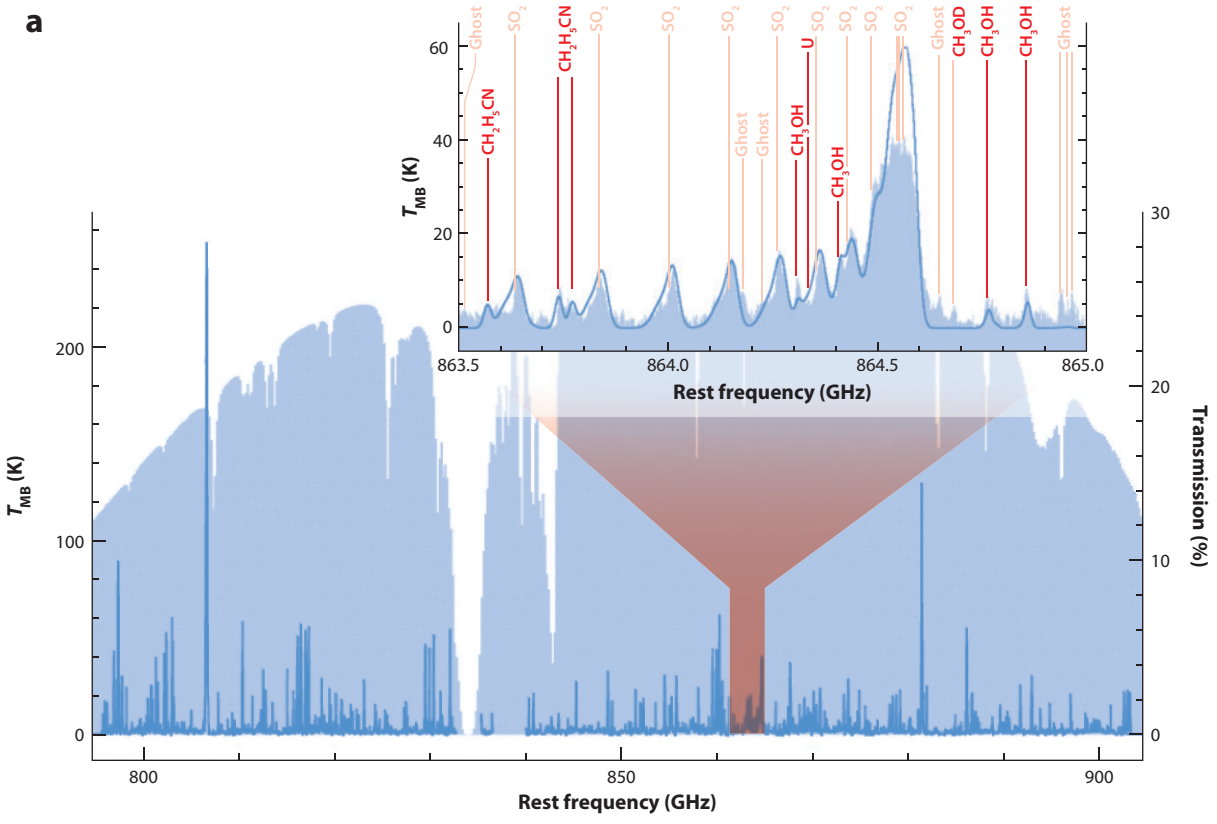

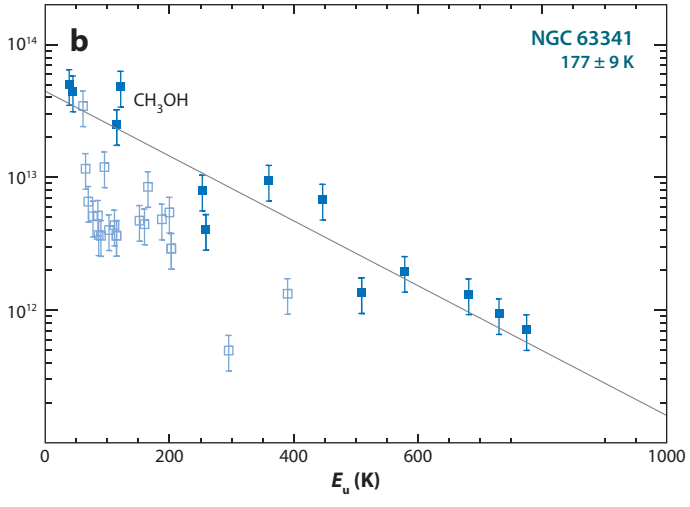

years apart. Small pointing offsets of observations taken on different dates can lead to varying intensities across the frequency window that, together with the intrinsic calibration errors, can lead to overall uncertainties of 20–30%.

The translation of the observed intensities to physical parameters (temperature, densities) and chemical abundances requires a determination of the excitation of the molecule and an understanding of how the photon is produced in the cloud and how it makes its way from the cloud to the telescope. If it is assumed that (*i*) the lines are optically thin, (*ii*) the level populations can be characterized by a single excitation temperature $T_{\rm rot}$, and (*iii*) the source is homogeneous and fills the telescope beam, the measured integrated main beam temperature $\int T_{\rm MB} dV$, typically in K km s^{-1}, can be related to the column density N_u in the upper level u by

$$N_u/g_u = \frac{N_{\rm tot}}{Q(T_{\rm rot})} e^{-E_u/T_{\rm rot}} = \frac{3k \int T_{\rm MB} dV}{8\pi^3 \nu \mu^2 \mathcal{S}}, \quad (1)$$

where g_u is the statistical weight of level u, $N_{\rm tot}$ is the total column density of the molecule, $Q(T_{\rm rot})$ is the rotational partition function, E_u is the energy of the upper level, k the Boltzmann constant, ν the transition frequency, μ the permanent dipole moment, and $\mathcal{S}$ the intrinsic line strength (e.g., Blake et al. 1987a, Turner 1991). Thus, a logarithmic plot of the quantity on the right-hand side as a function of E_u should provide a straight line with slope $-1/T_{\rm rot}$ and intercept $N_{\rm tot}/Q(T_{\rm rot})$. For diatomic molecules and linear rotors, the intrinsic molecular parameters are $\mathcal{S}(J) = J$ and $Q(T) = kT/hB$ in the high-temperature limit $hB \ll kT$, with B the rotational constant ($h/8\pi^2 I$ where I is the moment of inertia), and h the Planck constant. For nonlinear molecules, the formulae for $\mathcal{S}$ and Q become more complex (Townes & Schawlow 1955). Care should be taken to use internally consistent definitions of $\mathcal{S}$ and Q, especially for molecules with nuclear spin and internal rotation degeneracies. The above equation assumes that the vibrational partition function can be set to unity. For the large molecules discussed in this review, some vibrational levels become significantly populated even at 100–200 K and have to be included in the formulae.

3.2. Pitfalls and Uncertainties

This so-called rotation diagram method is by far the most widely used method to analyze spectra of complex molecules, but many of the underlying assumptions are often not valid. Lines of common molecules like CH_3OH and CH_3CN are usually optically thick, which will lead to an overestimate of $T_{\rm rot}$ and an underestimate of $N_{\rm tot}$. This problem can be corrected by using an escape probability formulation, in which the intensities are multiplied by a factor $C_\tau = \tau/(1 - e^{-\tau})$. An estimate of the optical depth τ can be obtained either from the total column density itself or through

Figure 3

(*a*) Line survey of Orion–KL in the 850 GHz (0.35 mm) atmospheric window obtained with the Caltech Submillimeter Observatory. The spectrum has been reconstructed from ∼300 double-sideband scans. The light blue area in the 800–900 GHz panel indicates the atmospheric transmission at these frequencies (right-hand vertical scale), which is at most 30% for good weather conditions on Mauna Kea (1 mm precipitable water vapor). The strongest lines in the Orion spectrum are due to CO, CH_3OH, SO_2, and SO. The blow-up from 863.5–865 GHz illustrates various lines, as well as some ghosts produced by the deconvolution method. Figures taken from Comito et al. (2005), with permission. (*b*) Rotation diagram of CH_3OH for NGC 6334 I based on Bisschop et al. (2007b), with permission. The rotation temperature is a fit to the optically thin lines only (shown in *blue*).

observations of isotopic lines, but it varies from line to line. Alternatively, the strongest lines can simply be discarded and only lines with small $\mu^2\mathcal{S}$ values or from optically thin isotopes can be taken into account in the rotation diagram (**Figure 3*b***).

The assumption that the source fills the beam is certainly not true for hot cores; here the observed antenna temperatures have to be corrected by the ratio of the solid angle of the antenna beam to that of the source, also called the dilution factor, Ω_a/Ω_s. Since hot cores are typically only $\sim 1''$ on the sky and single-dish beams are of order $15''$–$30''$, the correction factor can be more than a factor of 100. This effect, in turn, also increases the inferred optical depths. A variation on this theme is the situation in which there are multiple temperature components in the beam, or, as for YSOs, temperature and density gradients through the envelope. In this case, the filling factor of the emission becomes smaller with increasing excitation conditions, which leads to an artificial decrease in measured $T_{\rm rot}$. In some cases, two-temperature fits have been made to the rotation diagram to partly mitigate this problem, giving a "cold" and a "hot" component.

In the case of complete thermalization (that is, high densities), the rotational temperature should equal the kinetic temperature T_k. In the simplest case of a two-level system, the critical density for thermalization is $n_{\rm cr} = A_{u\ell}/q_{u\ell}$, where $A_{u\ell}$ is the Einstein A coefficient for spontaneous emission and $q_{u\ell}$ the rate coefficient for collisional de-excitation. Since $A_{u\ell}$ is proportional to $\mu^2\nu^3$ and since $q_{u\ell}$ does not vary much with energy level, $n_{\rm cr}$ increases steeply with frequency ν. Since the rotational energy level separation of (linear) molecules is proportional to the quantum number J, the higher-frequency, higher J transitions require higher densities and temperatures to be thermalized. For example, the critical density of the HC_3N $J = 10$–9 transition at 91 GHz is $\sim 10^5$ cm^{-3} ($E_u = 24$ K), whereas that of the 27–26 transition at 245 GHz is $\sim 2 \times 10^6$ cm^{-3} ($E_u = 165$ K). Thus, the higher-frequency transitions are more readily subthermally excited. As an extreme example, Johnstone, Boonman & van Dishoeck (2003) show that for CH_3OH at $T_k = 100$ K, the rotation diagram method using data in the 230 and 345 GHz atmospheric windows gives $T_{\rm rot}$ ranging from only 25 to 80 K even for densities as high as 10^7–10^9 cm^{-3}. The low excitation temperatures for CH_3OH of 10–20 K found in, for example, outflow or shocked regions therefore do not need to imply low kinetic temperatures but can simply be due to low densities, $<10^5$ cm^{-3} (e.g., Bachiller et al. 1995). Similarly, molecules in clouds in the Central Molecular Zone of the Galactic Center have rotation temperatures of at most 20 K, whereas kinetic temperatures are at least 100 K (e.g., Requena-Torres et al. 2006).

Lines can also be pumped by mid- or far-infrared radiation to give $T_{\rm rot} > T_k$. Well-known examples are HNCO (Churchwell et al. 1986) and b-type transitions of species like NH_2CHO, C_2H_3CN, and CH_3CHO (Nummelin et al. 2000). At centimeter wavelengths, strong radio continuum emission can invert the populations of the lowest rotational transitions of heavy rotors, thus boosting their intensities. This is certainly the case toward Sgr B2 where the radio continuum is extended and even fills large radio beams. It may be one of the reasons why so many complex species were first detected at low frequencies toward Sgr B2 (Menten 2004). Altogether, it is not surprising that rotational diagrams always show some degree of scatter around a single temperature because of different critical densities, optical depths, and special pumping mechanisms.

The rotation diagram method provides only column densities of the molecules. To obtain abundances relative to H_2, necessary to compare different regions with each other and with models, some tracer of the total gas column along the line of sight needs to be used (**Figure 4**). Traditionally, lines of optically thin isotopes of CO such as $C^{18}O$ or $C^{17}O$ have been adopted, assuming that the abundance of CO with respect to H_2 is constant at about 10^{-4}. It is now well established, however, that CO may have a very different abundance distribution throughout the source from that of the complex molecules and that CO freeze-out onto grains in the colder regions can significantly affect

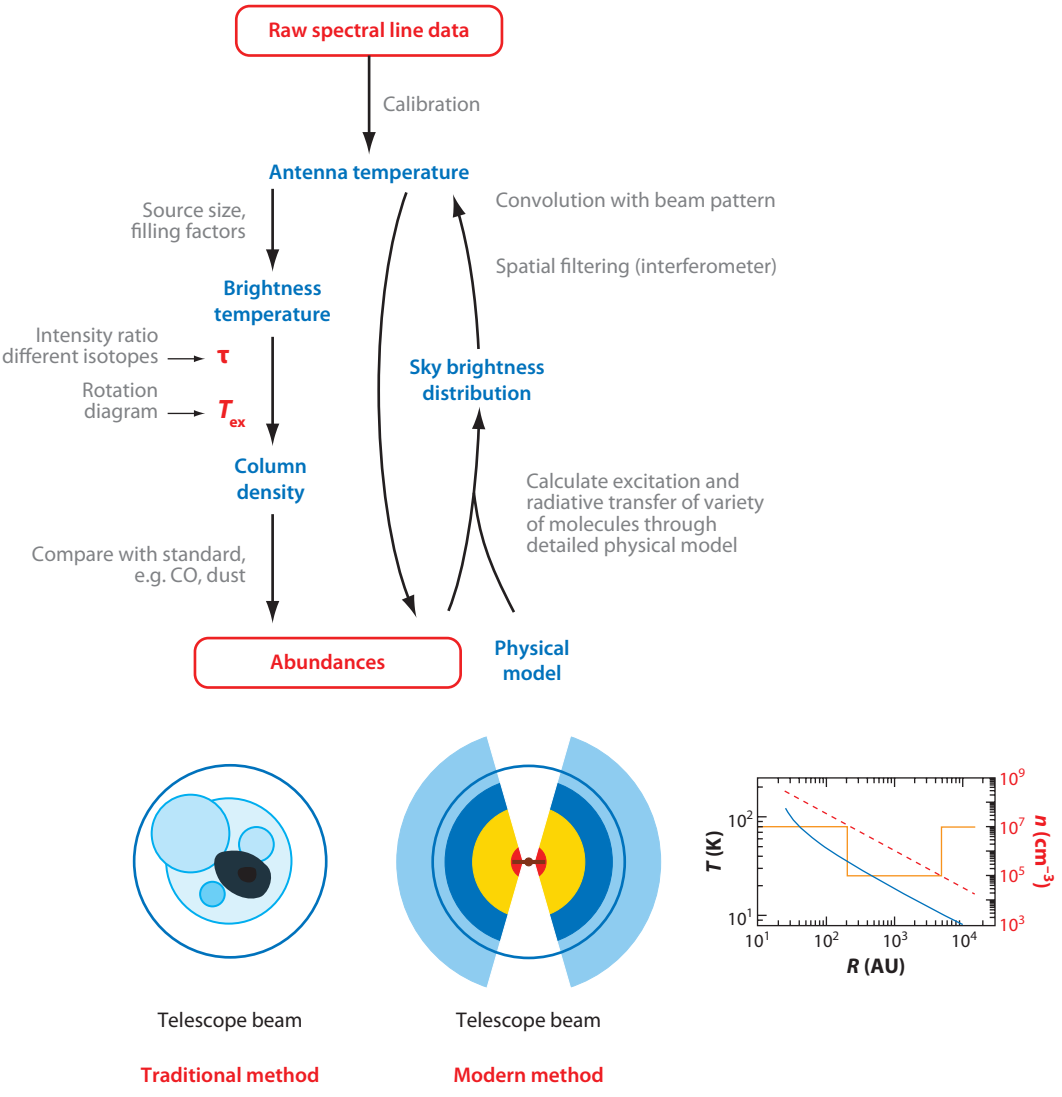

Figure 4

Traditional method for deriving column densities and abundances using the rotation diagram method compared with the more modern way of inferring abundance profiles using a full physical model of the source. Figure based on van Dishoeck & Hogerheijde (1999). The right-hand bottom graph indicates the typical temperature and density structure of the envelope around a Class 0 low-mass protostar as function of radius *R* (Jørgensen, Schöier & van Dishoeck 2005b). The orange step-function indicates the likely abundance profile, with freeze-out in the cold and dense middle region of the envelope and a jump in abundance in the inner "hot core" at the sublimation temperature. The dark blue circle indicates the telescope beam.

the results. A related point is that total gas column densities depend on the angular resolution of the tracer observations and do not necessarily scale in the same way as those of complex organics with increasing spatial resolution.

One step beyond the rotation diagram method is to calculate the steady-state non-LTE excitation of the molecule. Because the level of excitation is intimately coupled with the line radiative transfer (photons emitted at one position can be absorbed by a molecule elsewhere in the

cloud), this calculation needs to be coupled with a simple large-velocity-gradient (LVG) or escape probability radiative transfer method for a given set of temperatures and densities. The column density is then varied until a good fit to all lines is obtained. The physical parameters can be constrained from ratios of lines of the same or another molecule: Some sets of lines are good temperature probes whereas others are good density diagnostics (for a summary, see Genzel 1992, van der Tak et al. 2007). This method has been used to analyze the W3 line survey by Helmich & van Dishoeck (1997) and has most recently been applied to observations of CH_3OH in a variety of sources, where the physical conditions and column density are fitted simultaneously (Leurini et al. 2007). However, these parameters are not independent and variations throughout the source occur, with low-excitation lines arising in the cold region and high-excitation lines in the warm dense gas. If a low density of, say, 10^5 cm^{-3} is then used to fit a high excitation line, the column density can easily be overestimated by more than an order of magnitude.

The best way to analyze molecular line data is to build a good physical model of the source first, then compute the full non-LTE statistical equilibrium excitation of the molecule through this physical structure, calculate the emerging radiation from the source using nonlocal radiative transfer, convolve the simulated emission with the telescope beam or sample it with exactly the same baselines as the interferometer, and then compare with observations (see **Figure 4**). The adjustable parameter is the abundance of the molecule, which is varied until agreement with observations is reached. The physical model can be constrained by a variety of data; the most recent models use the submillimeter continuum maps coupled with the spectral energy distribution (SED) to constrain the dust temperature and density structure and assume that the gas temperature is equal to the dust temperature (for an example, see **Figure 4**, *bottom right*). For molecules with many observed lines originating from a wide range of energy levels, even the abundance profile through the source can then be determined. In its simplest form, this profile has a "jump" or "drop" at specific temperatures in the source where molecules can sublimate from the grains or freeze out. Abundance jumps by at least two orders of magnitude around the ~100 K ice sublimation radius have been inferred for CH_3OH in both high- and low-mass sources (e.g., Maret et al. 2005; Schöier et al. 2002; van der Tak, van Dishoeck & Caselli 2000).

This method requires the availability of collisional rate coefficients to compute the changing excitation through the source. Unfortunately, reliable molecular data are available for only one complex organic molecule, CH_3OH (Pottage, Flower & Davis 2004), and even there only for *E*-type sublevels in collisions with H_2 in its $J = 0$ state (see summary in Schöier et al. 2005) (**http://www.strw.leidenuniv.nl/~moldata**). Thus, for complex molecules, the only alternative is to assume LTE excitation with rotational temperatures equal to, or a fraction of, the kinetic temperature throughout the source.

A quantitative comparison of all three methods—rotation diagram, simple non-LTE excitation, and full physical model—has been done for only one source, IRAS 16293–2422 (Schöier et al. 2002, van Dishoeck et al. 1995). If the physical parameters are judiciously chosen, all three methods give beam-averaged abundances typically within a factor of 2, although excursions up to an order of magnitude are found. The error made by the assumption of a constant abundance (or, equivalently, a large source size for hot gas) or low optical depth is generally much larger. Also, not all molecules may be colocated within the observing beam. Because of the difficulties in deriving absolute abundances, observers often also give abundances relative to another molecule that is thought to have the same source size, excitation, and distribution as the molecule of interest. Methanol is often used as the reference for abundances of complex organic molecules.

3.3. What Constitutes a Firm Detection?

As discussed in Section 2 and illustrated in **Figure 2**, the spectrum of even a single complex molecule like $HCOOCH_3$-A can contain thousands of lines in the atmospheric windows. Thus, a collection of complex molecules as present in hot cores rapidly leads to confused spectra, especially in sources with intrinsically broad lines such as Sgr B2 [see figures 2 and 3 of Ziurys & Apponi (2005)], and identification of larger or minor species in between these "weeds" becomes a problem.

The currently accepted procedure for unequivocally identifying new molecules requires that at least the following criteria are met (Belloche et al. 2008, Snyder et al. 2005, Ziurys & Apponi 2005): (*i*) Rest frequencies are accurately known to $1{:}10^7$, either from direct laboratory measurements or from a high-precision Hamiltonian model; (*ii*) observed frequencies of clean, nonblended lines agree with rest frequencies for a single well-determined velocity of the source; if a source has a systematic velocity field as determined from simple molecules, any velocity gradient found for lines of a new complex molecule cannot be a random function of transition frequency; (*iii*) all predicted lines of a molecule based on an LTE spectrum at a well-defined rotational temperature and appropriately corrected for beam dilution are present in the observed spectrum at roughly their predicted relative intensities. A single anticoincidence (that is, a predicted line missing in the observational data) is a much stronger criterion for rejection than hundreds of coincidences are for identification. This last criterion is one of the strongest arguments for complete line surveys rather than targeted line searches.

Other criteria to strengthen the case for identification are to (*iv*) simulate the entire spectrum of a source using all identified molecules to check consistency and separate out contaminating blended features; and to (*v*) obtain interferometric images of the source and show that all lines of the new molecule originate from the same location. While full interferometric spectral surveys have to wait for the ALMA era, Belloche et al. (2008) used IRAM-Plateau de Bure images of 5 of their 88 blend-free lines to confirm their amino acetonitrile (NH_2CH_2CN) identification in Sgr B2(N). It is important that the less definitive identifications of complex molecules listed in **Table 1** be confirmed by at least some of the criteria discussed here.

4. OBSERVATIONS AND LINE SURVEYS

Ever since the first dedicated millimeter telescopes were built in the early 1970s, massive star-forming regions such as Orion-KL ($d \approx 400$ pc) and Sgr B2 ($d \approx 8$ kpc) have been prime targets for line surveys owing to their strong molecular lines (e.g., Cummins, Linke & Thaddeus 1986; Johansson et al. 1984; Turner 1991). Even though these surveys were carried out at low frequencies with large beams (typically 1′) and were not always centered on what we now know to be the positions of the YSOs, they emphasized the chemical richness of these sources and contributed hugely to the inventory of complex organic molecules. Of the many early surveys, one stands out: the Owens Valley Radio Observatory 1 mm survey of Orion-KL by Sutton et al. (1985) and Blake et al. (1987b). This survey was particularly influential not only because of the high quality of the observations but primarily because the data were accompanied by a detailed physical and chemical analysis.

The advent of large aperture (sub)millimeter telescopes equipped with heterodyne receivers close to the quantum limit has stimulated new and deeper surveys. Compared with the older data, the recent surveys refer to smaller beams of 10″–20″ that allow nearby sources to be observed separately [e.g., Orion hot core and compact ridge; Sgr B2(N) and (M)]. The high-frequency data measure higher-lying rotational transitions, thus probing directly the warmer and denser gas close to the YSO and rich in complex organic molecules rather than the extended cloud. Also, a much

larger variety of high-mass and low-mass objects has now been observed. **Table 2** summarizes single-dish (sub)millimeter surveys over the past 15 years, whereas **Figures 1** and **3** illustrate the richness of the line spectra. In the most extreme case of Orion, the lines contribute 50% or more of the broadband continuum at 350–650 GHz. Unfortunately, a significant fraction of these surveys are not yet published in the refereed literature, an illustration of the huge effort needed to go from observations to data analysis (see Section 3). A prime goal for the future should be to make the reduced and calibrated line survey data publicly available; this will be crucial input information for planning and analyzing data to be obtained with major new facilities such as *Herschel* and ALMA.

Millimeter arrays have been operational since the early 1990s but the number of interferometric chemical studies has been limited owing to the very long observing times needed to image even a single molecular line at high angular resolution. The SubMillimeter Array (SMA) with its 2 GHz broad bandwidth correlator is a major step forward because many molecules can be imaged simultaneously; other arrays with upgraded bandwidths will follow soon. This is particularly powerful for massive YSOs that have a plethora of strong lines in any frequency range (Beuther et al. 2006, Brogan et al. 2007) (see **Figure 5**).

The uncertainties and pitfalls in the derivation of molecular abundances have been amply discussed in Section 3. In the following discussion, only source averaged abundances are cited and compared; where needed, literature data have been corrected for (estimated) source size. Another cautionary note is that not all complex organic molecules are colocated so that abundance ratios derived from unresolved single-dish data have only limited meaning. Until the advent of full line surveys with ALMA (∼2013), this will remain an issue.

4.1. Cold Cores

Most studies of complex organic species in cold clouds have focused on the southern part of the core TMC-1 in Taurus, serendipitously discovered in the 1970s as a source with particularly strong lines of long carbon chains. All of the complex organic molecules in **Table 1** labeled with "cc" have been detected in TMC-1, many there for the first time. **Figure 6** shows the full 8.8–50.0 GHz line survey obtained with the 45m Nobeyama Radio Telescope (Kaifu et al. 2004). Of the 414 lines, only one remains unidentified. Targeted deeper line searches continue to reveal new molecules, such as the recently discovered more saturated propylene CH_3CHCH_2 (Marcelino et al. 2007), the carbon chain CH_3C_6H (Remijan et al. 2006), and the anions C_6H^- and C_8H^- (see Section 2).

How exceptional is TMC-1 in terms of long carbon chains? Suzuki et al. (1992) carried out a seminal survey of key molecules such as HC_5N toward a large number of cold clouds, including some cores that are now called "prestellar," with strong central density concentrations (e.g., L1498, L1544). When detected, the ratios of carbon chains such as HC_5N/HC_3N are rather constant at 3 ± 2. In contrast, the HC_5N/NH_3 ratio varies by more than two orders of magnitude between the clouds, with TMC-1 having the highest ratio at ∼0.3. Even across the TMC-1 core itself, which is known to be composed of small cloudlets, HC_7N/NH_3 varies by a factor of more than 30 on scales as small as 0.3 pc (e.g., Olano, Walmsley & Wilson 1988). Thus, models to explain the high abundances of complex organics toward the southern part of TMC-1 invoke some special condition (e.g., fresh injection of atomic carbon, an elemental abundance ratio C/O greater than unity) or time (early evolutionary state) compared with other cold clouds (see Section 5).

More recent studies have focused on ratios of long carbon chains with respect to a shorter chain, CCS, a molecule that is readily detected in cold clouds (e.g., Hirota, Maezawa & Yamamoto 2004; Hirota & Yamamoto 2006). The CCS line intensities are comparable with those of TMC-1, but the long carbon chains are weaker. Variations of carbon chains with respect to CCS are even seen

Table 2 Overview of recent unbiased (sub)millimeter line surveys of young stellar objects

Object	Frequency range (GHz)	Telescope	Reference
Orion-KL	80–115.5, 130–179	IRAM 30m	Tercero, Cernicharo & Pardo (2005)
	138.3–150.7	TRAO	Lee, Cho & Lee (2001)
	130–170	NRAO	Remijan et al. (2008b)
	197–281	IRAM 30m	Tercero, Cernicharo & Pardo (2005)
	260–328	CSO	Yoshida & Phillips (2005)
	325–365	CSO	Schilke et al. (1997)
	486–492, 541–577	ODIN	Persson et al. (2007)
	455–507	JCMT	White et al. (2003)
	607–725	CSO	Schilke et al. (2001)
	795–903	CSO	Comito et al. (2005)
Orion-S	130–170	NRAO	Remijan et al. (2008b)
	325–365	CSO	Groesbeck (1995)
SgrB2 (N,M,NW)	80–116	IRAM 30m	Belloche et al. (2007)
	65–116, 130–180	ARO 12m	Halfen & Ziurys (2008)
	130–170	NRAO	Remijan et al. (2008b)
	218–263	SEST	Nummelin et al. (2000)
	210–280	SMT	Halfen & Ziurys (2008)
	0.30–50	GBT	Remijan et al. (2008a)
AFGL 2591	332–373	JCMT	Plume et al. (2007)
G327.3–0.6	213–315, 335–362	APEX	Bisschop et al. (in preparation)
G34.3+0.15	84.7–115.7	TRAO	Kim et al. (2000)
	123.5–165.3	TRAO	Kim et al. (2000, 2001)
	330–360	JCMT	MacDonald et al. (1996)
G5.89–0.39	330–360	JCMT	Thompson & MacDonald (1999)
IRAS 16293–2422	80–280	IRAM 30m	Caux et al. (2005)
	328–366	JCMT	Caux et al. (2005)
IRAS 20126+4104	332–373	JCMT	Plume et al. (2007)
IRAS 23385+6053	330–360	JCMT	Thompson & MacDonald (2003)
NGC 1333 IRAS4	332–373	JCMT	Plume et al. (2007)
NGC 6334 I, I(N)	85–115, 133–160, 211–267	SEST	Thorwirth et al. (2007)
TMC-1	8.8–50	Nobeyama 45m	Kaifu et al. (2004)
W3 IRS5, IRS4	84.7–115.6	TRAO	Kim et al. (2006)
W3 (OH/H_2O)	130–170	NRAO	Remijan et al. (2008b)
	334–365	JCMT	Helmich & van Dishoeck (1997)
W49	332–373	JCMT	Plume et al. (2007)
W51M	130–170	NRAO	Remijan et al. (2008b)

*Only (nearly) complete spectral surveys within an atmospheric window obtained with heterodyne instruments ($R > 10^6$) since 1994 are listed. There are numerous additional partial line surveys or far-infrared surveys at lower spectral resolution in the literature (van Dishoeck 2001). APEX, Atacama Pathfinder Experiment 12m; ARO, Arizona Radio Observatory Kitt Peak 12m; CSO, Caltech Submillimeter Observatory 10m; GBT, Green Bank Telescope 100m; IRAM, Institute Radio Astronomie Millimetrique 30m; JCMT, James Clerk Maxwell Telescope 15m; NRAO, National Radio Astronomical Observatory 12m, now called ARO 12m; SEST, Swedish-ESO Submillimetre Telescope 15m; SMT, ARO SubMillimeter Telescope 10m; TRAO, Taeduk Radio Astronomy Observatory 14m.

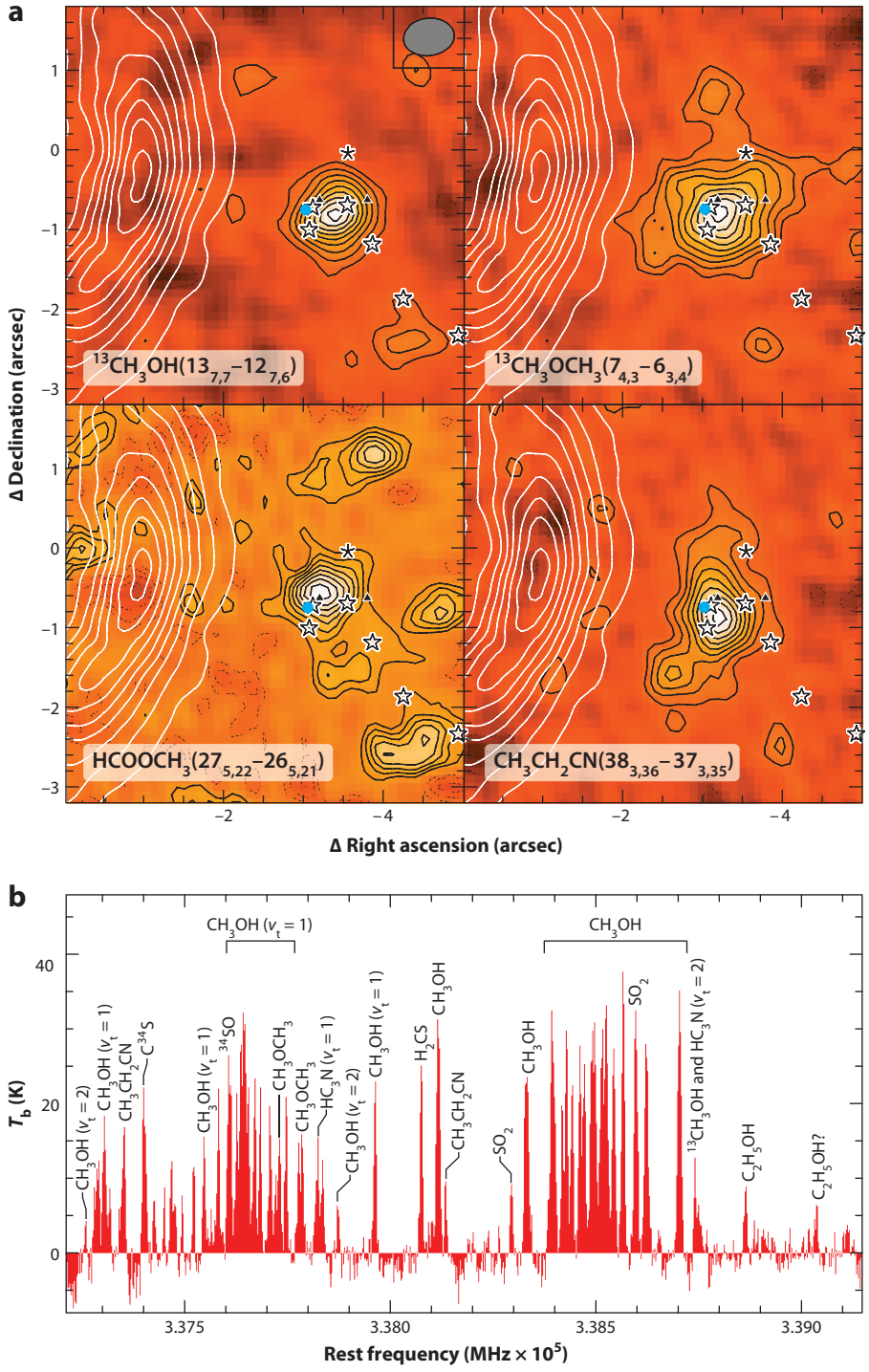

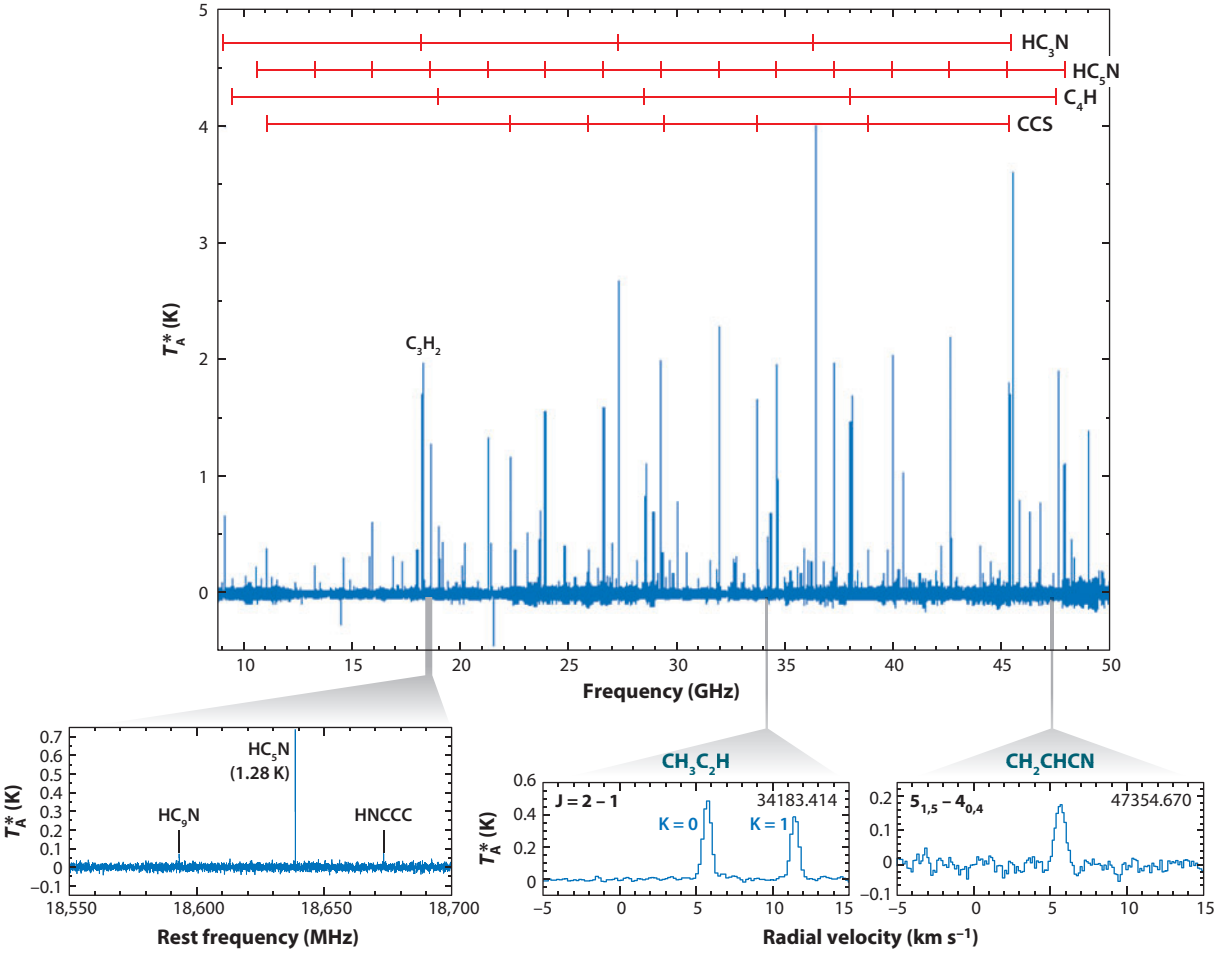

Figure 6

Line survey of the cold core TMC-1 ($d = 140$ pc) obtained in the 7-mm atmospheric window with the Nobeyama 45-m telescope. Note the prominent lines of long carbon chains. Figure based on Kaifu et al. (2004) with permission, and provided by M. Ohishi.

←

Figure 5

(*a*) Images of selected complex molecules obtained with the SubMillimeter Array toward the hot core G29.96–0.02 ($d \approx 6$ kpc, $L \approx 10^5\ L_\odot$) at subarcsec resolution of $0.64'' \times 0.47''$ (~3500 AU). The colors and black contours indicate the molecular emission, with contour values ranging from 15% to 95% of peak emission in steps of 10%. The white contours indicate the ultracompact (UC) HII region, whereas the white filled stars mark the submillimeter continuum peaks. The purple triangles mark the positions of the H_2O peaks, the light blue circles show the H_2CO maser, and the black star shows the mid-infrared peak emission. A CH_3OH maser is located close to the latter position. Note that none of the molecules peak on the UC HII region, and that they all have slightly different distributions, illustrating the need for high spatial resolution data. (*b*) Part of the interferometric spectrum toward G29.96–0.02, toward the peak molecular emission. Note that—in contrast with single-dish data—the vibrationally excited lines of CH_3OH are as strong as the ground-state lines. Figure based on Beuther et al. (2007), with permission.

within TMC-1 itself, with HC_7N/CCS changing by a factor of 3 to 5 on a 0.03 pc scale (Dickens, Langer & Velusamy 2001).

How about more saturated complex organic molecules? Methanol has been detected toward TMC-1 and a large number of other cold clouds, including even translucent ones (Friberg et al. 1988, Turner 1998), at abundances of a few $\times 10^{-9}$, well below its normal abundance in hot cores. Otherwise, observations are scarce. Acetaldehyde (CH_3CHO) is seen in TMC-1 and L134N at a fractional abundance less than 10^{-9}. Acetonitrile (CH_3CN) is seen in a few sources with CH_3CN/CH_3OH ratios of ~0.1, comparable with those found in hot cores (Turner, Terzieva & Herbst 1999). Dimethyl ether (CH_3OCH_3) has been detected toward at least one core, L183 (also known as L134N) (Friberg et al. 1988), but deep searches for C_2H_5OH and $HCOOCH_3$ have not revealed any lines (Requena-Torres et al. 2007). The upper limits on their abundances with respect to CH_3OH are comparable with those found for hot cores (see **Table 3**).

4.2. Outflows

When outflows from young stars impact the surrounding molecular cloud, they can destroy grain material and/or liberate ices, depending on the strength of the shock. Also, the high temperatures in the shock, up to a few thousand K, can drive chemical reactions not present in cold gas. Line surveys of shocks therefore provide an alternative way to probe the ice composition of cold clouds and any subsequent high temperature chemistry.

Methanol is readily detected in outflows of nearby low-mass YSOs at locations where the outflow can be spatially separated from the protostar itself. The fractional abundances of 10^{-6}–10^{-5} with respect to H_2 are orders of magnitude higher than those found in cold cores (Section 4.3) but consistent with sputtering of ices off the grains (Bachiller et al. 1995, Jørgensen et al. 2004). Because the total column densities of shocked gas are much lower than those toward the YSOs themselves, searches for other complex organics in shocks require very long integration times. A recent very deep search toward peak B1 in the blue lobe of the L1157 outflow has revealed $HCOOCH_3$ and C_2H_5OH, with abundance ratios relative to CH_3OH comparable to those found in hot cores and Galactic Center clouds (Arce et al. 2008) (see **Table 3**). Because the time scale for the warm outflowing gas is too short ($< 2 \times 10^3$ years) for the complex organics to have formed in the gas from evaporated CH_3OH, the more likely explanation is that all of these molecules originate from the ices. CH_3CN is not detected, but the quoted very low abundance (three orders of magnitude lower than that found in hot cores) assumes a much higher excitation temperature than that for other species.

The only spatially resolved outflow of a high-mass source for which a line survey has been performed is that emanating from Orion IRc2. Several complex organic species are seen in the plateau region (Sutton et al. 1995), but with similar abundance ratios as for other high-mass regions. However, CH_3CN does not have a plateau component.

4.3. High-Mass Young Stellar Objects and Galactic Center Clouds

Most complex organic species were first detected in the hot cores Orion-KL and Sgr B2(N), but over the past decade, observational studies have expanded to other targets for a variety of reasons. For example, the southern sources G 327.3–0.6 and NGC 6334 I have much narrower lines (~5 km s^{-1} versus ~20 km s^{-1} for Sgr B2), reducing the line confusion problem (e.g., Gibb et al. 2000a, Schilke et al. 2006). Also, similarities and differences in chemistry among high-mass YSOs in the same cloud can be studied. Examples include the 230 GHz surveys of Sgr B2(N), (M), and (NW) by Nummelin et al. (2000); the 230 and 345 GHz surveys of NGC 6334 I and I(N) by

Table 3 Abundance ratios of some gas-phase complex organic molecules with respect to CH_3OH[a]

	Low mass				High mass				Outflow	Dark Cloud	
Species	I16293[1]	N13 2A[2]	N13 4A[3]	N13 4B[2]	High-m[4]	GC[5]	Orion[6]	G327.3[7]	L1157[8]	TMC-1[9]	L134N[9]
$HCOOCH_3$	0.30	<1.7	0.56	0.26	0.10	~0.04	0.07	0.08	0.02	<0.4	<0.03
CH_3OCH_3	0.20	0.02	<0.22	<0.19	0.31	~0.04	0.05	~3	–	–	<0.13
C_2H_5OH	0.01	–	–	–	0.025	~0.04	0.004	0.003	0.006	–	<0.004
CH_3CN	0.02	0.02	0.01	0.01	0.06	–	0.01	0.035	6E-5	0.08	0.015
HC_5N	–	–	–	–	<0.1	–	<0.0003	–	–	2.8	<0.06

[a]CH_3OH abundances with respect to H_2 vary between 10^{-7}–10^{-5} except for dark clouds; typical uncertainties in ratios are a factor of a few.

[1]Ratios for IRAS 16293–2422 based on column densities from Cazaux et al. (2003) and van Dishoeck et al. (1995) for a 2″ source. C_2H_5OH from Bisschop et al. (2008).

[2]Ratios for NGC 1333 IRAS 2A and IRAS 4B based on column densities from Bottinelli et al. (2007) and Maret et al. (2005) scaled to the same (small) source size. CH_3OCH_3 for 2A from Jørgensen et al. (2005a).

[3]Ratios for NGC 1333 IRAS 4A based on column densities from Bottinelli et al. (2004a) and Maret et al. (2005) scaled to a 0.5″ source size.

[4]Average ratios for 7 high-mass YSOs from Bisschop et al. (2007b).

[5]Average ratios for a number of Galactic Center clouds from Requena-Torres et al. (2006).

[6]Ratios for the Orion Compact Ridge from Sutton et al. (1995); HC_5N from Blake et al. (1987b) for extended ridge.

[7]Ratios for the high-mass YSO G327.3–0.6 based on Gibb et al. (2000a) for a 2″ source.

[8]Ratios for the L1157 outflow from Arce et al. (2008) and Bachiller & Perez Gutierrez (1997).

[9]Ratios for TMC-1 at the cyanopolyyne peak and L134N based on Ohishi, Irvine & Kaifu (1992), Friberg et al. (1988), Turner, Terzieva & Herbst (1999), Suzuki et al. (1992) and Requena-Torres et al. (2007).

McCutcheon et al. (2000) and Thorwirth et al. (2007); and the 345 GHz surveys of W 3 IRS4, IRS5, and (H_2O) by Helmich & van Dishoeck (1997). The sources Sgr B2(N), NGC 6334 I, and W 3(H_2O) have typical hot-core spectra rich in complex organic species similar to Orion-KL, but the other massive YSOs in the same regions do not, in spite of very similar luminosities and distances (e.g., see **Figure 1**). Both Sgr B2(M) and W 3 IRS5 have spectra with very prominent lines of SO and SO_2, whereas the spectrum of W 3 IRS4 resembles that of a PDR with strong lines of radicals like CN and C_2H. In the former case, outflows likely dominate the single dish line fluxes whereas in the latter case the evolutionary state is such that UV from the young star can escape the envelope and illuminate the nearby cloud. Thus, not all hot cores defined as such by their physical conditions show complex organic molecules, that is, not all hot cores have a "hot-core chemistry." A key question is whether these sources would reveal complex organic species in deeper integrations. If detected at similar (relative) abundances as in traditional hot cores, it would indicate that it is the size of the hot-core region (and thus the filling factor in the single-dish beam) that is changing among these sources, rather than the chemistry itself.

Variation in chemical content is also revealed in high spatial resolution interferometric images of small clusters of massive YSOs, which show that complex organic species are usually associated with only one or two deeply embedded sources but not with the majority of the (ultracompact) H II regions traced by the radio continuum (see review by Kurtz et al. 2000) (**Figure 5**). A well-known example is CH_3CN, often used as a tracer of hot cores (Araya et al. 2005, Pankonin et al. 2001). Because it is readily detected and imaged, CH_3CN is often the molecule of choice to determine the velocity field of hot-core gas at high angular resolution and to search for evidence of rotation in disk-like structures (e.g., Beltrán et al. 2005, Cesaroni et al. 1997). Methanol masers are also a good signpost of nearby hot cores of complex chemistry, even if not fully coincident (**Figures 1** and **5**). Variations in chemistry can occur on scales as small as a few thousand AU (0.1 pc or less). Well-known examples include the separation of O- and N-bearing molecules in the Orion hot core and compact ridge (see above), and in W 3(H_2O) and W 3(OH) (Wyrowski et al. 1999).

Dedicated searches for individual (sets of) molecules in a large number of sources can often address specific chemical questions better than full line surveys of a single source. Ikeda et al. (2001) surveyed a number of complex organic molecules in sources with well-determined dust temperatures to find a correlation between abundances and temperature, consistent with ice evaporation. Hatchell et al. (1998) covered about 10 GHz in selected settings between 200 and 350 GHz for 14 ultracompact H II regions and found that only half of their sources are rich in lines of complex organic molecules. Remijan et al. (2005a) performed a survey for a few cyanides and their corresponding less stable isocyanide isomers to show that the two classes of species have different distributions, with the isocyanides avoiding the hot cores. Remijan et al. (2003) determined the relative abundances of the isomers CH_3COOH and $HCOOCH_3$ to be roughly 0.03:1, which, together with their different distributions, provide constraints on their formation pathways.

Bisschop et al. (2007b) surveyed a number of complex organic molecules. Although the absolute abundances vary by two orders of magnitude from source to source, the relative ones are remarkably constant within factors of a few. Strong correlations are found among the O-bearing molecules and the N-bearing ones, but not between the two families, providing additional (indirect) evidence that they are not necessarily colocated. This conclusion is further strengthened by small differences in velocity between the two families (Fontani et al. 2007). This latter study also finds a strong correlation among the N-bearing molecules, but with a link to some O-rich species as well.

For most molecules in hot cores, sufficient numbers of lines have been measured to determine rotation temperatures, which in turn provide further constraints on their chemical pathways. Many complex organics have high rotational temperatures of 120–300 K, consistent with the estimated

gas temperatures in the hot cores. Surprisingly, some complex organics have much lower rotational temperatures <60 K, suggesting that they are present mostly in the colder envelope. Examples include HCOOH, CH_2CO, CH_3CHO, and CH_3CCH (e.g., Bisschop et al. 2007b, Ikeda et al. 2001). Also, C_2H_5OH is found to have a cold component in some sources (e.g., Gibb et al. 2000a, Nummelin et al. 2000). These molecules are not exclusively present in the cold gas, however, and deeper single-dish searches or interferometer data often also reveal a hot component at comparable abundance to the cold component (see Section 4.6).

The surveys of complex molecules in the Central Molecular Zone of the Galactic Center region provide a very interesting, new, and complementary opportunity to test their chemical pathways (Requena-Torres et al. 2008, 2006). Because of their low rotational temperature ($T_{rot} < 20$ K) due to subthermal excitation, the spectra are much less confused and the emission is concentrated in only a small number of (low-frequency) lines (see **Figure 2**). As with massive YSOs, the CH_3OH abundance varies by two orders of magnitude, but the abundances of the other complex organic species relative to CH_3OH are remarkably similar within factors of a few, even for clouds hundreds of pc apart. Thus, if these molecules originate from sputtering of grain mantles by shocks, as proposed by the researchers, there must be a single grain mantle composition throughout the Galactic Center region. Moreover, many of the complex organic species have abundance ratios very similar to those found in massive YSOs in other parts of the Galaxy (see **Table 3**).

There may also be some differences. The isomer CH_2OHCHO (glycolaldehyde) is more abundant in the Central Molecular Zone than in massive YSOs, whereas CH_3COOH is not detected. There are also suggestions that saturated (that is, more hydrogenated molecules) are more abundant in the Galactic Center clouds (e.g., CH_3CHO vs H_2CCO).

4.4. Low-Mass Young Stellar Objects

4.4.1. IRAS16293-2422. Organic molecules including CH_3OH, CH_3CN and CH_3C_2H were detected in the low-mass deeply embedded "Class 0" protostar IRAS 16293–2422 in Ophiuchus ($L = 27\ L_\odot$, $M_{env>10\,K} = 5\,M_\odot$, $d = 125$ pc) by van Dishoeck et al. (1995), a source that subsequently proved to be exceptionally rich in complex organics in much deeper searches by Cazaux et al. (2003) (see also Ceccarelli 2005). This source has become the equivalent of Orion for low-mass YSO studies and is the only solar-mass protostar to date for which complete line surveys in the 230 and 345 GHz windows exist (**Figure 7**) (Caux et al. 2005).

For molecules like CH_3OH, which are present both in the hot corino and in the colder envelope, the abundance has a "jump" from $\sim 10^{-9}$ in the outer region to at least 10^{-7} in the inner part where the temperature is above ~90 K (150 AU radius) (Maret et al. 2005, Schöier et al. 2002). **Table 3** includes the source-averaged abundance ratios with respect to CH_3OH in the inner hot region derived from the rotation diagram method and assuming a source radius of ~150 AU. Such a procedure is similar to that used to determine abundance ratios for high-mass YSOs. The abundance ratios derived in this way are up to an order of magnitude lower than those presented by Bottinelli et al. (2007) and are closer to those found in high-mass YSOs.

Nearby sources like IRAS 16293–2422 can be spatially resolved with millimeter interferometers, in contrast to most of their high-mass counterparts. The source is actually a proto-binary, with the two YSOs separated by about 800 AU (5″) (Mundy et al. 1992). Each binary component has its own circumstellar disk of radius ~50 AU, and both are embedded in a circumbinary envelope of which the inner 600 AU radius region has been largely cleared of material (Jørgensen et al. 2005b). The more southern of the two sources has a prominent outflow traversing the envelope. Thus, the single YSO–passively heated envelope model used to analyze the data is clearly too simplistic for this source.

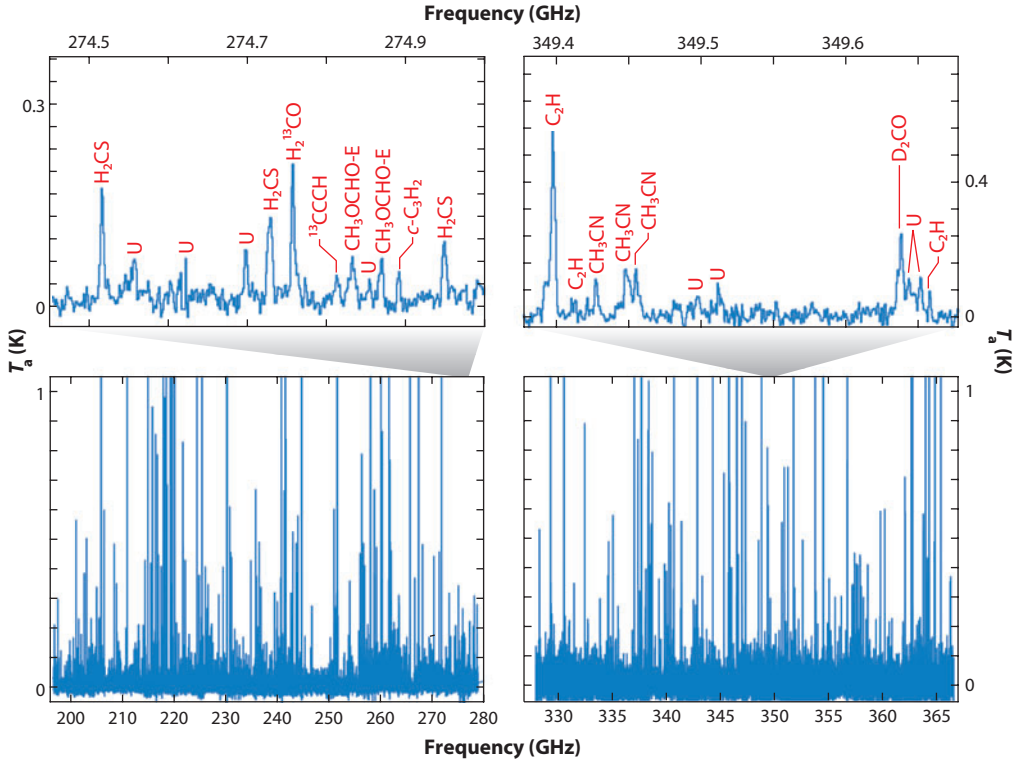

Figure 7

Line survey of the low-mass protobinary object IRAS 16293–2422 ($d = 125$ pc, $L = 27$ $L_\odot$) obtained in the 1-mm atmospheric window with the IRAM 30-m telescope and in the 0.8-mm atmospheric window with the James Clerk Maxwell Telescope. Note the richness of the spectra and the presence of complex organic molecules in spite of the orders-of-magnitude lower luminosity compared with massive regions like Orion. (Figure based on Caux et al. 2005.)

Interferometric images show that the abundances of the complex molecules change significantly between the two binary components, with the southern component richer in nitrogen-bearing species (Bottinelli et al. 2004b, Kuan et al. 2004b, Remijan & Hollis 2006) (see **Figure 8**). The abundance ratios of organics like HNCO and CH_3CHO with respect to CH_3OH change by more than an order of magnitude between the two sources, even though their sum is quite consistent with the single-dish abundance ratios (Bisschop et al. 2008). Also, molecules like CH_3CHO, which were found to be "cold" in single-dish studies, turn out to have a compact "hot" component as well. Further questions on the location of the complex organics have been raised by the high-resolution observations of Chandler et al. (2005), which show that the molecular emission near the southern component coincides with the shock seen at centimeter wavelengths and is slightly offset ($\sim$0.2″) from the disk continuum at submillimeter wavelengths. Combined with their broad line profiles, this observation would be consistent with sputtering of ices in the interaction zone of the outflow with the inner envelope, rather than passive heating of the envelope.

IRAS 16293–2422 is a true gold mine for studies of deuterated molecules, with ratios of deuterated species relative to the normal ones orders of magnitude higher than the overall [D]/[H] ratio of $\sim 1.5 \times 10^{-5}$ (e.g., Ceccarelli et al. 1998, van Dishoeck et al. 1995). This deuterium fractionation can be up to a factor of 10^{9-13} for doubly and triply deuterated species like D_2CO and CD_3OH (Ceccarelli et al. 2007, Parise et al. 2004). The deuteration patterns (e.g., CDH_2OH

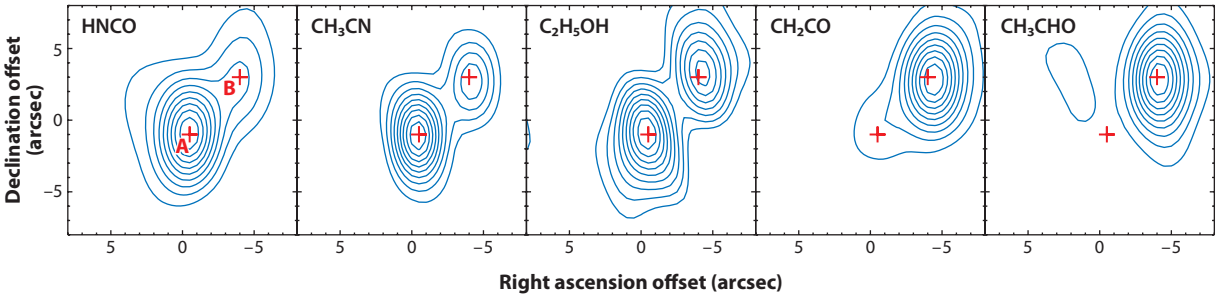

Figure 8

Interferometric line images of the low-mass protobinary object IRAS 16293–2422 obtained with the SubMillimeter Array. The maps show the emission integrated over the width of the lines toward the northern (*B*) component. Different distributions of the oxygen- and nitrogen-rich complex organic molecules are seen, even though the two sources are separated by only about 800 AU. Figure from Bisschop et al. (2008), with permission.

versus CH_3OD) in principle hold important clues on the chemical pathways toward the formation of the complex organics, an area that needs to be further developed in the coming decade.

4.4.2. Other low-mass young stellar objects. How unique is IRAS 16293–2422? Several other low-mass embedded YSOs have been surveyed for CH_3OH and a few other characteristic complex organics. Because the envelope masses and luminosities of these sources are lower than those of IRAS 16293–2422 and their distances larger, the lines are correspondingly weaker and in many cases below the current detection limits even for hours of integration. CH_3OH itself is readily detected, but convincing abundance jumps providing evidence for a hot core have been found for only a handful of sources, primarily in NGC 1333 (Blake et al. 1995; Jørgensen, Schöier & van Dishoeck 2005a; Maret et al. 2005). In one source, NGC 1333 IRAS 4B, the CH_3OH lines are very broad, consistent with the outflow dominating the single-dish emission, as also revealed in interferometric data (Jørgensen et al. 2007); in another source, NGC 1333 IRAS 2A, the line profiles and physical structure are consistent with a passively heated envelope. Since the infall time scale in the hot corino region is short (a few $\times 10^2$ years) (Schöier et al. 2002), dynamically more stable regions such as the disk surface layers have also been proposed as the location for the complex species (Jørgensen et al. 2005a).

Of the other complex molecules, only $HCOOCH_3$ and CH_3CN have been detected toward NGC 1333 IRAS 2A, 4A, and 4B, with upper limits on HCOOH and C_2H_5CN (Bottinelli et al. 2004a, 2007; Jørgensen, Schöier & van Dishoeck 2005a); CH_3OCH_3 has been detected only in 2A in interferometric data (Jørgensen et al. 2005a). Their abundance ratios with respect to CH_3OH are comparable to those found for IRAS 16293–2422, except that CH_3OCH_3 is an order of magnitude lower in NGC 1333 IRAS 2A. The values listed in **Table 3** refer to the rotation diagram method for a small ($\sim 2''$ or less) source size and are again lower than in Bottinelli et al. (2007).

The source L1527 in Taurus is a special case. This class 0 object ($L_{\rm bol} = 2\ L_\odot$, $M_{\rm env>10\,K} = 0.9\,M_\odot$) shows particularly strong lines of carbonaceous molecules, including carbon chains and negative ions (Sakai et al. 2008, 2007). It has been dubbed a "lukewarm" corino because the beam-averaged temperature on $\sim 20''$ scales is around 30 K, even though warmer gas and dust up to 100 K or more must be present as well. Its appearance as lukewarm may simply be the result of a rather flat density profile ($n \propto r^{-\alpha}$ with $\alpha = 0.6$) so that most of the emission picked up in the single-dish beams comes from larger and cooler regions (few thousand AU) than for the case of hot

corinos ($\alpha = 1.5$ to 2.0). If a temperature of 30 K applies to a sizeable region, the sublimation of CH_4 from grain mantles leads to an ion-molecule chemistry that produces carbon chains (Hassel, Herbst & Garrod 2008). Another characteristic of L1527 is a prominent outflow in the plane of the sky, filling a large fraction of the single-dish beams (e.g., Hogerheijde et al. 1998). UV radiation can escape through this outflow and affect the chemistry in the surrounding envelope, liberating atomic carbon or a hydrocarbon such as methane needed to build carbon chains. Such a situation is also found for the class 0 source L483, where photoproducts like CN are found to be enhanced along the outflow cavity walls (Jørgensen 2004). Thus, these sources form an excellent laboratory to study complex organic chemistry under conditions different from the standard hot cores.

4.5. Disks

Observational studies of the chemistry of protoplanetary disks are currently limited to small molecules because disk sizes and masses are orders of magnitude smaller than those of low-mass YSO envelopes. Also, a large fraction of the molecules is frozen onto the surfaces of grains in the cold high-density midplane of the disk (see Bergin et al. 2007 for a review). Taken together, this results in huge beam dilution and very weak signals in single-dish beams even for molecules as simple as the organics HCN and H_2CO (e.g., Dutrey, Guilloteau & Guelin 1997; Thi, van Zadelhoff & van Dishoeck 2004). No detection of a complex organic molecule has yet been reported in a disk, not even CH_3OH, but the limits of 10^{-9}–10^{-10} are not yet stringent compared with cold clouds.

An exciting recent development is the mid-infrared detection of the precursors of complex organics, in particular HCN and C_2H_2, in the inner few AU of disks (Carr & Najita 2008, Lahuis et al. 2006). The inferred abundances of 10^{-5}–10^{-6} are orders of magnitude larger than those found in the outer disk or in the cold surrounding cloud. Detection of the complex organics themselves, if present, will be possible with ALMA only beyond ~10 AU.

4.6. Ices

Full spectral surveys at mid-infrared wavelengths provide an inventory of the ices in dense clouds, seen as broad absorption bands on the strong dust continuum from YSOs or background field stars. The ~15 brightest high-mass YSOs have been surveyed with the Infrared Space Observatory (ISO) at 2.5–20 μm (see the summary by Gibb et al. 2004), whereas a large sample of about 50 low-mass YSOs has been covered with the Spitzer Space Telescope at 5–20 μm (e.g., Boogert et al. 2008) and ground-based 8-m class telescopes at 3–5 μm (e.g., Pontoppidan et al. 2003). Results for a few background field stars probing the quiescent cloud material have been published as well (e.g., Knez et al. 2005, Whittet et al. 2007). The complex organics themselves cannot be detected in ices, because their features overlap and their optical depths are too small to be seen on top of the strong mid-infrared continuum. The only exception is CH_3OH, which is detected through its bands at 3.54 and/or 9.7 μm in about 30% of the sources. Acetaldehyde (CH_3CHO) ice has been proposed as a candidate for the 7.41 μm feature seen in a few high-mass YSOs but alternative assignments exist (Schutte et al. 1999). Precursors to complex organics such as HCOOH, CH_4, NH_3, and OCN^-, and perhaps H_2CO, are commonly detected. C_2H_2 ice, another potential building block of complex organics, has not yet been convincingly seen, but the limits are not very stringent because of its weak infrared features when embedded in H_2O ice (Boudin, Schutte & Greenberg 1998). High abundances of C_2H_2 gas are commonly found in infrared spectra of hot cores (e.g., Lahuis & van Dishoeck 2000).

The fractional abundances of the molecules in ices can be orders of magnitude larger than those inferred from beam-averaged gas-phase submillimeter line data. The CH_3OH ice abundance varies from <1% to 30% with respect to that of H_2O ice, which corresponds to $<10^{-6}$ to 3×10^{-5} with respect to H_2. For comparison, inferred source-averaged CH_3OH abundances in the hot gas range from $<10^{-7}$ to 10^{-6}. For the few sources for which both CH_3OH ice and gas have been detected along the line of sight, the solid/gas ratio is about 10 (Bisschop et al. 2007a). For HCOOH and CH_3CHO (if confirmed), solid/gas ratios range from 10^4 to 10^5. Both are classified as cold molecules that are mostly present in the cold outer envelope of these high-mass YSOs, where only nonthermal desorption processes can get the molecules off the grains. Their absence or low abundance in the hot gas suggests that these molecules are efficiently destroyed just prior to or after evaporation of the ices.

The limit on C_2H_5OH (ethanol) is 1% of H_2O ice (Boudin, Schutte & Greenberg 1998), giving a $C_2H_5OH/CH_3OH < 0.1$ ice ratio consistent with the gas-phase data (**Table 3**). The most significant nondetection is that of CH_3CN ice. Any nitrile band is expected to have strong features at 4.35–4.55 μm, a wavelength range covered only by ISO toward high-mass YSOs. CH_3CN is one of the most prominent species in the gas in hot cores, with abundances up to a few $\times 10^{-7}$. If the CH_3CN solid/gas ratio were similar to that of CH_3OH, ice abundances of $>10^{-6}$ are expected. The observed limits indicate ice abundances less than 10^{-6} (Gibb et al. 2000a). The limit on the 5.62 μm ice feature of the simplest amino acid, glycine (NH_2CH_2COOH), is about 0.3% of H_2O ice, or $<3 \times 10^{-7}$ (Gibb et al. 2004).

Although some molecules, such as CH_4, have very constant abundances from source to source, other species, including CH_3OH and OCN^-, show variations on scales as small as a few hundred AU (Pontoppidan, van Dishoeck & Dartois 2004; van Broekhuizen et al. 2005). This indicates that local conditions such as temperature and amount of (UV) radiation can play a role in setting the overall abundances of complex organics. It also strengthens models in which the observed separation of O- and N-bearing species has its roots in different ice distributions.

Greenberg et al. (1995) and Gibb & Whittet (2002) have argued that the 5–8 μm residual feature once all known bands have been subtracted (the component labeled C_5 by Boogert et al. 2008) is at least partly due to refractory complex organic species produced by photoprocessing of simple ices, but other identifications have been proposed as well. H_2CO is known to polymerize quickly upon heating, leaving also a nonvolatile residue (Schutte et al. 1993).

4.7. Prebiotic Molecules

Prebiotic molecules are defined as molecules that are thought to be involved in the processes leading to the origin of life. Usually, molecules in this category are taken to be species with structural elements in common with those found in living organisms and are also called molecules of biological interest. Biogenic molecules are species that are necessary for the maintenance of life (including water) and those produced by living organisms or biological processes (such as CH_4). Of the interstellar prebiotic molecules, many were first detected toward Sgr B2(N-LMH). For example, Hollis et al. (2004a) detected the first interstellar "sugar" glycolaldehyde (CH_2OHCHO), The tri-carbon sugar, glyceraldehyde (a true sugar in the chemical sense), has not yet been detected (Hollis et al. 2004b) nor has 1,3-dihydroxyacetone [$(CH_2OH)_2CO$] a three-carbon keto sugar (Apponi et al. 2006), whereas ethylene glycol ($HOCH_2CH_2OH$), a hydrogenated sugar better known as antifreeze, was found by Hollis et al. (2002), albeit with only several lines. Acetamide, CH_3CONH_2, the largest interstellar molecule with a peptide bond, was detected by Hollis et al. (2006), and amino acetonitrile (NH_2CH_2CN), a direct precursor of the simplest amino acid glycine, has recently been found (Belloche et al. 2008).

Many ring molecules are of biological importance. For example, the imidazole (c-$C_3N_2H_4$) structure occurs in purines and in the amino acid histidine, but was not detected in an early search (Irvine et al. 1981). Aziridine (c-C_2H_5N) and pyrimidine (c-$C_4H_4N_2$) have also not yet been seen at abundance levels of a few $\times 10^{-11}$–10^{-10} (Kuan et al. 2004a). The latter molecule is the unsubstituted ring analog for three of the RNA and DNA bases.

As discussed in Section 7, the dominant form of carbon delivered to young planetary systems is likely to be aromatic in nature. Large PAHs and macromolecular carbon networks more readily survive the intense UV radiation near young stars and in the surface layers of disks.

4.8. Differences and Similarities

From the summary of key abundance ratios in **Table 3**, a few conclusions stand out:

1. In some dark cores, long unsaturated carbon chains such as HC_5N have orders-of-magnitude higher abundance ratios with respect to saturated molecules such as CH_3OH than in other clouds. Among cold cores, and even within a single cold core, the abundances of long chains can vary by more than a factor of 10, indicating that their chemistry is tied to special conditions or specific time scales.
2. In hot cores, saturated molecules are likely to be more abundant than are nonsaturated ones, although there is a high abundance of C_2H_2.
3. The abundance ratios of many complex molecules derived from single-dish data are remarkably similar (within factors of a few) for massive YSOs spread across the Milky Way Galaxy and for clouds in the Central Molecular Zone in the Galactic Center hundreds of parsec across (**Table 3**). Abundance ratios of complex organics in dense low-mass regions surrounding YSOs (e.g., L1157), where ice mantles are liberated by shocks, are also comparable to those found for high-mass YSOs. The simplest interpretation is that the grain mantle compositions are very similar in these regions.
4. Low-mass YSOs can have a chemical complexity as rich as that found for high-mass YSOs.
5. The origin of the complex organic species in low-mass YSOs and the mechanism for getting the ices off the grains can differ from source to source, with both passive heating and liberation by shocks playing a role. Because of short infall time scales compared with high-mass YSOs, more stable structures such as disks have been invoked as well.
6. A significant fraction of high- and low-mass YSOs do not show emission from complex molecules in spite of similar luminosities, masses, and distances. Deeper integrations are needed to determine whether these sources simply have much smaller hot-core regions or whether they have a different chemistry linked to their evolutionary state.
7. Spatial differences between O- and N-rich complex organics are found for both high- and low-mass YSOs, on scales as small as a few hundred AU. Abundance ratios derived from high-resolution interferometer data can differ by more than an order of magnitude from the larger scale values.
8. The ice composition observed toward large samples of low- and high-mass YSOs is remarkably similar (within factors of 2) across the Milky Way for many of the major ice species. Methanol, together with OCN^- and NH_3, shows larger variations by more than an order of magnitude, even on scales as small as a few hundred AU.

In summary, the overall picture emerging from observations of both gases and ices is that the bulk of the quiescent material in the Galaxy prior to star formation ($T = 10$–30 K) has a similar grain mantle composition independent of global environment. Local conditions (heating, UV) appear to affect specific molecules on smaller scales.

5. CHEMISTRY AND COMPLEX MOLECULES IN COLD CORES

Although molecules and dust particles are produced in stellar atmospheres, especially in older stars, as the gas and dust are expelled, all but the largest molecules are photodissociated by the harsh UV radiation in the unshielded interstellar medium on time scales of ≈100 years (van Dishoeck 1988). The existence of molecules in the interstellar medium thus indicates that the chemistry that forms the molecules is local in nature. As the gas and dust gradually condense into cool diffuse interstellar matter, chemical processes begin to synthesize molecules from the mainly atomic gas. Although molecules as large as formaldehyde (H_2CO) are known to exist in diffuse and translucent clouds (Liszt, Lucas & Pety 2006), the production of complex species appears to be limited to denser regions. The major molecule produced in diffuse regions is H_2, where it is formed on the surfaces of dust particles (Gould & Salpeter 1963). Details of both modern theoretical and experimental approaches to the study of H_2 formation on grains can be found in Section H of Lis, Blake & Herbst (2005).

5.1. Basic Chemistry

5.1.1. Gas-phase chemistry. Once H_2 is ejected into the gas, a gas-phase chemistry occurs leading to complex species. At the low temperatures of cold dense cores ($T_{gas} \approx T_{grain} \approx 10$ K), the chemistry must occur via reactions that are exothermic (that is, give off energy) and that have no potential ("activation energy") barriers between reactants and products. Reactions involving positive ions and neutrals (ion-neutral reactions) often obey this constraint and dominate the chemistry (Herbst & Klemperer 1973, Watson 1973). Although most exothermic reactions between two neutral species do possess considerable activation energy, there are exceptions, which must be taken into account. Networks of reactions for use in simulations of the gas-phase chemistry can be obtained on two web sites; the Rate06 site (Woodall et al. 2008) and the OSU (Ohio State) site (Herbst & Wakelam 2008). These networks currently have ≈5000 reactions with gas-phase species up to 12–13 atoms in size. The Rate06 network can be used at somewhat higher temperatures than the OSU network.

Positive ions are formed in dense regions mainly by cosmic ray bombardment and subsequent reactions; the formation of the simplest polyatomic ion H_3^+ is a case in point: $H_2 + CR \rightarrow H_2^+ + e^- + CR$, $H_2^+ + H_2 \rightarrow H_3^+ + H$. Here CR stands for a cosmic ray proton. A significant portion of the ionization actually occurs via secondary electrons, as they relax to thermal conditions (Cravens & Dalgarno 1978). The flux of cosmic rays and its penetration into dense regions is normally parameterized by a rate of ionization for H_2 molecules designated ζ, which is typically set at $\approx 1\text{–}5 \times 10^{-17}$ s^{-1} for dense sources. In addition to ionization, cosmic rays lead to the internal production of UV photons via a mechanism in which secondary electrons excite H_2, which then reradiates back to the ground electronic state (Gredel et al. 1989, Prasad & Tarafdar 1983). These photons are a source of destruction of molecules since they can photodissociate and photoionize many species despite high visual extinction.

Chains of ion-molecule reactions starting with H_3^+ and primeval atomic species lead to a variety of complex molecular ions. These ions tend to be unsaturated because many "H-atom transfer" reactions involving molecular ions (X^+) of the type $X^+ + H_2 \rightarrow XH^+ + H$, which is the main process for hydrogenation, are either endothermic or possess potential barriers, so that they do not occur at low temperatures. For example, for hydrocarbon ions $C_nH_m^+$ with $n > 3$, H-atom transfer reactions cannot produce ions with $m > 2$ (McEwan et al. 1999). Moreover, once the positive molecular ions are formed, dissociative recombination processes such as $C_nH_2^+ + e^- \rightarrow C_nH + H$, etc., produce neutral fragments that tend to have one or more hydrogen atoms fewer than the

ionic structure. Although other chemical reactions such as radiative association reactions between ions and H_2 lead to somewhat more saturated ions (Bates 1987), the net result is that the complex molecules produced in gas-phase chemical models of cold sources tend to be very unsaturated. Combined with the fact that ion-molecule reactions with C^+ or C and neutral-neutral reactions with C lead to carbon insertion at low temperatures, this chemistry naturally produces long carbon chains. A figure showing the ion-molecule pathways from H_3^+, C, and C^+ to neutrals as complex as C_6H is shown in Smith (1992). Herbst & Millar (2008) have recently reviewed ion-molecule chemistry in cold cores in some detail. A few researchers have speculated about the syntheses of molecules considerably larger than those detected and in current large gas-phase networks but achievable by an extension of ion-molecule chemistry (Bettens & Herbst 1995, Herbst 1991, Thaddeus 1994).

5.1.2. Grain-surface chemistry. As the gas-phase chemistry proceeds, atoms and molecules (adsorbates) also accrete onto dust particles, since sublimation at 10 K can only occur efficiently for very light weakly bound adsorbates such as H, H_2, and He. Accretion occurs via weak van der Waals forces, known as physisorption, or via chemical valence forces, known as chemisorption. Often, chemisorption has a potential barrier, and it is normally but not universally assumed that in cold sources, sticking occurs via physisorption. As adsorbates accrete onto a cold surface, a complex surface chemistry occurs, leading to the production of ices (Hasegawa, Herbst & Leung 1992; Pickles & Williams 1977; Ruffle & Herbst 2001; Tielens & Hagen 1982). There are three major mechanisms for surface reactions: the diffusive, or Langmuir-Hinshelwood; the Eley-Rideal; and the hot atom, all of which are depicted in **Figure 9**, which shows a regular surface with a periodic potential. Accretion, with a sticking efficiency S, occurs onto the potential minima, known as binding sites, which here represent physisorption sites. "Desorption" is also possible, with a minimum energy E_D, either by thermal evaporation (sublimation) for very light species or by nonthermal mechanisms. A more general sublimation occurs for all species on the ice as the surface temperature increases to 100–300 K in YSOs. In the Langmuir-Hinshelwood mechanism, diffusion occurs by tunneling or thermal hopping over the barrier E_b between binding sites. Once reactive adsorbates (mainly atoms and radicals) lie in the same minimum, they can react, typically by sticking together with the grain receiving the excess energy. Reaction can also occur via the Eley-Rideal mechanism, in which a gas-phase species lands atop an adsorbate and reacts with it, and via the hot-atom mechanism, in which a gas-phase species lands on a surface and moves considerably before thermalization, so that it is able to collide with an adsorbate.

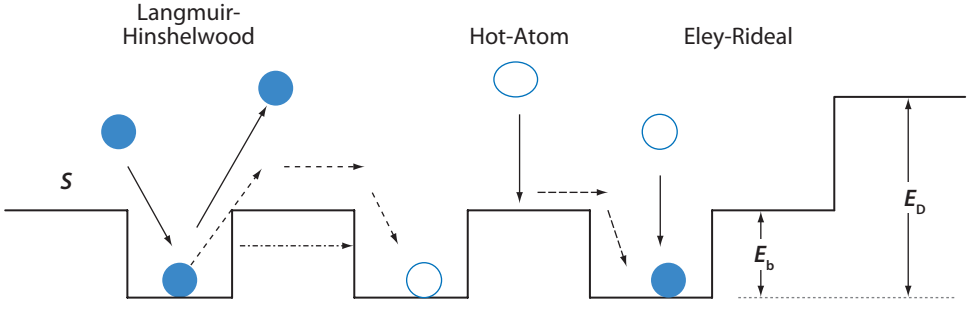

Figure 9

Three mechanisms for surface reactions on a regular grain surface. S is the sticking efficiency of a gas-phase species, E_D is the binding, or desorption, energy of the adsorbate to the surface, and E_b is the barrier from one site to an adjacent one.

Of these three mechanisms for surface reactions, astrochemical models most often include only the diffusive (Langmuir-Hinshelwood) since it is the best studied (Kolasinski 2002). In general, the surface species thought to be produced via diffusive chemistry are saturated ones, unlike those produced in the gas, because atomic hydrogen, which accretes from the gas and then diffuses very rapidly, is a very efficient reactant on surfaces. The dominant ice species—water ice—is produced by the sequential hydrogenation of O atoms landing on a grain: $O \rightarrow OH \rightarrow H_2O$, as well as via the more complex hydrogenation of O_2 and O_3 (Tielens & Hagen 1982). Similar syntheses convert N atoms into NH_3 and C atoms into CH_4. Likewise, once CO is produced in the gas and accretes onto grains, it can be hydrogenated to the complex molecule methanol via another sequence of reactions involving atomic hydrogen (Charnley, Tielens & Rodgers 1997):

$$CO \rightarrow HCO \rightarrow H_2CO \rightarrow H_2COH \rightarrow CH_3OH, \quad (2)$$

as studied in the laboratory by two groups (Ioppolo et al. 2007, Watanabe & Kouchi 2002). The process occurs competitively at low temperatures despite the fact that small potential barriers exist for two of the reactions. The possibility that more complex species than methanol are formed at low temperatures on surfaces has been pursued by Charnley and coworkers, who have assumed that heavier atoms can also be reactive even if they diffuse more slowly than atomic hydrogen (Charnley 2001a, 1997a). For example, ethanol and acetaldehyde can be produced from CO by suitable additions of C and H atoms (see also Section 6.1):

$CO \rightarrow HCO \rightarrow HCCO \rightarrow CH_2CO \rightarrow CH_3CO \rightarrow CH_3CHO \rightarrow C_2H_5OH$. The sizes of any activation energy barriers for these reactive steps involving C atoms are not known, although the last step has been measured to be moderately efficient (Bisschop et al. 2007a).

The mathematical treatment of grain-surface reactions is tricky because of the small size and heterogeneity of individual grains. Rate equations, used for the gas-phase chemistry, are least inadequate for diffusive chemistry on homogeneous larger grains, on which at least several reactive adsorbate species exist on average (Green et al. 2001, Tielens & Hagen 1982). So-called macroscopic stochastic methods such as the master equation approach and the Monte Carlo method eliminate the problem caused by the small numbers of adsorbates, especially on smaller grains, but do not tackle the problem of inhomogeneity (Barzel & Biham 2007; Charnley 2001b; Green et al. 2001; Stantcheva, Shematovich & Herbst 2002). A special Monte Carlo method known as the "continuous-time, random-walk" approach handles this latter problem (Chang, Cuppen & Herbst 2007). Because it is very difficult to merge stochastic treatments of surface chemistry with deterministic treatments of the gas-phase chemistry, most gas-grain models, such as the Ohio State gas-grain model (Garrod, Wakelam & Herbst 2007), still utilize rate equations for the surface chemistry. Model results for abundances of molecules in grain mantles must therefore be taken with caution, especially if grains smaller in radius than the standard 0.1 μm are used.

A new approximate macroscopic stochastic method, known as the method of moments, shows promise in both delimiting when rate equations are accurate and in being used to calculate surface abundances when rate equations are inaccurate (Barzel & Biham 2007). Most recently, Vasyunin et al. (2009) have reported a new macroscopic Monte Carlo method that treats both surface and gas-phase chemistry for periods of up to 10^6 years using grains of radius 0.1 μm. The results do not significantly differ from those obtained by rate equations if it is assumed that H atoms diffuse on the surface only by classical hopping from site to site. If, on the other hand, H atoms tunnel rapidly from site to site, the Monte Carlo results differ strongly from those of the rate equation method. Similar calculations on smaller grains would be very interesting. Another new contribution has been reported by Garrod (2008), who showed that standard rate equations can be modified to reproduce most aspects of macroscopic stochastic treatments of surface chemistry on small grains.

5.2. Negative Ions

With the recent discovery of negative molecular ions in the cold core TMC-1, the AGB stellar envelope IRC+10216, and the lukewarm protostellar envelope L1527, gas-phase ion-molecule chemistry has become more complex. Not only must the formation and depletion of negative ions be understood, but the importance of negative ions in the chemistry of the other classes of species must also be considered. So far, four negative ions have been definitely detected: C_3N^-, C_4H^-, C_6H^-, and C_8H^-, of which only the latter two fit our definition of complex species. The anion C_5N^- has been probably detected in IRC+101216. The major formation mechanism is thought to be simple radiative attachment of an electron to the parent neutral; e.g., $C_6H + e^- \rightarrow C_6H^- + h\nu$. With a large electron binding energy (affinity) to the neutral precursor of 3–4 eV and a size of at least 4–5 atoms, the attachment can be quite efficient (Herbst & Osamura 2008). Another formation mechanism is known as dissociative attachment; here the nonradiative sticking of an electron is accompanied by the breaking of a chemical bond (Herbst & Osamura 2008, Petrie 1996, Sakai et al. 2007). This process is only exothermic for weakly bound neutral reactants; e.g., $HNCCC + e^- \rightarrow C_3N^- + H$.

Negative ions are destroyed in the gas by associative detachment reactions with atoms such as $C_6H^- + H \rightarrow C_6H_2 + e^-$ (Barckholtz, Snow & Bierbaum 2001), by normal ion-molecule reactions, by mutual neutralization reactions with positive ions (e.g., $C_6H^- + H_3^+ \rightarrow C_6H + H_2 + H$), and by photodetachment: $C_6H^- + h\nu \rightarrow C_6H + e^-$. Detailed experimental and theoretical studies are needed for most of these classes of reactions. The role of negatively charged PAHs has been looked at anew by Wakelam & Herbst (2008) in cold cores using similar reactions.

5.3. Chemical Models of Cold Cores

For noncollapsing cold cores such as TMC-1, purely gas-phase models using either the Rate06 or OSU networks are typically run in the "pseudo-time-dependent" mode, in which homogeneous, time-independent physical conditions are assumed with initial species either atomic or, for the case of hydrogen, at least partially molecular based on the assumption that much molecular hydrogen is made in diffuse stages (Wakelam, Herbst & Selsis 2006). Most recently, models including anionic chemistry have been run, with the major goal being to reproduce the anion-to-neutral ratios in TMC-1 and other sources (Millar et al. 2007), which range upward to $\approx$0.05–0.10. For models with and without anions, both the best overall agreement with observation and the largest abundances of carbon-chain complex species typically occur at so-called early times of 10^{5-6} years with normal oxygen-rich elemental abundances (C/O = 0.4), since the steady-state abundances, reached at times of 10^7 years, are too low for most complex species. Modern comparisons between observational and theoretical results are aided by sensitivity analyses of the model results, in which the uncertainties in rate coefficients and physical conditions are translated into standard deviations in calculated abundances as functions of time by a Monte Carlo method (Vasyunin et al. 2004, Wakelam et al. 2005). Agreement for a molecule occurs if the observational and theoretical uncertainties overlap. Other comparisons used are the simple order-of-magnitude criterion for individual species and the so-called mean confidence level method, in which an average confidence level κ is computed as a function of time. A κ of 1 indicates perfect agreement for all observed molecules, whereas a κ of 0.317 indicates a one-order-of-magnitude average departure from observed values (Garrod, Wakelam & Herbst 2007).

Gas-phase pseudo-time-dependent models are capable of achieving order-of-magnitude agreement or better for up to 80% of the observed molecules if the gas-phase elemental abundances are treated as parameters. In particular, agreement is poor for TMC-1 with the standard reaction

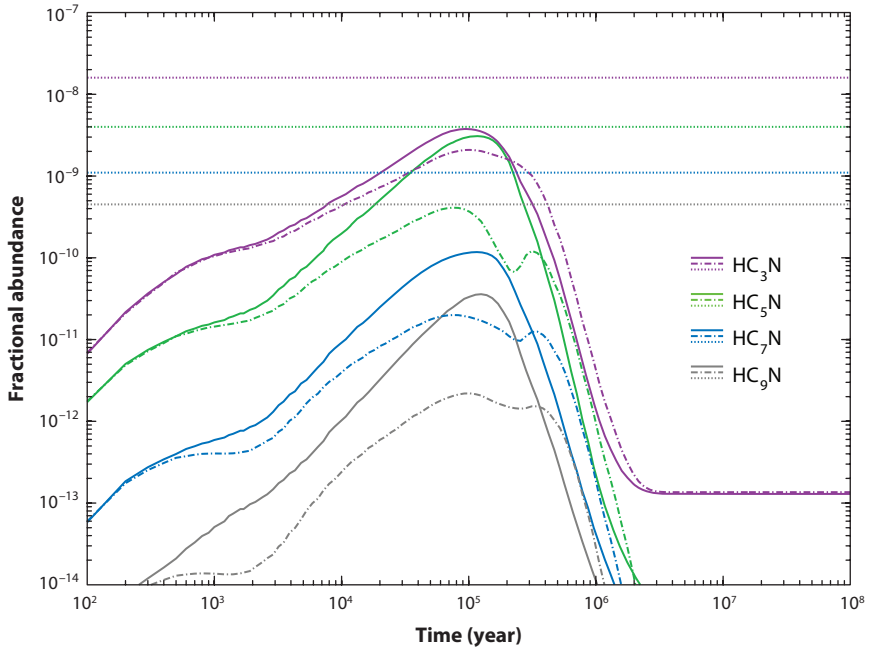

Figure 10

Comparison of fractional abundances with respect to H_2 for cyanopolyynes in a pure gas-phase model calculated with anions (*solid lines*) and without anions (*dashed-dotted lines*). Oxygen-rich (C/O = 0.4) low-metal abundances are used. The model parameters are $T = 10$ K, $n_H = 2 \times 10^4$ cm^{-3}, and a cosmic ray ionization rate per H_2 molecule of $\zeta = 1.3 \times 10^{-17}$ s^{-1}. Horizontal lines represent observed abundances in TMC-1. Figure provided by C. Walsh.

networks unless the elemental abundances are carbon-rich (C/O = 1.2; Wakelam, Herbst & Selsis 2006). In this case, calculated early time abundances of some of the largest complex molecules detected in this source (e.g., HC_9N, CH_3C_5N, CH_3C_6H) are in reasonable agreement with observation (Quan & Herbst 2007; Smith, Herbst & Chang 2004). One possible source for the excess carbon is a high abundance of C I, detected in HCL2, the dark cloud surrounding TMC-1 (Maezawa et al. 1999). The inclusion of negatively charged PAHs (Wakelam & Herbst 2008) improves the agreement between model and observation with the standard oxygen-rich elemental abundances (C/O = 0.4). The inclusion of small anions and their uncertain chemistry does not result in great improvement in the overall agreement with observation in TMC-1 when oxygen-rich abundances are used, although it does enhance the early time abundances of classes of carbon chain species, such as the cyanopolyynes, as shown in **Figure 10**. Other cold cores such as L134N are fit reasonably with oxygen-rich abundances at early times even in the absence of PAHs, suggesting that PAHs may be clustered into smaller numbers of larger units (Wakelam & Herbst 2008). Despite these complications, the gas-phase chemistry in cold cores is still the most plausible explanation of the gaseous molecular abundances in cold cores. With such a chemistry, the observed variation in abundance ratios such as HC_5N/NH_3 demands a heterogeneity in structure or chemical lifetime.

Some molecules with abundances in cold cores not explained well by this approach are the more saturated species CH_3OH, CH_3CHCH_2, and CH_3CHO. The case of methanol is worth discussing in detail. It was once thought that this species could be produced from the methyl ion

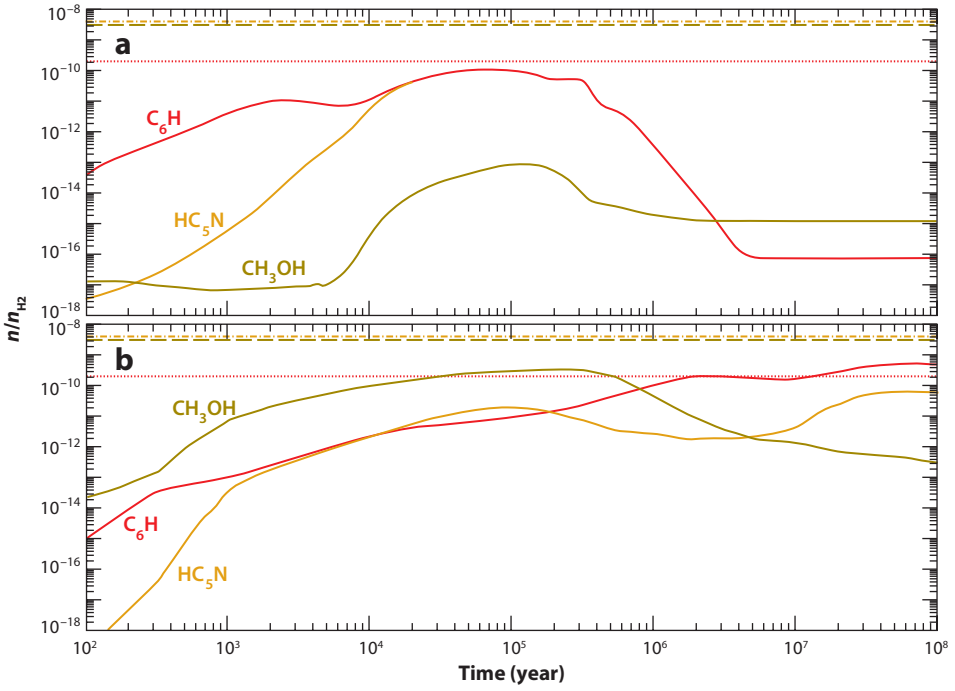

Figure 11

Comparison of fractional abundances calculated with gas-phase (*a*) and gas-grain (*b*) models for a cold core with oxygen-rich abundances (C/O = 0.4). The Ohio State networks were used without anions. The model parameters are $T = 10$ K, $n_H = 2 \times 10^4$ cm^{-3}, and the cosmic ray ionization rate per H_2 molecule of $\zeta = 1.3 \times 10^{-17}$ s^{-1}. Horizontal lines represent observed species in TMC-1. Provided by D. Quan.

(CH_3^+) by a radiative association reaction with water followed by a dissociative recombination reaction: $CH_3^+ + H_2O \rightarrow CH_3OH_2^+ + h\nu$, $CH_3OH_2^+ + e^- \rightarrow CH_3OH + H$. However, when the initial reaction was finally studied in the laboratory, it was found to be much slower than the earlier theoretical prediction (Luca, Voulot & Gerlich 2002). In addition, experiments using storage rings show that saturated molecular ions such as protonated methanol tend to fragment more completely upon dissociative recombination rather than just breaking one bond to a hydrogen atom. In particular, the fraction of reactions leading to methanol and H was found to be only $3 \pm 2\%$ (Geppert et al. 2006, 2005). These two difficulties render the production of methanol in the cold gas phase exceedingly inefficient (Garrod et al. 2006, Geppert et al. 2005) (**Figure 11*a***).

Models of cold cores that include dust chemistry are more physically realistic than gas-phase models, but without nonthermal desorption processes, which are poorly understood, all species containing elements heavier than He are depleted almost totally from the gas at times exceeding 10^6 years if the gas density is 10^4 cm^{-3} (Roberts & Millar 2000). A recent model including nonthermal desorption mechanisms, in particular the ejection of molecules produced in exothermic surface reactions (Garrod, Wakelam & Herbst 2007), leads to the production of a much larger abundance of methanol than produced in gas-phase models. **Figure 11** contains a comparison of the abundances versus time obtained from this gas-grain model and those obtained from the OSU gas-phase model for the gaseous molecules CH_3OH, HC_5N, and C_6H with oxygen-rich elemental abundances. Of the three species, the effect for methanol is the most dramatic. The model also indicates that partially saturated hydrocarbons are produced on surfaces, which may

mean that gaseous propylene (CH_3CHCH_2) can be formed in such a manner if its desorption is efficient. As with gas-phase models, the best agreement with gas-phase observations occurs at times in the range of 10^4–10^6 years, depending on the efficiency of the nonthermal desorption. Agreement with observations of ice mantle abundances towards field stars behind the Taurus complex is mixed but best for water ice. Although this model does not include direct photodesorption, it includes desorption via photodissociation on surfaces followed by exothermic reactions between the newly produced fragments. In addition to this mechanism, direct photodesorption by cosmic ray-induced photons is now being included by modelers (Hassel, Herbst & Garrod 2008) in their gas-grain codes based on recent experiments from the Leiden group (Öberg et al. 2007).

More detailed models of cold cores abandon the pseudo-time-dependent assumption altogether. A new model of this type, in which the cores are formed via a shock through diffuse gas while the chemistry starts to occur, is being prepared by Hassel, Herbst, and Bergin, based on the shock model of Bergin et al. (2004). Even this degree of detail is insufficient for the clumpy nature of TMC-1; a gas-grain model intended to explain the chemical diversity and structure within this source has been developed by Markwick, Millar & Charnley (2000). Here precursor organic material comes off the grains as the result of Alfvén waves, which reach the different cloudlets at different times.

6. CHEMISTRY AND COMPLEX MOLECULES IN HOT CORES AND CORINOS

To analyze the chemistry of hot cores and corinos, the most recent studies contain up to three phases. The initial (cold) phase occurs as the cold core ages and undergoes isothermal collapse. At this time, an icy mantle is built up around granular cores of silicates and carbon. The next (warm-up) phase occurs during the passive warm-up of the inner envelope of the protostar to temperatures of 100–300 K and the attendant sublimation of the ice mantles. The final (hot-core) phase occurs at the temperature of the hot core or corino. The individual chemistries during the cold, warm-up and hot-core stages produce what can be termed zeroth-generation, first-generation, and second-generation organic molecules (see sidebar, Definitions of Generational Species). This three-phase approach represents the simplest manner of accounting for the history of hot cores/corinos, an accounting in which physical conditions are time-dependent but not

DEFINITIONS OF GENERATIONAL SPECIES

Zeroth-generation species: Large molecules formed in the gas and on granular mantles during the cold core era. An example is methanol (CH_3OH), which is produced by the surface hydrogenation of carbon monoxide, a gas-phase species that accretes onto cold grains.

First-generation species: Large molecules formed at least partially in and on granular mantles during the warm-up period as a cold core becomes a YSO. Here photodissociation of species such as methanol and formaldehyde, produced in the cold era, produces radicals such as CH_3O and HCO. At surface temperatures significantly above 10 K, the radicals can diffuse readily and associate to form larger molecules such as methyl formate ($HCOOCH_3$).

Second-generation species: Large molecules formed once the core has become a hot core or corino with a temperature of 100–300 K, which is high enough to evaporate the mantles completely. The chemistry now occurs only in the gas-phase via both ion-molecule and neutral-neutral reactions. Eventually complex molecules are destroyed by the gas-phase chemistry unless incorporated into disks.

heterogeneous. The approach must be revised for regions such as the Galactic Center clouds, where ices are thought to be removed from grains at any time during the cold or warm-up phases by shocks or ablation. New models for the formation of complex gaseous species via sputtering or ablation are needed.

6.1. The Cold Phase

During the cold era, atoms accrete onto cold grain surfaces followed by molecules formed in the gas phase such as CO and unsaturated carbon chains. Surface chemistry produces both simple ices such as water and CO_2, as well as more complex and saturated first-generation species, as discussed in Section 5.1. In addition to the formation of methanol and ethanol, where H and C atoms play major roles, many other reactions of this type were suggested by Charnley and coworkers (Charnley 2001a, 1997a), leading to a host of organic species, as shown in **Figure 12**. Complex molecule syntheses on cold surfaces were also considered by Caselli, Hasegawa & Herbst (1993), especially for nitrogen-containing species such as propionitrile (C_2H_5CN).

6.2. The Warm-Up Phase

This passively heated phase occurs as material streams inward toward the protostar and warms from 10 K to 100–300 K. The sublimation of the mixed-ice mantles on the dust grains does not occur in a simple manner, since each species can affect the process for other species (Sandford & Allamandola 1988), as most recently studied in temperature-programmed desorption (TPD) experiments (Collings et al. 2004). The first group to treat gas-phase chemistry in the warm-up phase was Viti & Williams (1999). Later, Viti et al. (2004) considered the complex desorption of individual species from the ice mantle based on the TPD work of Collings et al. (2004).

Following upon this work, Garrod & Herbst (2006) considered the gaseous and surface chemistries occurring during the warm-up phase. The temporal details of the warm-up phase were taken from the earlier models of Viti & Williams (1999) and Viti et al. (2004), although no allowance was made for complex desorption effects seen in the laboratory (Collings et al. 2004). Although the gas-phase processes change somewhat as the temperature increases, the changes in the surface chemistry are far greater. As the surface temperature increases past 20 K, H atoms no longer reside long enough on the grain surfaces to be dominant reactants, and some of the more vaporizable species such as CO, CH_4, and N_2 start to sublimate. At the same time, the heavier species remaining on the grain surfaces begin to diffuse more quickly. These species are too stable to be very reactive; in order to create reactive neutral species, or radicals, Garrod & Herbst (2006) considered an active photochemistry powered by cosmic ray-induced UV photons. The idea of radical-radical reactions on surfaces had first been suggested by Allen & Robinson (1977), albeit for dark cloud conditions. More recently, Hollis & Churchwell (2001) also considered the role of radicals, which they termed functional groups.

Studies of high-energy surface chemistry in general, and surface photochemistry in particular, have been undertaken in the laboratory by a number of groups over the past 20 years. Notable advances in the photochemistry of simple ices have been made in Leiden, Orsay, and NASA-Ames. [For some recent work, see Elsila et al. (2007), Muñoz Caro & Schutte (2003), and Nuevo et al. (2008).] Other groups in Hawaii, Catania, and NASA-Goddard have studied the surface chemistry following both electron and proton bombardment of ices [see, e.g., Bennett & Kaiser (2007), Mennella et al. (2002), and Ruiterkamp et al. (2005)]. The problems in utilizing the photochemical data have been twofold: (*i*) The results are obtained over very much shorter times than occur in interstellar cores even if the total fluence (flux onto a surface multiplied by time) is comparable, and (*ii*) detailed absolute rates for specific elementary processes are normally not

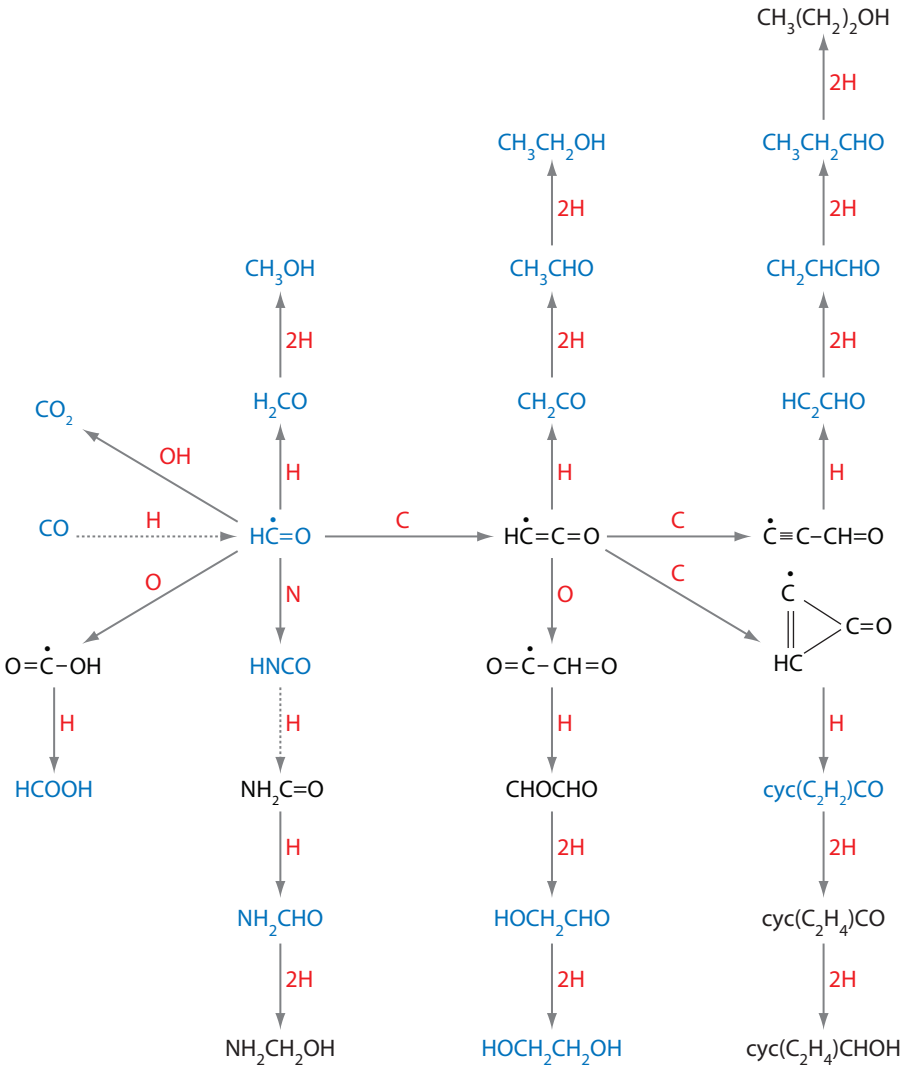

Figure 12

Organic chemistry on interstellar grains resulting from cold H addition reactions to CO. Broken arrows indicate reactions with activation energy barriers; where 2H is shown, a barrier penetration reaction followed by an exothermic addition is implicitly indicated. Molecules in blue are detected in star-forming regions. Provided by S. Charnley, and adapted from Charnley (2001a, 1997a).

reported. Given these problems, Garrod & Herbst (2006) chose to assume that photodissociation rates and radical products for species on and in ices are the same as in the gas phase, where the results of elementary processes are available. That this assumption is simplistic is shown by recent work on the photodissociation of water ice (Andersson & van Dishoeck 2008).

Assuming that reactions between radicals are mainly associative in nature, Garrod & Herbst (2006) posited the formation of surface methyl formate, dimethyl ether, and formic acid (HCOOH) by the surface reactions $HCO + CH_3O \rightarrow HCOOCH_3$, $CH_3 + CH_3O \rightarrow CH_3OCH_3$, and $HCO + OH \rightarrow HCOOH$. These products are examples of first-generation species (see sidebar,

Definitions of Generational Species). The radicals derive from the zeroth-generation precursors water, formaldehyde (H_2CO), methanol, and methane.

Whereas the work of Garrod & Herbst (2006) only added a small number of radical-radical reactions to the surface chemistry, Garrod, Weaver & Herbst (2008) suggested the addition of many surface reactions involving a large number of radicals. They made a chemical distinction between primary and secondary radicals: The primary radicals are those made initially via photodissociation of stable molecules produced during the cold era, and the secondary radicals are made from reactions involving primary radicals that do not lead to stable or saturated products.

6.3. The Hot Core/Corino Phase

Because the ices on the grain mantles sublimate during the warm-up phase, the only chemistry that can occur in the next, or hot-core, phase, is a gas-phase chemistry. Because the temperature (100–300 K) is much larger than that of cold cores, many more reactions, including endothermic processes and exothermic processes with barriers, can occur efficiently. It is the hot-core phase that was initially the focus of chemical models of hot cores, beginning with the work of Blake et al. (1987b). They presented a gas-phase chemistry to explain the oxygen-containing complex molecules in the so-called Orion Compact Ridge; the chemistry starts with the radiative association of CH_3^+ and H_2O to produce protonated methanol, followed by dissociative recombination to produce methanol (see Section 5.3), a sequence now known to be inefficient. Once produced, methanol acts as a precursor in ion-molecule reaction chains leading to species such as dimethyl ether and methyl formate. In a subsequent study of the Orion Compact Ridge by Millar, Herbst & Charnley (1991), these researchers used much of the chemistry of Blake et al. (1987b) but found that it was necessary that methanol be injected into the source. Some of the hot-core chemistry used in this and subsequent studies is based on the laboratory work of Mautner and coworkers, as discussed by Ehrenfreund & Charnley (2000). Additional suggestions of the chemistry were made by Charnley et al. (1995) for complex alcohols.

It was not until much later that two problems emerged with complex molecule synthesis in the hot-core phase. The first problem has to do with the final step in a gas-phase synthesis, which is typically a dissociative recombination reaction in which the complex neutral molecule is produced in a product channel where one hydrogen atom is broken off. As discussed in Section 5.3 for the case of methanol in cold cores, the product channel $CH_3OH + H$ is only a very minor one. Other storage ring experiments show a similar pattern, although totally deuterated ions are often used to improve the resolution. For example, the formation of deuterated dimethyl ether from its deuterated ionic form $CD_3ODCD_3^+ + e^- \rightarrow CD_3OCD_3 + D$ only occurs with a branching fraction of 5% (M. Hamberg, F. Österdahl, R.D. Thomas, V. Zhaunerchyk, M. Kaminska, et al., in preparation). These small branching fractions are much less than assumed in earlier models and strongly reduce the formation rates of the complex hot-core neutrals. The second problem is that there is no very efficient process to synthesize protonated methyl formate [$HC(OH)OCH_3^+$] (Horn et al. 2004). Because methyl formate is perhaps the molecule most strongly associated with hot cores given its huge number of lines, failure to produce the protonated precursor to this species in the warm gas suggests most strongly that additional synthetic mechanisms are needed.

With these problems, the previously considered chemistry in the hot-core phase clearly could not explain the saturated species without revisions such as the synthesis of far larger ions than the neutral products of dissociative recombination reactions, resulting in a loss of efficiency. If the cold and warm-up stages are efficient in making most organic species on grains, then the warm gas-phase chemistry of the hot-core stage may be more important for the destruction of these species than for their formation.

CATEGORIES OF MODELS

Hot-core phase models: An initial gas-phase composition in the hot-core phase is assumed following sublimation, and the second-generation gas-phase chemistry is run for up to 10^5 years.

Cold-core and hot-core phase models: The zeroth and second-generation chemistries of the cold and hot-core stages are followed with instantaneous sublimation in between. Surface chemistry can be considered in the cold stage.

Cold-core and warm-up phase models: One follows the zeroth and first-generation gas and possibly surface chemistries during the cold and warm-up stages ending at the asymptotic temperature of the hot core or corino.

All-phase models: Here, the gas-phase and surface chemistries are followed through all phases.

6.4. Models and Predictions

The results of individual models are strongly dependent on whether surface reactions are included during the first two phases, and what the timescales and physical conditions are during all three phases. We can divide the models into a number of classes depending upon which phases and types of chemistry are considered. The categories are listed in a sidebar (see sidebar, Categories of Models). The models discussed in this section do not incorporate inhomogeneous physical conditions; models incorporating heterogeneity; that is, position-dependent physical conditions, are discussed in Section 6.6.

The best-known hot-core phase model is that of Charnley, Tielens & Millar (1992), who started with warm gas-phase initial molecular abundances considered to be variable parameters, in an attempt to explain why the Orion Hot Core and Compact Ridge have such differing chemistries. For the Hot Core, assumed to have constant physical conditions $T = 200$ K and $n_{\rm H} = 2 \times 10^7$ cm^{-3} after the warm-up phase, reasonable agreement with observational abundances was found at a time of 6.3×10^4 years with an initial gas-phase rich in ammonia although the only complex molecule calculated was CH_3CN. For the cooler and less dense Compact Ridge, the initially high abundance of methanol was sufficient to produce large abundances of dimethyl ether and methyl formate in 10^4 years. These results have been called into question by new results for the chemical processes, as discussed above. Despite the incompleteness of the second-generation approach, it is still used to determine hot-core lifetimes. The use of sulfur chemistry has shown some promise (Charnley 1997b, Wakelam et al. 2004). Nevertheless, the gas-phase time scales needed for hot corino chemistry may still be too long because they exceed the transit time of infalling gas (Schöier et al. 2002).

The initial cold-core and hot-core phase model was that of Brown, Charnley & Millar (1988), who used it to study the chemistry in the Orion Hot Core. Although accretion was considered during the cold stage, the surface chemistry was not followed. Following this work, Caselli, Hasegawa & Herbst (1993) used a similar model with surface chemistry to study the chemical differences between the Orion Hot Core and Compact Ridge. In their model, these differences stem from the density and temperature in the cold stage: the 40 K surface and gas temperature of the Hot Core does not allow many of the species more weakly bound to the grain to remain there long enough to react, whereas the 20 K surface and gas temperature of the Compact Ridge allows more heavy species to remain on the grain and react. In particular, any CO that lands on a 40 K grain cannot remain there, so that the hydrogenation to methanol does not occur in the Hot Core. On the other hand, enough gas-phase and surface chemistry occur to produce nitrogen-rich species such as propionitrile (C_2H_5CN) (Charnley 2001a, 1997a; Hasegawa & Herbst 1993). The overall

agreement with observation is reasonable in both sources within 10^4–10^5 years after the start of the hot-core stage, although once again, the hot methanol-based gas-phase chemistry of the Compact Ridge is not as efficient as estimated.

Following earlier work, Viti et al. (2004) reported a cold-core and warm-up phase model with sublimation treated in the latter phase by dividing up the adsorbates into five groups based on the TPD work of Collings et al. (2004). They did not include the surface chemistry in this phase, but were able to produce a high abundance of gaseous $HCOOCH_3$ toward the end of the warm-up phase for the case of a 15-$M_\odot$ protostar, presumably by the gas-phase chemistry starting from methanol. Their figures of gaseous abundances versus time during warm-up show a number of steep steps, corresponding to the desorption of various classes of adsorbates.

In their subsequent cold-core and warm-up phase model, Garrod & Herbst (2006) incorporated the formation of complex molecules both on cold surfaces and on surfaces that are warming up. The reaction network for the cold surface chemistry, however, is much smaller than that suggested by Charnley (2001a, 1997a). Large surface abundances of the complex species methyl formate and dimethyl ether are formed from radical-radical surface reactions during the warm-up phase, and sublimation at still higher temperatures during this phase creates high abundances in the gas-phase. **Figure 13** shows the surface and gas-phase abundances of methyl formate and other complex species during the warm-up phase for a medium-mass (10 $M_\odot$) star. The final results are

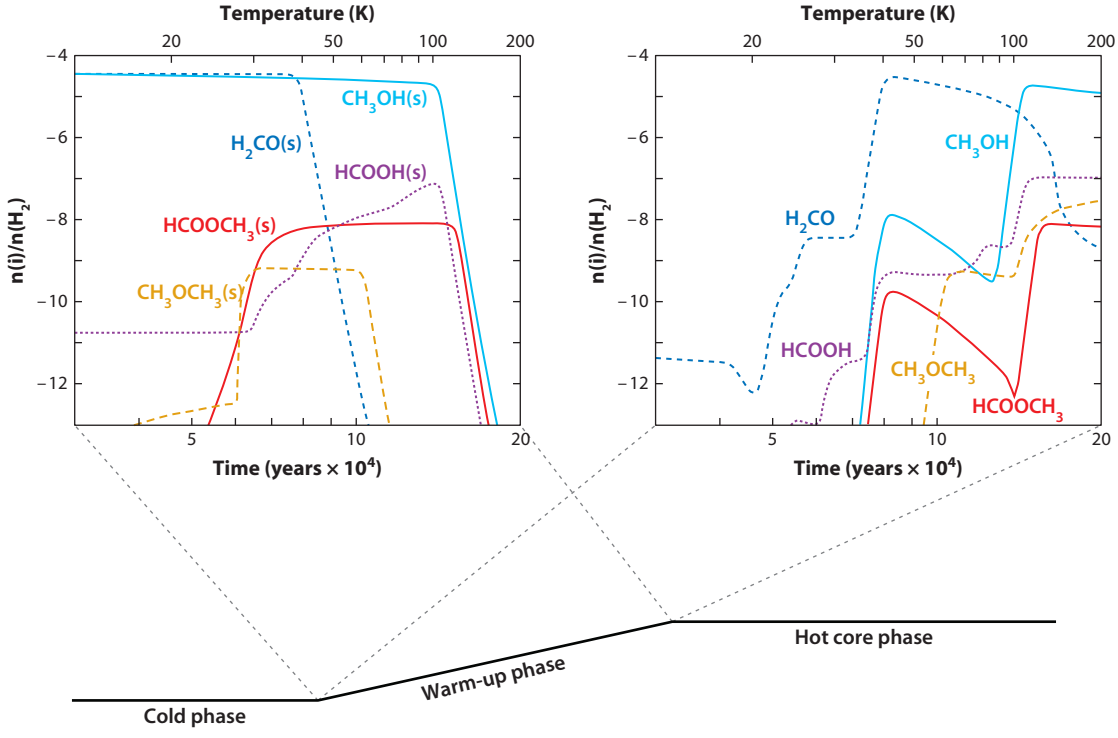

Figure 13

The abundances of methyl formate, dimethyl ether, formic acid, methanol, and formaldehyde during the warm-up phase around a star of intermediate mass (around 10 $M_\odot$), which lasts 2×10^5 years, after which the temperature of the core is 200 K. The heat-up occurs quadratically with time. The species in the ice mantles are designated by (s). Taken from Garrod & Herbst 2006, and provided in part by R. Garrod.

dependent on the details of the warm-up, such as its time scale (10^4–10^6 years), which is longer for lower mass stars, and whether the temperature rise is linear or quadratic with time. It is incorrect to state that surface chemistry is responsible for all of the synthesis of methyl formate and dimethyl ether during the warm-up stage; rather, considerable portions can still be formed in the gas during frequent recycling between gas and grain, depending on the details of the warm-up.

Garrod & Herbst (2006) compared the abundances of gaseous methyl formate, formic acid, dimethyl ether, formaldehyde and methanol at the time of peak methyl formate abundance (near the end of the warm-up phase) with observed abundances in the Orion Hot Core and Compact Ridge, and in two hot corinos—IRAS 16293–2422 and NGC 1333 IRAS 4A. No difference in physical conditions in the cold phase was assumed. The agreement is mixed for both the hot cores and the corinos. In general, the abundance of gas-phase $HCOOCH_3$ increases with the time of the warm-up whereas the dependence of the gas-phase CH_3OCH_3 abundance is more complex. Note that the more recent observations of Orion used in the comparison show that significant abundances of oxygen-containing molecules can be found in the Hot Core although they are less than those in the Compact Ridge (Sutton et al. 1995).

The recent study by Garrod, Weaver & Herbst (2008), an extension of the earlier model by Garrod & Herbst (2006), is the most complex example of a cold-core and warm-up phase model. This model makes predictions for abundances of a large number of first-generation neutral organic species during the warm-up period, and compares gaseous results with observations in Sgr B2(N). Moreover, the temperature of peak abundance for each molecular species during warm-up is associated with its measured rotational temperature, and a distinction is made, following Bisschop et al. (2007b), between "cold" and "hot" species. Agreement is quite reasonable for both peak abundances and their temperatures. Note that the model effectively incorporates heterogeneity in temperature although it does not follow physical structure as a function of time.

Another extension of the work of Garrod & Herbst (2006) has been undertaken by Hassel, Herbst & Garrod (2008), who ran hot-core/corino models with all three phases. Although inclusion of the second-generation chemistry in the hot-core phase showed that the abundances of saturated organic species eventually decrease, the work led to the unexpected prediction that observable abundances for unsaturated carbon-chain species exist.

6.5. Carbon-Chain Species?

Although models indicate why hot cores and corinos are likely to have saturated organic molecules, they do not indicate that unsaturated carbon chains are not present. Hassel, Herbst & Garrod (2008) used a three-phase model designed primarily to study the envelope of the protostellar source L1527, which has a temperature of only 30 K for much of the envelope (but see Section 4.4.2). This source was found to be rich in gaseous carbon chain species (e.g., C_nH, $HC_{2n+1}N$) by Sakai et al. (2008), who argued that the chemistry was similar to the models of hot corinos except that at 30 K, only a few vaporizable species come off the grain mantles, the most important of which is methane (CH_4) because it is the precursor of an ion-molecule gas-phase chemistry. The model reproduces the observations well, but a continuation of the warm-up to the temperatures of hot corinos and cores followed by the hot-core phase shows that the carbon-chain species do not decrease in abundance but rather have even higher abundances, which last for a considerable amount of time. More recently, Chapman et al. (2009) presented a gas-phase chemical model of a hot core with high but transitory abundances of the cyanopolyynes, thought to form from the precursor acetylene (C_2H_2) in the gas phase (see also Lahuis & van Dishoeck 2000).

In the main, unsaturated species are not detected in hot cores via rotational emission with the exception of HC_3N, although there is some evidence for them in the hot corino IRAS 16293–2422

(E. Caux, personal communication). Upper limits to the abundance ratios C_4H/CH_3OH and HC_5N/CH_3OH for seven hot cores have kindly been provided to us by S. and J. Jørgensen-Bisschop; these ratios lie around 0.01–0.1. The peak theoretical ratios at 200 K are also in the range 0.01–0.1 (Hassel, Herbst & Garrod 2008). Given that the abundance of methanol is typically high in hot cores, significant amounts of C_4H and HC_5N are not ruled out by the observations. One reason for the apparent nondetection of carbon chains in hot cores may be that the spectra of the saturated species are so dense that it is difficult to detect the less dense spectra of unsaturated linear species (see **Figure 2**).

6.6. Physical Structure

Most of the models discussed up to now are one-point (0-dimensional) models, in which although physical conditions can change with time, there is no explicit allowance made for inhomogeneity at a given time. Such inhomogeneity can encompass the physical conditions assumed in the one-point models discussed above; e.g., the outer envelope can be cold (cold phase), the middle envelope can have temperatures in the range 10–100 K (warm-up phase), and the inner envelope can have still higher temperatures (hot-core phase). Models with inhomogeneity in physical conditions are known as multipoint models; these can be either time-independent or time-dependent. An example of a time-independent model is one where concentric spherical shells of differing physical conditions are added together to form a noncollapsing core. Such a model is often used for prestellar cores (Roberts, Herbst & Millar 2004). At its most detailed, the time-dependence of the physical conditions can be handled by hydrodynamics (Aikawa et al. 2005).

To illustrate some different approaches to physical structure and dynamics, let us look at a few models of the chemistry that occurs during the formation of low-mass protostellar cores and their hot corinos. Doty, Schöier & van Dishoeck (2004) adapted a time-independent physical structure for the protostellar envelope/hot corino IRAS 16293–2422 and two sets of initial gas-phase abundances, including polyatomic species, depending on the temperature. In the structure, the temperature ranges from 10 K up to near 300 K and the density from below 10^5 cm^{-3} to upwards of 10^9 cm^{-3} (**Figure 4**, *bottom right*). Time-dependent gas-phase chemistry is followed and the effects of freeze-out onto and desorption from grains are treated approximately. Molecules come off the grains inside specific radii according to their surface binding energies, resulting in distinct spatial zones in the envelope with their own characteristic chemistries. The model also treats radiative transfer so that line strengths can be calculated as output. At times of 3×10^3–3×10^4 years after turn-on of the protostar, the model can reproduce many line strengths to better than 50%.

Lee, Bergin & Evans (2004) calculated molecular abundances and line profiles for a protostellar core model with a time-dependent physical structure. The structure starts out as a cold hydrostatic sphere, and undergoes inside-out collapse (Shu 1977) as matter moves inwards to warmer and denser regions while time-dependent gas-phase chemistry occurs (see **Figure 14**). Once again, adsorption and desorption of species is included, but no grain surface chemistry. The species-dependent evaporation fronts move outwards as the protostar increases in luminosity. Although the qualitative features of adsorption and desorption are similar, the calculated molecular abundance profiles and line shapes for heterogeneous models with time-dependent physical conditions differ from those from a static calculation because static models do not account for infall (Lee, Evans & Bergin 2005).

More recently, Aikawa et al. (2008) combined a model with both gas-phase and grain-surface chemistry and one-dimensional hydrodynamic collapse to calculate abundances as functions of time and position for a low-mass spherical core collapsing from the prestellar to the protostellar stage. Similar to the study of Lee, Bergin & Evans (2004), shells of material fall inward towards

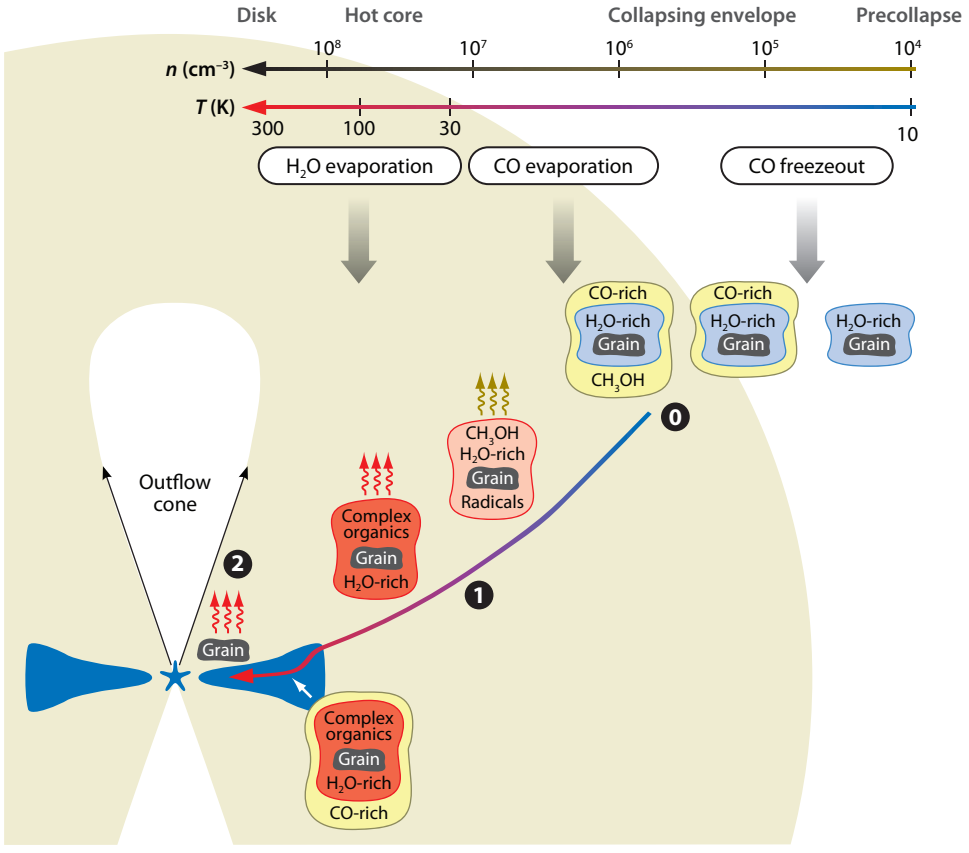

Figure 14

Cartoon representation of the evolution of material from the prestellar core stage through the collapsing envelope (size ~0.05 pc) into a protoplanetary disk. The formation of zeroth- and first-generation organic molecules in the ices is indicated with 0 and 1, and the second-generation molecules in the hot-core/corino region when the envelope temperature reaches 100 K, and even strongly bound ices start to evaporate, are designated 2. The grains are typically 0.1 μm and are not drawn to scale. The temperature and density scale refer to the envelope, not to the disk (see also **Figure 4**). Once material enters the disk, it will rapidly move to the cold midplane where additional freeze-out and grain surface chemistry occur. All ices evaporate inside the (species-dependent) sublimation radius. For H_2O and trapped complex organic molecules, this "snow line" lies around a few astronomical units in a disk around a solar mass star. Figure by E. van Dishoeck & R. Visser.

the protostar and warm up. As in the one-point model of Hassel, Herbst & Garrod (2008), much of the chemistry leading to the synthesis of complex molecules occurs between radicals on the surfaces of warming dust particles. The model is in reasonable agreement with observed gas-phase abundances in the hot corino IRAS 16293–2422 including some complex molecules, and with ice-mantle abundances in the low-mass protostar Elias 29.

Although it does not contain an explicit complex molecule chemistry, an even more recent treatment follows the evolution of matter from a collapsing envelope into a circumstellar disk via a two-dimensional semianalytical model (Visser et al. 2009). The chemical history of material in the disk depends on its location: In the inner disk, weakly bound species like CO have adsorbed and desorbed from the grains multiple times during their journey from cloud to disk, whereas the outer disk still contains pristine CO ice from the prestellar stage. Strongly bound molecules like H_2O

stay mostly as ice until they enter the inner few AU of disks (see **Figure 14**). One looks forward to the inclusion of complex chemistry into this multiphase picture, but initial results indicate that the material that ends up in the planet- and comet-forming zones of disks spends enough time at temperatures of 20–40 K for some complex surface chemistry to occur.

7. RELATION TO OTHER ORGANIC COMPOUNDS

The complex organic molecules discussed in this review comprise only a small fraction of the total carbon budget: <0.1% for the long chains in cold clouds, and up to a few% for the saturated organic molecules in hot cores or corinos. The majority of carbon in interstellar clouds (at least 30%) is in some form of carbonaceous solids with grain sizes large enough that they lack any clear spectroscopic signature other than continuous opacity. Another fraction of the carbon (about 30%) can be in gaseous C, C^+, and/or CO. In the coldest clouds, most of this carbon is frozen out and transformed into volatile ices, including CO, CO_2, CH_4, CH_3OH, and HCOOH. The remaining ∼20%–40% is in some form of small grains and carbonaceous molecules (gas or ice) whose composition cannot be unambiguously established (for summary and references, see van Dishoeck 2008).

Most of the information on the composition of this remaining 20%–40% comes from observations of diffuse clouds. A fraction consists of PAHs, as seen by their characteristic infrared emission bands (Tielens 2008): ∼4% of carbon is in small PAHs containing up to ∼100 carbon atoms, ∼2% in larger PAHs. Very Small Grains (VSGs) contain a similar amount. The carrier of the 2175 Å bump observed in the UV extinction curve contains about ∼15%. The leading candidates for the identification of this carrier are graphite and hydrogenated amorphous carbon (HAC), a material consisting of islands of aromatic C joined by a variety of peripheral hydrocarbons (e.g., Draine 2003). This type of carbonaceous material is consistent with that proposed for the carrier of the 3.4 μm absorption feature and from new *Spitzer* observations of the 5–8 μm region in diffuse clouds, both of which also require ∼15% of the available carbon (Dartois & Muñoz-Caro 2007), suggesting that the UV and infrared data indeed probe the same material.

7.1. Comets and Meteorites

Many volatile organic molecules, including several complex ones, have been detected in bright comets like Hale-Bopp with modern millimeter and infrared telescopes (Bockelée-Morvan et al. 2004). Most of them are parent species evaporating directly from the ices. A strong correlation is found between their abundances and those observed in hot cores and corinos covering many orders of magnitude, suggesting that at least some of the volatile ices observed in star-forming regions are incorporated unaltered into icy solar system bodies. Observations of a diverse sample of comets show that—just as in interstellar clouds—variations in ice abundances exist, with organics like CH_3OH and C_2H_2 depleted by a factor of 3 or more in some comets.

Complex organic molecules have been found in the cometary granular samples returned from the *Stardust* mission, with a heterogeneous distribution in abundance and composition among particles (Sandford 2008). Here, many of the organic species are PAHs, with typical sizes of just a few rings, that is, generally smaller than the PAH size inferred in the diffuse clouds. Also, a new class of aromatic-poor organic material has been found compared with that seen in interplanetary dust particles.

The most primitive and least processed meteorites—the so-called carbonaceous chondrites—also contain ample organic material. Well-known examples are the Murchison, Orgueil, and Tagish Lake meteorites. Most of the organic species (60%–80%) are in an insoluble macromolecular

form, often described as kerogen-like. The remaining ~20% is in a soluble form and has been found to contain carboxylic acids, PAHs, fullerenes, purines, amides, and other prebiotic molecules including amino acids (Botta & Bada 2002, Cronin & Chang 1993). Enantiomeric excess (chirality) has been found for at least some meteoritic amino acids (Cronin & Pizzarello 1997). Note that most of these organic molecules are not the original interstellar ones but are likely formed from reactions with liquid water under the high pressure in the parent body.

8. THE FUTURE

Molecular astronomy will be strongly influenced by the imminent arrival of three major new telescopes: the *Herschel Space Observatory*, the *Atacama Large Millimeter/submillimeter Array* (ALMA), and the *Stratospheric Observatory for Infrared Astronomy* (SOFIA). These facilities will allow molecular astronomers to detect new molecules, study nearby objects at high spatial and spectral resolution, and open up the field of extragalactic molecular astronomy. The improved spatial resolution will strongly affect chemical models of interstellar sources; inclusion of heterogeneity and dynamics will become mandatory. The evolutionary stages of stellar and planetary formation will be better understood, especially the formation of intermediate- and high-mass stars and the evolution of disks around low-mass stars.

In the 35-year lifetime during which polyatomic molecules have been observed in the interstellar medium, the study of complex interstellar molecules has enriched our knowledge of how these species are produced and what their existence tells us about the formation of both low-mass and high-mass stars. In the next 35 years, we can expect that complex molecules will become far better probes of star formation than they currently are. We can also hope that our increased knowledge of molecular complexity throughout the universe will help us to gain a greater comprehension of one of the true current mysteries in science: the formation of life.

FUTURE ISSUES

1. The observation of new classes of complex molecules. Such species include molecules of obvious biological interest such as glycine, the simplest amino acid, and other prebiotic molecules of minor abundance; large carbonaceous molecules such as linear chains with many more than 10 carbon atoms, large single-ring molecules, and fullerenes (e.g., C_{60}); large anions such as negatively charged PAHs; and doubly charged positive molecular ions.
2. An improvement in our knowledge of relevant chemical processes. To understand the chemistry of complex molecules better, modelers will need a better understanding of a number of chemical processes. In the gas phase, these include the formation and destruction of negative ions, and, more generally, the improvement in our knowledge of reactions shown by sensitivity analyses to influence strongly the abundances of many species in models. In the solid phase, many more rates for specific chemical reactions need to be studied and quantified in the laboratory; for example, the bulk of the reactions in **Figure 12** have not yet been measured. We also need to understand how to better extrapolate such laboratory results to interstellar time scales and how to better model surface reactions on small grains, where rate equations are inadequate and stochastic methods too time-consuming. Finally, we need to understand both the rates and mechanisms of nonthermal desorption mechanisms better.

3. An understanding of the physical structure and dynamics of hot cores and corinos and how they relate to the formation of complex molecules. There are clearly many more YSOs than there are hot cores and corinos. Although hot corino sources are typically small and weak, the same cannot be said for hot cores. Why then are they so few in number? Also, since the hot-core stage is a fecund one for the formation of complex molecules, a deeper understanding of how these complex molecules are formed and destroyed will help us to elucidate many astrophysical aspects of hot cores.
4. An understanding of the complex molecules present in sources where they are currently not found, such as protoplanetary disks. A set of complex molecules similar to those detected in hot corinos and hot cores will likely soon be found in these disks. The inventory and spatial heterogeneity of complex molecules will help us to constrain the molecules that might be present as planets form.
5. A better understanding of the environments in the Galactic Center where complex molecules are currently found. Why are complex saturated molecules found in dense regions of the Galactic Center in addition to the hot cores and not found in similar regions in the Orion Molecular Cloud?

DISCLOSURE STATEMENT

The authors are not aware of any affiliations, memberships, funding, or financial holdings that might be perceived as affecting the objectivity of this review.

ACKNOWLEDGMENTS

We acknowledge the assistance of S. Bruenken, S. Charnley, W. Irvine, J. Martín-Pintado, K. Öberg, M. Ohishi, A. Remijan, L. Snyder, and S. Widicus Weaver for reading and criticizing portions of the manuscript. We are grateful to R. Bachiller, E. Bergin, A. Belloche, H. Beuther, S. Bisschop, S. Bottinelli, E. Caux, C. Ceccarelli, J. Cernicharo, H. Cuppen, R. Garrod, J. Jørgensen, J. Martín-Pintado, K. Menten, T. Millar, K. Öberg, M. Ohishi, D. Quan, C. Qi, P. Schilke, M. Tafalla, S. Thorwirth, A. Tielens, R. Visser, and A. Walters for answering many questions, checking numbers, and providing figures. E. H. acknowledges the support of the National Science Foundation and NASA for his research programs in astrochemistry and spectroscopy, and E. v. D. acknowledges support from the Netherlands Research School for Astronomy (NOVA) and from a Spinoza grant from the Netherlands Organization for Scientific Research (NWO).

LITERATURE CITED

Aikawa Y, Herbst E, Roberts H, Caselli P. 2005. *Ap. J.* 620:330
Aikawa Y, Wakelam V, Garrod RT, Herbst E. 2008. *Ap. J.* 674:984
Allamandola LJ, Tielens AGGM, Barker JR. 1989. *Ap. J. Suppl.* 71:733
Allen M, Robinson GW. 1977. *Ap. J.* 212:396
Andersson S, van Dishoeck EF. 2008. *Astron. Astrophys.* 491:907
Apponi AJ, Halfen DT, Ziurys LM, Hollis JM, Remijan AJ, Lovas FJ. 2006. *Ap. J. Lett.* 643:L29
Araya E, Hofner P, Kurtz S, Bronfman L, DeDeo S. 2005. *Ap. J. Suppl.* 157:279
Arce HG, Santiago-García J, Jørgensen JK, Tafalla M, Bachiller R. 2008. *Ap. J. Lett.* 681:L21

Bachiller R, Liechti S, Walmsley CM, Colomer F. 1995. *Astron. Astrophys.* 295:L51
Bachiller R, Perez Gutierrez M. 1997. *Ap. J. Lett.* 487:L93
Barckholtz C, Snow TP, Bierbaum VM. 2001. *Ap. J. Lett.* 547:L171
Barzel B, Biham O. 2007. *J. Chem. Phys.* 127:144703
Bates DR. 1987. *Ap. J.* 312:363
Belloche A, Comito C, Hieret C, Menten KM, Mueller HSP, Schilke P. 2007. See LeMaire & Combes 2007, p. 65 (*ArXiv e-print* arXiv:0801.3214)
Belloche A, Menten KM, Comito C, Müller HSP, Schilke P, et al. 2008. *Astron. Astrophys.* 482:179
Beltrán MT, Cesaroni R, Neri R, Codella C, Furuya RS, et al. 2005. *Astron. Astrophys.* 435:901
Bennett CJ, Kaiser RI. 2007. *Ap. J.* 661:899
Bergin EA, Aikawa Y, Blake GA, van Dishoeck EF. 2007. See Reipurth, Jewitt & Keil 2007, p. 751
Bergin EA, Hartmann LW, Raymond JC, Ballesteros-Paredes J. 2004. *Ap. J.* 612:921
Bergin EA, Tafalla M. 2007. *Annu. Rev. Astron. Astrophys.* 45:339
Bettens RPA, Herbst E. 1995. *Int. J. Mass Spect. Ion Proc.* 149:321
Beuther H, Zhang Q, Bergin EA, Sridharan TK, Hunter TR, Leurini S. 2007. *Astron. Astrophys.* 468:1045
Beuther H, Zhang Q, Sridharan TK, Lee CF, Zapata LA. 2006. *Astron. Astrophys.* 454:221
Bisschop SE, Fuchs GW, van Dishoeck EF, Linnartz H. 2007a. *Astron. Astrophys.* 474:1061
Bisschop SE, Jørgensen JK, Bourke TL, Bottinelli S, van Dishoeck EF. 2008. *Astron. Astrophys.* 488:959
Bisschop SE, Jørgensen JK, van Dishoeck EF, de Wachter EBM. 2007b. *Astron. Astrophys.* 465:913
Blake GA, Laughlin KB, Cohen RC, Busarow KL, Saykally RJ. 1987a. *Ap. J. Lett.* 316:L45
Blake GA, Sandell G, van Dishoeck EF, Groesbeck TD, Mundy LG, Aspin C. 1995. *Ap. J.* 441:689
Blake GA, Sutton EC, Masson CR, Phillips TG. 1987b. *Ap. J.* 315:621
Bockelée-Morvan D, Crovisier J, Mumma MJ, Weaver HA. 2004. In *The Composition of Cometary Volatiles. Comets II*, ed. MC Festou, HU Keller, HA Weaver, p. 391. Tucson: Univ. Arizona Press
Boogert ACA, Pontoppidan KM, Knez C, Lahuis F, Kessler-Silacci J, et al. 2008. *Ap. J.* 678:985
Botta O, Bada JL. 2002. *Surv. Geophys.* 23:411
Bottinelli S, Ceccarelli C, Lefloch B, Williams JP, Castets A, et al. 2004a. *Ap. J.* 615:354
Bottinelli S, Ceccarelli C, Neri R, Williams JP, Caux E, et al. 2004b. *Ap. J. Lett.* 617:L69
Bottinelli S, Ceccarelli C, Williams JP, Lefloch B. 2007. *Astron. Astrophys.* 463:601
Boudin N, Schutte WA, Greenberg JM. 1998. *Astron. Astrophys.* 331:749
Brogan CL, Chandler CJ, Hunter TR, Shirley YL, Sarma AP. 2007. *Ap. J. Lett.* 660:L133
Brown PD, Charnley SB, Millar TJ. 1988. *MNRAS* 231:409
Brünken S, Gupta H, Gottlieb CA, McCarthy MC, Thaddeus P. 2007. *Ap. J. Lett.* 664:L43
Carr JS, Najita JR. 2008. *Science* 319:1504
Carvajal M, Willaert F, Demaison J, Kleiner I. 2007. *J. Mol. Spec.* 246:158
Caselli P, Hasegawa TI, Herbst E. 1993. *Ap. J.* 408:548
Caux E, Bacmann A, Castets A, Cazaux S, Ceccarelli C, et al. 2005. In *Astrochemistry: Recent Successes and Current Challenges*, IAU Symp. 231, Poster 12 Sess. 2; **http://asilomar.caltech.edu**
Cazaux S, Tielens AGGM, Ceccarelli C, Castets A, Wakelam V, et al. 2003. *Ap. J. Lett.* 593:L51
Ceccarelli C. 2005. See Lis, Blake & Herbst 2005, p. 1
Ceccarelli C, Caselli P, Herbst E, Tielens AGGM, Caux E. 2007. See Reipurth, Jewitt & Keil 2007, p. 47
Ceccarelli C, Castets A, Loinard L, Caux E, Tielens AGGM. 1998. *Astron. Astrophys.* 338:L43
Cesaroni R, Felli M, Testi L, Walmsley CM, Olmi L. 1997. *Astron. Astrophys.* 325:725
Chandler CJ, Brogan CL, Shirley YL, Loinard L. 2005. *Ap. J.* 632:371
Chang Q, Cuppen HM, Herbst E. 2007. *Astron. Astrophys.* 469:973
Chapman JF, Wardle M, Millar TJ, Burton MG, Walsh AJ. 2009. *MNRAS* 394:221
Charnley SB. 2001a. In *The Bridge Between the Big Bang and Biology: Stars, Planetary Systems, Atmospheres, Volcanoes: Their Link to Life*, ed. F Giovannelli, p. 139. Rome: Cons. Naz. Ric.
Charnley SB. 1997a. In *Astronomical and biochemical origins and the search for life in the universe. Proc.*, ed. CB Cosmovici, S Bowyer, D Werthimer. *IAU Colloq.* 161:89. Bologna, Italy: Ed. Compos.
Charnley SB. 1997b. *Ap. J.* 481:396

Charnley SB. 2001b. *Ap. J. Lett.* 562:L99
Charnley SB, Kress ME, Tielens AGGM, Millar TJ. 1995. *Ap. J.* 448:232
Charnley SB, Tielens AGGM, Millar TJ. 1992. *Ap. J. Lett.* 399:L71
Charnley SB, Tielens AGGM, Rodgers SD. 1997. *Ap. J. Lett.* 482:L203
Churchwell E, Wood D, Myers PC, Myers RV. 1986. *Ap. J.* 305:405
Collings MP, Anderson MA, Chen R, Dever JW, Viti S, et al. 2004. *MNRAS* 354:1133
Comito C, Schilke P, Phillips TG, Lis DC, Motte F, Mehringer D. 2005. *Ap. J. Suppl.* 156:127
Cox NLJ, Spaans M. 2006. *Astron. Astrophys.* 451:973
Cravens TE, Dalgarno A. 1978. *Ap. J.* 219:750
Cronin JR, Chang S. 1993. In *The Chemistry of Life's Origins*. NATO ASI Ser., ed. JM Greenberg, CX Mendoza-Gomez, V. Pirronello, 416:209
Cronin JR, Pizzarello S. 1997. *Science* 275:951
Cummins SE, Linke RA, Thaddeus P. 1986. *Ap. J. Suppl.* 60:819
Dartois E, Muñoz-Caro GM. 2007. *Astron. Astrophys.* 476:1235
De Lucia FC, Helminger P, Cook RL, Gordy W. 1972. *Phys. Rev. A* 5:487
Dickens JE, Langer WD, Velusamy T. 2001. *Ap. J.* 558:693
Doty SD, Schöier FL, van Dishoeck EF. 2004. *Astron. Astrophys.* 418:1021
Draine BT. 2003. *Annu. Rev. Astron. Astrophys.* 41:241
Dutrey A, Guilloteau S, Guelin M. 1997. *Astron. Astrophys.* 317:L55
Ehrenfreund P, Charnley SB. 2000. *Annu. Rev. Astron. Astrophys.* 38:427
Elsila JE, Dworkin JP, Bernstein MP, Martin MP, Sandford SA. 2007. *Ap. J.* 660:911
Fontani F, Pascucci I, Caselli P, Wyrowski F, Cesaroni R, Walmsley CM. 2007. *Astron. Astrophys.* 470:639
Friberg P, Hjalmarson A, Madden SC, Irvine WM. 1988. *Astron. Astrophys.* 195:281
Garrod RT. 2008. *Astron. Astrophys.* 491:239
Garrod RT, Park IH, Caselli P, Herbst E. 2006. *Faraday Discuss.* 133:51
Garrod RT, Wakelam V, Herbst E. 2007. *Astron. Astrophys.* 467:1103
Garrod RT, Herbst E. 2006. *Astron. Astrophys.* 457:927
Garrod RT, Weaver SLW, Herbst E. 2008. *Ap. J.* 682:283
Genzel R. 1992. In *Saas-Fee Advanced Course 21: The Galactic Interstellar Medium*, ed. WB Burton, BG Elmegreen, R Genzel, p. 275. Swiss Soc. Astrophys. Astron.
Geppert WD, Hamberg M, Thomas RD, Österdahl F, Hellberg F, et al. 2006. *Far. Disc.* 133:177
Geppert WD, Hellberg F, Österdahl F, Semaniak J, Millar TJ, et al. 2005. See Lis, Blake & Herbst 2005, p. 117
Gibb E, Nummelin A, Irvine WM, Whittet DCB, Bergman P. 2000a. *Ap. J.* 545:309
Gibb EL, Whittet DCB. 2002. *Ap. J. Lett.* 566:L113
Gibb EL, Whittet DCB, Boogert ACA, Tielens AGGM. 2004. *Ap. J. Suppl.* 151:35
Gibb EL, Whittet DCB, Schutte WA, Boogert ACA, Chiar JE, et al. 2000b. *Ap. J.* 536:347
Gordy W, Cook RL. 1984. *Microwave Molecular Spectra*. New York: Wiley
Gould RJ, Salpeter EE. 1963. *Ap. J.* 138:393
Gredel R, Lepp S, Dalgarno A, Herbst E. 1989. *Ap. J.* 347:289
Green NJB, Toniazzo T, Pilling MJ, Ruffle DP, Bell N, Hartquist TW. 2001. *Astron. Astrophys.* 375:1111
Greenberg JM, Li A, Mendoza-Gomez CX, Schutte WA, Gerakines PA, de Groot M. 1995. *Ap. J. Lett.* 455:L177
Groesbeck TD. 1995. *The Contribution of Molecular Line Emission to Broadband Flux Measurements at Millimeter and Submillimeter Wavelengths*. PhD thesis, Calif. Inst. Technol.
Groner P. 1997. *J. Chem. Phys.* 107:4483
Halfen DT, Ziurys LM. 2008. See Kwok & Sanford 2008, p. 27
Hasegawa TI, Herbst E. 1993. *MNRAS* 261:83
Hasegawa TI, Herbst E, Leung CM. 1992. *Ap. J. Suppl.* 82:167
Hassel GE, Herbst E, Garrod RT. 2008. *Ap. J.* 681:1385
Hatchell J, Thompson MA, Millar TJ, MacDonald GH. 1998. *Astron. Astrophys. Suppl.* 133:29
Helmich FP, van Dishoeck EF. 1997. *Astron. Astrophys. Suppl.* 124:205
Herbst E. 1991. *Ap. J.* 366:133

Herbst E, Klemperer W. 1973. *Ap. J.* 185:505
Herbst E, Millar TJ. 2008. In *Low Temperatures and Cold Molecules*. ed. IWM Smith, p. 1. London: Imperial College Press
Herbst E, Osamura Y. 2008. *Ap. J.* 679:1670
Herbst E, Wakelam V. 2008. The Ohio State University astrophysical chemistry group. **http://www.physics.ohio-state.edu/~eric/research.html**
Hirota T, Maezawa H, Yamamoto S. 2004. *Ap. J.* 617:399
Hirota T, Yamamoto S. 2006. *Ap. J.* 646:258
Hogerheijde MR, Jansen DJ, van Dishoeck EF. 1995. *Astron. Astrophys.* 294:792
Hogerheijde MR, van Dishoeck EF, Blake GA, van Langevelde HJ. 1998. *Ap. J.* 502:315
Hollis JM, Churchwell E. 2001. *Ap. J.* 551:803
Hollis JM, Jewell PR, Lovas FJ, Remijan A. 2004a. *Ap. J. Lett.* 613:L45
Hollis JM, Jewell PR, Lovas FJ, Remijan A, Møllendal H. 2004b. *Ap. J. Lett.* 610:L21–24
Hollis JM, Lovas FJ, Jewell PR, Coudert LH. 2002. *Ap. J. Lett.* 571:L59
Hollis JM, Lovas FJ, Remijan AJ, Jewell PR, Ilyushin VV, Kleiner I. 2006. *Ap. J. Lett.* 643:L25
Horn A, Møllendal H, Sekiguchi O, Uggerud E, Roberts H, et al. 2004. *Ap. J.* 611:605
Iglesias-Groth S, Manchado A, García-Hernández DA, González Hernández JI, Lambert DL. 2008. *Ap. J. Lett.* 685:L55
Ikeda M, Ohishi M, Nummelin A, Dickens JE, Bergman P, et al. 2001. *Ap. J.* 560:792
Ioppolo S, Fuchs GW, Bisschop SE, van Dishoeck EF, Linnartz H. 2007. See LeMaire & Combes 2007, p. 275
Irvine WM, Ellder J, Hjalmarson A, Kollberg E, Rydbeck OEH, et al. 1981. *Astron. Astrophys.* 97:192–94
Johansson LEB, Andersson C, Ellder J, Friberg P, Hjalmarson A, et al. 1984. *Astron. Astrophys.* 130:227
Johnstone D, Boonman AMS, van Dishoeck EF. 2003. *Astron. Astrophys.* 412:157
Jørgensen JK. 2004. *Astron. Astrophys.* 424:589
Jørgensen JK, Bourke TL, Myers PC, Di Francesco J, van Dishoeck EF, et al. 2007. *Ap. J.* 659:479
Jørgensen JK, Bourke TL, Myers PC, Schöier FL, van Dishoeck EF, Wilner DJ. 2005a. *Ap. J.* 632:973
Jørgensen JK, Hogerheijde MR, Blake GA, van Dishoeck EF, Mundy LG, Schöier FL. 2004. *Astron. Astrophys.* 415:1021
Jørgensen JK, Lahuis F, Schöier FL, van Dishoeck EF, Blake GA, et al. 2005b. *Ap. J. Lett.* 631:L77
Jørgensen JK, Schöier FL, van Dishoeck EF. 2005a. *Astron. Astrophys.* 437:501
Jørgensen JK, Schöier FL, van Dishoeck EF. 2005b. *Astron. Astrophys.* 435:177
Kaifu N, Ohishi M, Kawaguchi K, Saito S, Yamamoto S, et al. 2004. *Publ. Astron. Soc. Jpn.* 56:69
Kim HD, Cho SH, Chung HS, Kim HR, Roh DG, et al. 2000. *Ap. J. Suppl.* 131:483
Kim HD, Cho SH, Lee CW, Burton MG. 2001. *J. Korean Astron. Soc.* 34:167
Kim SJ, Kim HD, Lee Y, Minh YC, Balasubramanyam R, et al. 2006. *Ap. J. Suppl.* 162:161
Kimura Y, Saito M, Sakon I, Kaito C. 2007. In *Lunar Planet. Inst. Conf., 38th. Abstr.* 1338:1511
Kleiner I, Hougen JT. 2003. *J. Chem. Phys.* 119:5505
Knez C, Boogert ACA, Pontoppidan KM, Kessler-Silacci J, van Dishoeck EF, et al. 2005. *Ap. J. Lett.* 635:L145
Kobayashi K, Ogata K, Tsunekawa S, Takano S. 2007. *Ap. J. Lett.* 657:L17
Kolasinski KW. 2002. *Surface Science*. Chichester: Wiley. 1st ed.
Kuan YJ, Charnley SB, Huang HC, Kisiel Z, Ehrenfreund P, et al. 2004a. *Adv. Space Res.* 33:31
Kuan YJ, Charnley SB, Huang HC, Tseng WL, Kisiel Z. 2003. *Ap. J.* 593:848
Kuan YJ, Huang HC, Charnley SB, Hirano N, Takakuwa S, et al. 2004b. *Ap. J. Lett.* 616:L27
Kurtz S, Cesaroni R, Churchwell E, Hofner P, Walmsley CM. 2000. *Protostars and Planets IV*, ed. V Mannings, AP Boss, SS Russell, p. 299. Tucson: Univ. Ariz. Press
Kwok S, Sanford S, eds. 2008. *Organic Matter in Space*, IAU Symp. 251. Cambridge, UK: Cambridge Univ. Press
Lahuis F, van Dishoeck EF. 2000. *Astron. Astrophys.* 355:699
Lahuis F, van Dishoeck EF, Boogert ACA, Pontoppidan KM, Blake GA, et al. 2006. *Ap. J. Lett.* 636:L145
Lee CW, Cho SH, Lee SM. 2001. *Ap. J.* 551:333
Lee JE, Bergin EA, Evans NJ. 2004. *Ap. J.* 617:360

Lee JE, Evans NJ II, Bergin EA. 2005. *Ap. J.* 631:351
Léger A, D'Hendecourt L, Defourneau D. 1989. *Astron. Astrophys.* 216:148
Leurini S, Schilke P, Wyrowski F, Menten KM. 2007. *Astron. Astrophys.* 466:215
Lis DC, Blake GA, Herbst E, eds. 2005. *Astrochemistry: Recent Successes and Current Challenges*, IAU Symp. 231. Cambridge, UK: Cambridge Univ. Press
Liszt HS, Lucas R, Pety J. 2006. *Astron. Astrophys.* 448:253
Lovas FJ, Hollis JM, Remijan AJ, Jewell PR. 2006. *Ap. J. Lett.* 645:L137
Luca A, Voulot D, Gerlich D. 2002. WDS'02 Proc. Contributed Papers, Part ii, p. 294. Prague
MacDonald GH, Gibb AG, Habing RJ, Millar TJ. 1996. *Astron. Astrophys.* 119:333
Maeda A, Medvedev IR, De Lucia FC, Herbst E, Groner P. 2008. *Ap. J. Suppl.* 175:138
Maezawa H, Ikeda M, Ito T, Saito G, Sekimoto Y, et al. 1999. *Ap. J. Lett.* 524:L129
Marcelino N, Cernicharo J, Agúndez M, Roueff E, Gerin M, et al. 2007. *Ap. J. Lett.* 665:L127
Maret S, Ceccarelli C, Tielens AGGM, Caux E, Lefloch B, et al. 2005. *Astron. Astrophys.* 442:527
Markwick AJ, Millar TJ, Charnley SB. 2000. *Ap. J.* 535:256
Markwick-Kemper AJ. 2003. astrochemistry.net. **http://astrochemistry.net/**
McCarthy MC, Gottlieb CA, Gupta H, Thaddeus P. 2006. *Ap. J. Lett.* 652:L141
McCutcheon WH, Sandell G, Matthews HE, Kuiper TBH, Sutton EC, et al. 2000. *MNRAS* 316:152
McEwan MJ, Scott GBI, Adams NG, Babcock LM, Terzieva R, Herbst E. 1999. *Ap. J.* 513:287
Medvedev IR, De Lucia FC. 2007. *Ap. J.* 656:621
Mennella V, Brucato JR, Colangeli L, Palumbo P. 2002. *Ap. J.* 569:531
Menten KM. 2004. In *The Dense Interstellar Medium in Galaxies*, ed. S Pfalzner, C Kramer, C Staubmeier, A Heithausen, p. 69, Springer Proc. Phys., Vol. 91. Berlin: Springer
Millar TJ, Herbst E, Charnley SB. 1991. *Ap. J.* 369:147
Millar TJ, Walsh C, Cordiner MA, Ní Chuimín R, Herbst E. 2007. *Ap. J. Lett.* 662:L87
Muñoz Caro GM, Schutte WA. 2003. *Astron. Astrophys.* 412:121
Mundy LG, Wootten A, Wilking BA, Blake GA, Sargent AI. 1992. *Ap. J.* 385:306
Nuevo M, Auger G, Blanot D, d'Hendecourt L. 2008. *Orig. Life Evol. Biosph.* 38:37
Nummelin A, Bergman P, Hjalmarson Å, Friberg P, Irvine WM, et al. 2000. *Ap. J. Suppl.* 128:213
Öberg KI, Boogert ACA, Pontoppidan KM, Blake GA, Evans NJ, et al. 2008. *Ap. J.* 678:1032
Öberg KI, Fuchs GW, Awad Z, Fraser HJ, Schlemmer S, et al. 2007. *Ap. J. Lett.* 662:L23
Ohishi M, Irvine WM, Kaifu N. 1992. In *Astrochemistry of Cosmic Phenomena*, ed. PD Singh. IAU Symp. 150, p. 171. Dordrecht: Kluwer
Ohishi M, Kaifu N. 1998. In *Chemistry and Physics of Molecules and Grains in Space*. *Faraday Discuss.* 109:205
Olano CA, Walmsley CM, Wilson TL. 1988. *Astron. Astrophys.* 196:194
Olofsson H. 2005. See Lis, Blake & Herbst 2005, p. 499
Pankonin V, Churchwell E, Watson C, Bieging JH. 2001. *Ap. J.* 558:194
Pardo JR, Cernicharo J, Goicoechea JR, Guélin M, Asensio Ramos A. 2007. *Ap. J.* 661:250
Parise B, Castets A, Herbst E, Caux E, Ceccarelli C, et al. 2004. *Astron. Astrophys.* 416:159
Persson CM, Olofsson AOH, Koning N, Bergman P, Bernath P, et al. 2007. *Astron. Astrophys.* 476:807
Petrie S. 1996. *MNRAS* 281:137
Pety J, Teyssier D, Fossé D, Gerin M, Roueff E, et al. 2005. *Astron. Astrophys.* 435:885
Pickett HM. 1991. *J. Mol. Spectrosc.* 148:371
Pickles JB, Williams DA. 1977. *Astrophys. Space Sci.* 52:443
Plume R, Fuller GA, Helmich F, van der Tak FFS, Roberts H, et al. 2007. *Publ. Astron. Soc. Pac.* 119:102
Pontoppidan KM, Fraser HJ, Dartois E, Thi WF, van Dishoeck EF, et al. 2003. *Astron. Astrophys.* 408:981
Pontoppidan KM, van Dishoeck EF, Dartois E. 2004. *Astron. Astrophys.* 426:925
Pottage JT, Flower DR, Davis SL. 2004. *MNRAS* 352:39
Prasad SS, Tarafdar SP. 1983. *Ap. J.* 267:603
Quan D, Herbst E. 2007. *Astron. Astrophys.* 474:521
Reipurth B, Jewitt D, Keil K, eds. 2007. *Protostars and Planets V*. Tucson: Univ. Arizona Press
Remijan A, Snyder LE, Friedel DN, Liu SY, Shah RY. 2003. *Ap. J.* 590:314
Remijan AJ, Hollis JM. 2006. *Ap. J.* 640:842
Remijan AJ, Hollis JM, Jewell PR, Lovas FJ. 2008a. *Bull. Am. Astron. Soc.* 40:188

Remijan AJ, Hollis JM, Lovas FJ, Plusquellic DF, Jewell PR. 2005a. *Ap. J.* 632:333
Remijan AJ, Hollis JM, Snyder LE, Jewell PR, Lovas FJ. 2006. *Ap. J. Lett.* 643:L37
Remijan AJ, Leigh DP, Markwick-Kemper AJ, Turner BE. 2008b. arXiv:0802.2273
Remijan AJ, Markwick-Kemper A, ALMA Work. Group on Spectral Line Frequencies. 2007. In *Bull. Am. Astron. Soc.* 39:963
Remijan AJ, Wyrowski F, Friedel DN, Meier DS, Snyder LE. 2005b. *Ap. J.* 626:233
Requena-Torres MA, Marcelino N, Jiménez-Serra I, Martín-Pintado J, Martín S, Mauersberger R. 2007. *Ap. J. Lett.* 655:L37
Requena-Torres MA, Martín-Pintado J, Martín S, Morris MR. 2008. *Ap. J.* 672:352
Requena-Torres MA, Martín-Pintado J, Rodríguez-Franco A, Martín S, Rodríguez-Fernández NJ, de Vicente P. 2006. *Astron. Astrophys.* 455:971
Roberts H, Herbst E, Millar TJ. 2004. *Astron. Astrophys.* 424:905
Roberts H, Millar TJ. 2000. *Astron. Astrophys.* 361:388
Ruffle DP, Herbst E. 2001. *MNRAS* 322:770
Ruiterkamp R, Peeters Z, Moore MH, Hudson RL, Ehrenfreund P. 2005. *Astron. Astrophys.* 440:391
Sakai N, Sakai T, Hirota T, Yamamoto S. 2008. *Ap. J.* 672:371–381
Sakai N, Sakai T, Osamura Y, Yamamoto S. 2007. *Ap. J. Lett.* 667:L65
Sandford SA. 2008. See Kwok & Sanford 2008, p. 299
Sandford SA, Allamandola LJ. 1988. *Icarus* 76:201
Schilke P, Benford DJ, Hunter TR, Lis DC, Phillips TG. 2001. *Ap. J. Suppl.* 132:281
Schilke P, Comito C, Thorwirth S, Wyrowski F, Menten KM, et al. 2006. *Astron. Astrophys.* 454:L41
Schilke P, Groesbeck TD, Blake GA, Phillips TG. 1997. *Ap. J. Suppl.* 108:301
Schöier FL, Jørgensen JK, van Dishoeck EF, Blake GA. 2002. *Astron. Astrophys.* 390:1001
Schöier FL, van der Tak FFS, van Dishoeck EF, Black JH. 2005. *Astron. Astrophys.* 432:369
Schutte WA, Allamandola LJ, Sandford SA. 1993. *Icarus* 104:118
Schutte WA, Boogert ACA, Tielens AGGM, Whittet DCB, Gerakines PA, et al. 1999. *Astron. Astrophys.* 343:966
Shu FH. 1977. *Ap. J.* 214:488
Smith D. 1992. *Chem. Rev.* 592:1473
Smith IWM, Herbst E, Chang Q. 2004. *MNRAS* 350:323
Snow TP, McCall BJ. 2006. *Annu. Rev. Astron. Astrophys.* 44:367
Snyder LE. 2006. *Proc. Natl. Acad. Sci. USA* 103:12243
Snyder LE, Lovas FJ, Hollis JM, Friedel DN, Jewell PR, et al. 2005. *Ap. J.* 619:914
Stantcheva T, Shematovich VI, Herbst E. 2002. *Astron. Astrophys.* 391:1069
Sutton EC, Blake GA, Masson CR, Phillips TG. 1985. *Ap. J. Suppl.* 58:341
Sutton EC, Peng R, Danchi WC, Jaminet PA, Sandell G, Russell APG. 1995. *Ap. J. Suppl.* 97:455
Suzuki H, Yamamoto S, Ohishi M, Kaifu N, Ishikawa S, et al. 1992. *Ap. J.* 392:551
Tercero B, Cernicharo J, Pardo JR. 2005. In *Astrochemistry: Recent Successes and Current Challenges*, IAU Symp. 231, Poster 57 Sess. 2. **http://asilomar.caltech.edu**
Thaddeus P. 1994. In *Molecules and Grains in Space*, ed. I Nenner. *Am. Inst. Phys. Conf. Ser.*, 312:312
Thi WF, van Zadelhoff GJ, van Dishoeck EF. 2004. *Astron. Astrophys.* 425:955
Thompson MA, MacDonald GH. 1999. *Astron. Astrophys. Suppl.* 135:531
Thompson MA, MacDonald GH. 2003. *Astron. Astrophys.* 407:237
Thorwirth S, Walsh AJ, Wyrowski F, Schilke P, Beuther H, et al. 2007. See LeMaire & Combes 2007, p. 141
LeMaire JL, Combes F, eds. 2007. *Molecules in Space & Laboratory*. Paris, France: DIANA
Thorwirth S, Winnewisser G, Megeath ST, Tieftrunk AR. 2003. In *Galactic Star Formation Across the Stellar Mass Spectrum*, ed. JM De Buizer, NS van der Bliek. *Astron. Soc. Pac. Conf. Ser.* 287:257
Tielens AGGM. 2008. *Annu. Rev. Astron. Astrophys.* 46:289
Tielens AGGM, Hagen W. 1982. *Astron. Astrophys.* 114:245
Townes CH, Schawlow AL. 1955. *Microwave Spectroscopy*. Microwave Spectroscopy, New York: McGraw-Hill
Turner BE. 1991. *Ap. J. Suppl.* 76:617

Turner BE. 1998. *Ap. J.* 501:731
Turner BE, Terzieva R, Herbst E. 1999. *Ap. J.* 518:699
van Broekhuizen FA, Pontoppidan KM, Fraser HJ, van Dishoeck EF. 2005. *Astron. Astrophys.* 441:249
van der Tak FFS, Black JH, Schöier FL, Jansen DJ, van Dishoeck EF. 2007. *Astron. Astrophys.* 468:627
van der Tak FFS, van Dishoeck EF, Caselli P. 2000. *Astron. Astrophys.* 361:327
van Dishoeck EF. 1988. In *Rate Coefficients in Astrochemistry*, ed. TJ Millar, DA Williams, p. 49. Dordrecht: Kluwer
van Dishoeck EF. 2001. In *The Promise of the Herschel Space Observatory*, ed. GL Pilbratt, J Cernicharo, AM Heras, T Prusti, R Harris. *ESA Special Publ.*, 460:185
van Dishoeck EF. 2008. See Kwok & Sanford 2008, p. 3
van Dishoeck EF, Blake GA. 1998. *Annu. Rev. Astron. Astrophys.* 36:317
van Dishoeck EF, Blake GA, Jansen DJ, Groesbeck TD. 1995. *Ap. J.* 447:760
van Dishoeck EF, Hogerheijde MR. 1999. In *NATO ASIC Proc. 540: The Origin of Stars and Planetary Systems*, ed. CJ Lada, ND Kylafis, p. 97
Vasyunin AI, Semenov DA, Wiebe DS, Henning T. 2009. *Ap. J.* 691:1459
Vasyunin AI, Sobolev AM, Wiebe DS, Semenov DA. 2004. *Astron. Lett.* 30:566
Visser R, van Dishoeck EF, Doty SD, Dullemond CP. 2009. *Astron. Astrophys.* 495:881
Viti S, Collings MP, Dever JW, McCoustra MRS, Williams DA. 2004. *MNRAS* 354:1141
Viti S, Williams DA. 1999. *MNRAS* 305:755
Wakelam V, Caselli P, Ceccarelli C, Herbst E, Castets A. 2004. *Astron. Astrophys.* 422:159
Wakelam V, Herbst E. 2008. *Ap. J.* 680:371
Wakelam V, Herbst E, Selsis F. 2006. *Astron. Astrophys.* 451:551
Wakelam V, Selsis F, Herbst E, Caselli P. 2005. *Astron. Astrophys.* 444:883
Watanabe N, Kouchi A. 2002. *Ap. J. Lett.* 571:L173
Watson WD. 1973. *Ap. J. Lett.* 183:L17
White GJ, Araki M, Greaves JS, Ohishi M, Higgenbottom NS. 2003. *Astron. Astrophys.* 407:589
Whittet DCB. 2003. *Dust in the Galactic Environment*. Bristol: Inst. Phys. 2nd ed.
Whittet DCB, Shenoy SS, Bergin EA, Chiar JE, Gerakines PA, et al. 2007. *Ap. J.* 655:332
Willaert F, Møllendal H, Alekseev E, Carvajal M, Kleiner I, Demaison J. 2006. *J. Mol. Struc.* 795:4
Woodall J, Agúndez M, Markwick-Kemper AJ, Millar TJ. 2008. The UMIST database for astrochemistry. **http://www.udfa.net/**
Woon DE. 2008. *The astrochymist*. **http://www.astrochymist.org**
Wyrowski F, Schilke P, Walmsley CM, Menten KM. 1999. *Ap. J. Lett.* 514:L43
Xu LH, Fisher J, Lees RM, Shi HY, Hougen JT, et al. 2008. *J. Mol. Spect.* 251:305
Yoshida H, Phillips TG. 2005. In *Astrochemistry: Recent Successes and Current Challenges*, IAU Symp. 231, Poster 63, Sess. 1. **http://asilomar.caltech.edu**
Ziurys LM, Apponi AJ. 2005. See Lis, Blake & Herbst 2005, p. 207

Annual Review of Astronomy and Astrophysics

Volume 47, 2009

Contents

Indexes

Errata

An online log of corrections to *Annual Review of Astronomy and Astrophysics* articles may be found at http://astro.annualreviews.org/errata.shtml